UNIVERSITÀ DEGLI STUDI DI NAPOLI "FEDERICO II"

Tesi di Dottorato

Effect of MGO accumulation on vascular function in mouse experimental models in vitro and in vivo.

Coordinatore
Prof. Giuseppe Cringoli

Candidato
Dott.ssa Immacolata Prevenzano

Tutor
Prof. Francesco Beguinot

Index

Chapter 2 The role of miRNAs in MGO-induced insulin resistance in mouse aortic endothelial cells.

Index

Aknownledgement

List of abbreviations

ACE: Angiotensin-converting enzyme
AGEs: Advanced glycation end-products
AGO: Argonaute
Akt2 KO: Akt2 Knockout
ALDH: Aldehyde dehydrogenase
Ang II: Angiotensin II
AR: Aldose reductase
DAG: Diacylglycerol
DHAP: Dydhdroxyacetone phosphate
DKO: Double Knockout mice
DM: Diabetes mellitus
ECs: Endothelial cells
ED: endothelial dysfunction
eNOS: Endothelial nitric oxide synthase
ERK1/2: Extracellular signal-regulated protein kinase 1/2 E
ET-1: Endothelin-1
FBS: Fetal bovine serum
G3P: Glycerol- 3 phosphate
GFAT: glutamine fructose-6-phosphatase amidotrasferase
GK: Goto-Kakizaki rats
GlcNAc: N-acetilglucosamine
Glo1 ^{KD}: Glo1-Knockdown
Glo1: Glyoxalase 1
Glo2: Glyoxalase 2
GSH: Glutathione
GSIS: Glucose-stimulates insulin secretion
GSK3: Glycogen syntase kinase
HbA1c: Glycated hemoglobin
ipGTT: intraperitoneal Glucose Tolerance Test
IRS-1 KO: IRSKO mouse
IRS1: insulin receptor substrate
ITT: Insulin Tolerance Test
KRAS: GTPase kirsten rat sarcoma homolog
LDL: low-density lipoproteins
LIRKO: Liver-specific insulin receptor Knockout
MAECs: Mouse aortic endothelial cells
MAPK: Mitogen-actived protein kinase
MCP-1: Monocyte chemotactic protein-1
MGOO: Methylglyoxal

List of abbreviations

MGO-H1: Methylglyoxal hydroimidazolone
microRNA: miRNAs
MOLD: 1,3-di(Nε-lysino)-4-methyl-imidazolium
NAD: nicotinamide adenine dinucleotide
NADPH: nicotinamide adenine dinucleotide phosphate hydrogen
NF-kB: Transcription factor nuclear factor kB
NO: Nitric oxide
PAI-1: Plasminogen activator inhibitor-1
PDK1: Phosphoinositide-dependent kinase-1
PHLPP1: protein phosphatase 1
PHLPP2: protein phosphatase 2
PI: Phosphatidyl inositol
PI3K: Phosphatidyl inositol 3 kinase
PKB: Protein kinase B
PKC: Protein kinase C
PTEN: Phosphatase and tensin homolog
PTP1B: Protein tyrosine phosphatase 1B
RISC: RNA-induced silencing complex
ROSs: Reactive oxygen species
SDH: Sorbitol dehydrogenase
SHR: Spontaneously hypertensive rats
SNPs: Single nucleotide polymorphisms
SOD: Superoxide dismutase
STZ: Streptozotocin
T2DM: Type 2 diabetes mellitus
TNF-α: Tumor necrosis factor α:
TP: miScript target protector
t-PA: tissue-type plasminogen activator
VCAM-1: Vascular cell adhesion molecule-1
VSMC: Vascular smooth muscle cells
vWf: Von Willebrand factor
WKY: Wistar-Kyoto rats
ZDF: Zucher Diabetic Fatty Rats

List of figures

List of figures

List of tables

List of tables

Abstract

Methylglyoxal (MGO), a highly reactive dicarbonyl compound formed as by-product of glycolysis, is an ubiquitous metabolite of cellular metabolism. Therefore, it is produced in all cells, both under normal and pathological conditions. Under physiological circumstances, MGO is detoxified through the glyoxalase system, of which Glyoxalase 1 (Glo1) is the rate limiting enzyme. In pathological conditions, as in chronic hyperglycemia, high blood glucose levels lead to increased MGO accumulation. It is known that MGO plays a major role in endothelial cell damage and development of vascular disease. We have previously demonstrated that MGO induces endothelial insulin resistance both in vitro and in animal models. In the last few years, many evidence has provided a link between microRNAs (miRNAs) and diabetic complications. Indeed, miRNAs regulate cellular molecular pathways, including insulin signaling, thus controlling the pathophysiology of vascular bed. This study includes the investigation of two aspects of MGO effects on the pathophysiology of diabetes mellitus (DM) and its associated complications: 1. the evaluation of MGO accumulation on glucose homeostasis and vascular function in a mouse model knockdown for Glo1 ($Glo1^{KD}$) and 2. the analysis of miRNAs contribution in MGO induced damaging effect on insulin responsiveness in mouse aortic endothelial cells (MAECs).

The results obtained *in vivo* demonstrated that the endogenous accumulation of MGO in mice with a reduced expression of Glo1 leads to an age-dependent development of glucose intolerance, in absence of hyperglycemia. Indeed, despite the reduced glucose tolerance at 10 months of age, $Glo1^{KD}$ mice have no differences in body weight and in the glucose levels, compared to WT mice, neither at 5 months nor at 10 months of age. While no alterations in the whole-body insulin-sensitivity have been observed by insulin tolerance tests, $Glo1^{KD}$ mice show a basal hyperinsulinemia and impaired glucose-stimulated insulin-secretion, compared to WT mice. Moreover, an increased systolic blood pressure accompanied by impaired endothelium-dependent vasodilation are already shown starting from 5 months of age in $Glo1^{KD}$ mice.

A deeper analysis of the molecular mechanisms involved in the endothelial dysfunction has been performed *in vitro*, in MAECs exposed to MGO, which we have previously demonstrated to display insulin resistance and an imbalanced production of vasoactive molecules: NO and ET-1. Our results demonstrate that MGO induces the down-regulation of 4 out of 84 diabetes-associated miRNAs. Among these, the reduced expression of miR-190a and miR-214 has been validated both in MAECs exposed to MGO and in aortae

from Glo1^{KD} mice. The inhibition of miR-190a and miR-214 impairs the insulin-induced activation of Akt1/eNOS pathway, whereas their overexpression prevents the MGO-induced insulin resistance in MAECs. In detail, we have identified the kinase KRAS and the phosphatase PHLPP2 as targets of miR-190a and miR-214, respectively. In MAECs increased KRAS levels result from the reduced expression of miR-190a and sustain the ERK hyperactivation, which is in turn responsible for the impairment of the insulin-stimulated IRS1/Akt/eNOS signal transduction in MAECs treated with MGO. Moreover, a reduced insulin-dependent activation of Akt in MGO-treated MAECs is fostered by higher protein levels of PHLPP2, which we validate here to be a direct target of miR-214.

In conclusion, our results demonstrate that Glo1 silencing is enough to induce MGO accumulation *in vivo* in Glo1^{KD} mice, causing glucose intolerance and β-cell dysfunction, which are characteristic of T2DM pathogenesis, together with the impairment of hemodynamic function (i.e blood pressure and endothelial-dependent vasodilation), in a context of normoglycemia. Moreover, miR-190a and miR-214 play a role in the endothelial insulin-resistance induced by MGO in MAECs. Thus, representing potential biomarkers of vascular dysfunction. Further efforts in the development of pharmacological intervention to interfere with these pathogenic events will be useful to provide new therapeutic options aimed at preventing the onset and progression of vascular complications in diabetes.

1. Endothelial cell function

The endothelium was considered to be a selective barrier to the diffusion of macromolecules from the vessel lumen to interstitial space. During the past years, different studies have highlighted additional roles for the endothelium. Indeed, the endothelium regulates vascular tone, cell-cell interaction, permeability and the coagulation system through the production of several factors, in response to various stimuli (Nigro et al. 2017, Schalkwijk et al. 2005). To carry out its above-mentioned functions, the endothelium produces components of the extracellular matrix such as collagen and a variety of regulatory mediators, including nitric oxide (NO), prostanoids, endothelin-1 (ET-1), angiotensin II (Ang II), tissue-type plasminogen activator (t-PA), plasminogen activator inhibitor-1 (PAI-1), von Willebrand factor (vWf), adhenosin molecular and cytokines (Schalkwijk et al. 2005). In physiological conditions, the endothelium actively decreases vascular tone, limits leucocyte adhesion and, thus, inflammatory activity in the vessel wall. It maintains vascular permeability to nutrients, hormones, other macromolecules and inhibits platelet adhesion and aggregation by producing prostacyclin and NO. Moreover, it limits the activation of the coagulation cascade by the thrombomodulin/protein C, heparan sulphate/antithrombin and tissue factor/tissue factor pathway inhibitor interactions and regulates fibrinolysis by producing t-PA and its inhibitor PAI-1. As mentioned above, the endothelium is able to synthesize NO, an important molecule that has vasodilator, anti-platelet, anti-proliferative, permeability-decreasing and anti-inflammatory properties. NO inhibits leucocyte adhesion and rolling, as well as cytokine-induced expression of vascular cell adhesion molecule-1 (VCAM-1) and monocyte chemotactic protein-1 (MCP-1), effects that are at least in part attributable to the inhibition of the transcription factor nuclear factor κB (NF-κB) (Schalkwijk et al. 2005). Disturbing this tightly regulated equilibrium leads to endothelial dysfunction (ED). In particular, ED is the first step in the initiation, progression and clinical outcome of vascular complications, such as retinopathy, nephropathy and hypertension, that are the principal causes of mortality and morbidity of diabetic patients (Nigro et al. 2017). Anyway, the mechanisms leading to ED are not very completely clarified. Several studies have shown that hyperglycemia associated with impaired glucose tolerance and diabetes causes insulin resistance and ED (Du et al. 2001).

2. Hyperglycemia and endothelial dysfunction

The hallmark of ED is represented by the impaired NO bioavailability. Additionally, ED is established when one or more of the following features occur: reduced endothelium-mediated vasorelaxation, hemodynamic deregulation, impaired fibrinolytic ability, enhanced turnover and /or overproduction of growth factors, increased expression of adhesion molecules and inflammatory genes, excessive generation of reactive oxygen species (ROSs), increased oxidative stress and enhanced permeability of the endothelial cells (ECs) layer (Taddei et al. 2003, Addabbo et al. 2009, Sena et al. 2013). The increased production of ROSs is due to the activation of nicotinamide adenine dinucleotide phosphate hydrogen (NADPH) oxidase, inactivation and reduced expression of the antioxidant enzymes, catalase and superoxide dismutase (SOD) or uncoupling of endothelial nitric oxide synthase (eNOS) (Dhananjayan et al. 2016). The increased ROSs production is one of the factors involved in the activation of transcription factors such as NF-κB. NF-κB is a key mediator that regulates multiple pro-inflammatory and pro-atherosclerotic target genes in ECs, vascular smooth muscle cells (VSMCs) and macrophages. Activation of NF-κB leads to an increased production of adhesion molecules, leukocyte-attracting chemokines and cytokines activating inflammatory cells in the vascular wall. In ED, a pro-thrombotic state is generated by the increased production of lesion-based coagulants, such as tissue factor, and the inhibitors of fibrinolysis, such as PAI-1. Vascular tone and remodeling are enhanced through reduced NO and an increased activity and production of vasoconstrictors (i.e. ET-1, angiotensin II, and prostanoids).

There are several factors contributing to ED, among which the most important are: hypertension, smoking, dyslipidemia and hyperglycemia (Sena et al. 2013). Hyperglycemia is one of major characteristic of type 2 diabetes mellitus (T2DM), a common metabolic disease with a high and growing prevalence (American Diabetes Association 2009). In both animal and human studies, it has been proven that hyperglycemia impairs endothelial function in both macro- and microvascular beds (Sena et al. 2013). Hyperglycemia causes vascular damage in different cell types of the vascular wall through the activation of several pathways including: 1) the increased flux of glucose and other sugars through the polyol pathway; 2) the augmented intracellular formation of advanced glycation end products (AGEs); 3) the increment of the expression of the receptor for AGEs (RAGE); 4) the activation of protein kinase C (PKC) isoforms; and 5) the

overactivation of the hexosamine pathway (Fig. 1). The activation of these biochemical ways promotes increased vascular oxidative stress, inflammation, apoptosis, atherogenesis and impaired endothelial function (Brownlee 2001).

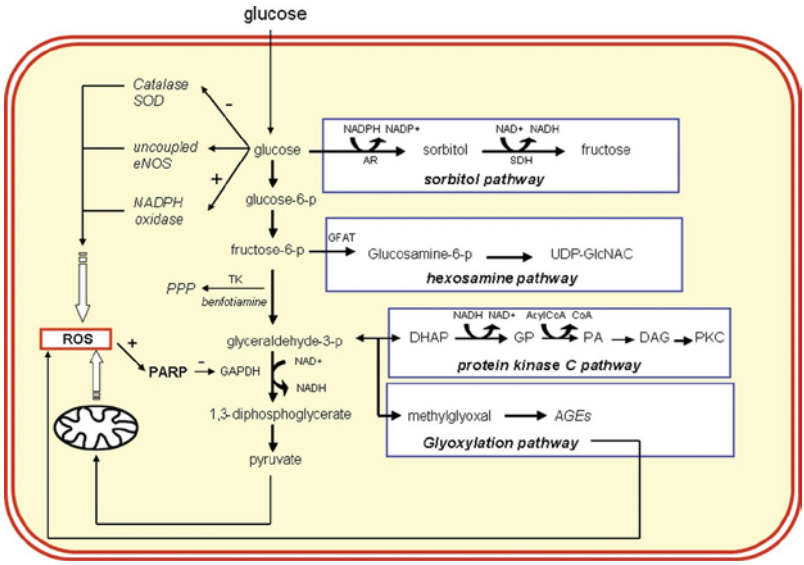

Figure 1: Molecular pathways activated chronic hyperglycemia. (Schalkwijk and Stehouwer 2005).

In hyperglycemic condition, the excess of glucose can be metabolized to sorbitol and fructose by aldose reductase (AR) and sorbitol dehydrogenase (SDH), respectively. In the hexosamine pathway, fructose 6-phosphate is converted into glucosamine 6-phosphate by the enzyme glutamine fructose-6-phosphate amidotransferase (GFAT) and subsequently into N-Acetylglucosamine (GlcNAc). The mechanism responsible for the activation of PKC by hyperglycemia is related to *de novo* synthesis of the PKC activator, diacylglycerol (DAG) from a stepwise acylation of glycerol 3-phosphate (G3P). A major pathway activated by increased levels of the upstream glycolytic metabolite glyceraldehyde-3-phosphate is the AGEs non-enzymatic formation where the major intracellular AGEs precursor methylglyoxal (MGO) is generated from triose-phosphates fragmentation.

3. Methylglyoxal metabolism

MGO is a highly reactive α-oxaldehyde, whose formation rate depends on the organism, tissue, cell metabolism and physiological condition (Igor et al. 2015). The endogenous MGO is derived from metabolic intermediates of carbohydrates, proteins and fatty acids (Fleming et al. 2011). In mammals, the glycolytic pathway is the principal source of MGO via fragmentation of triosephosphates G3P and dihydroxyacetone phosphate (DHAP) (Rabbani et al. 2016). Under normal physiological conditions, MGO is maintained at low levels. The latter are increased in conditions leading to higher triosephosphate levels, like happens in hyperglycemia when glucose metabolism is increased, in the impairment of pentose pathway with decreased G3P or in case of the increased anaerobic glycolysis occurring in hypoxia (Nigro et al. 2017). Although the production of MGO constitutes only 0.1% of glucotriose flux, its biological effect is important considering its high reactivity with proteins and nucleic acids. The irreversible reaction of MGO with proteins is directed to arginine residues forming hydroimidazolone adducts. The hydroimidazolone (MGO-H1) derived from MGO is the most abundant MGO-derived AGEs, as it accounts for >90% of all MGO adducts, equivalent to MGO-H1 residues in 1-5% of all proteins (Maessen et al. 2015).

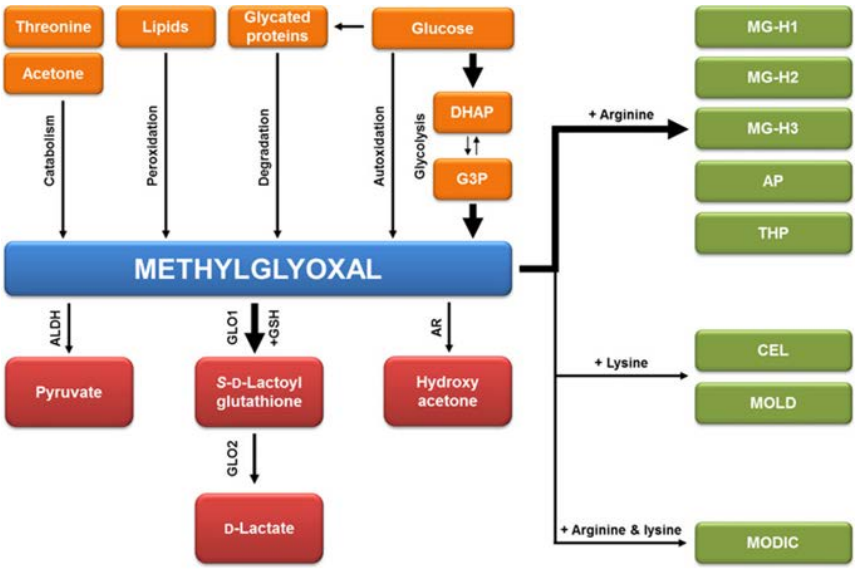

Figure 2. Pathways involved in MGO formation and detoxification. *MGO is generated as a byproduct of glycolysis. Other sources of MGO are constitute by: autoxidation of glucose, catabolism of threonine and acetone, lipid peroxidation and degradation of glycated proteins. MGO is detoxified mainly by the glyoxalase system. Other minor pathways are aldehyde dehydrogenase (ALDH) and aldose reductase (AR). Otherwise, it may react with amino groups of proteins and other biomolecules to form 1-carboxyethyl-lysine (CEL) methylglyoxal-lysine dimer: 1,3-di(Nε-lysino)-4-methyl-imidazolium (MOLD), while it forms 2-ammonio-6-{(2-[(4-ammonio-5-oxido-5-oxopentyl)amino]-4-methyl-4,5-dihydro-1H-imidazol-5-ylidene) amino}hexanoate (MODIC) following dimer crosslink with arginine and lysine (Maessen et al. 2015).*

Other minor contributors to MGO formation are from the oxidation of acetone (Beisswenger et al. 2006), the catabolism of ketone bodies that are increased in ketoacidosis (Lyles and Chalmers 1992), lipid peroxidation and degradation of glycated proteins and monosaccharides (Kalapos 1999, Thornalley et al. 1999) (Fig. 2). It is now known that MGO is observed at relative higher plasma levels (2–6 fold) in diabetic patients than in healthy subjects and are also found in many food products, beverages and cigarette smoke (Nigro et al. 2017). In detail, in physiological conditions, MGO levels is 50–150 nM in human plasma and 1–4 μM in human cells. Nevertheless, the contribution of exogenous MGO is still controversial. Several studies report that free MGO is rapidly degraded during digestion in the intestine and, thus, it does not influence plasma levels in vivo (Rabbani et al. 2016, Nigro et al. 2017), while others report that in rodents fed with MGO-

supplemented diet there is a major brain and plasma MGO accumulation (Cai et al. 2014). When reactive dicarbonyl concentration increases beyond physiological levels, they produce protein and cell dysfunction leading to impaired health and disease (Rabbani et al. 2016).
Under physiological circumstances, MGO is detoxified by different mechanisms such us the glyoxalase, aldose reductase, aldehyde dehydrogenase and carbonyl reductase pathways (Maessen et al. 2015). Undoubtedly, the glyoxalase system, an ubiquitous enzymatic pathway, is the main detoxification system for MGO.

4. The glyoxalase pathway

The glyoxalase pathway consists of two enzymes, glyoxalase 1 (Glo1) and glyoxalase 2 (Glo2) and a catalytic amount of glutathione (GSH) (Fig. 3).

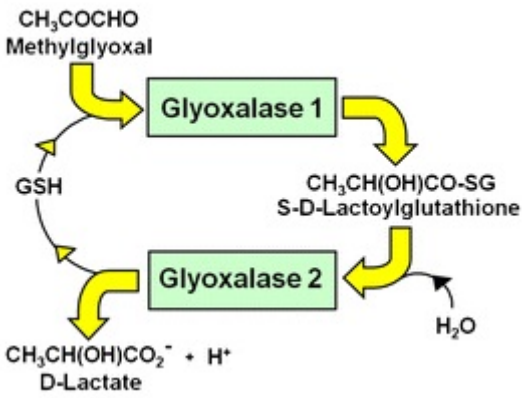

Figure 3. The Glyoxalase System. *Glyoxalase system is formed by two enzymes. Glyoxalase 1 catalyzes the conversion the MGO-GSH hemi-thioacetal to the thioester S-D-lactoyglutahione. Glyoxalase 2 catalyzes the hydrolysis of S-D-lactoylglutathione to form the end-product D-lactate (Rabbani et al. 2016).*

In this process, Glo1 is the most crucial enzyme as it is defined the rate limiting enzyme by converting the MGO-GSH hemi thioacetal to the thioester S-D-lactoyglutahione (Sousa et al. 2013). Its activity is directly proportional to GSH concentration. Thus, when cellular GSH concentration declines, as in oxidative stress, there is an associated impairment of Glo1 activity. Glo2 is the second enzyme in the glyoxalase system and it catalyzes hydrolysis of S-D-lactoylglutathione to D-lactate and GSH (Thornalley 1993, Nigro et al. 2017). Glo1 gene is expressed in all tissues

of prokaryotic and eukaryotic organisms (Aronsson and Mannervik 1978, He et al. 2000), and is the protein localized in the cytoplasmic compartment (Rabbani and Thornalley 2014). Several studies demonstrated that Glo1 activity can be modulated by both gene expression regulation and post-translational modifications (Ranganathan 1999). While genetic polymorphisms of Glo2 are extremely rare, different SNPs (single nucleotide polymorphisms) have been identified in the Glo1 gene that reduce the Glo1 activity and correlate with an increase of the diabetic neuropathy (Groener et al. 2013) and an increase risk of cardiovascular complications (Rabbani and Thornalley 2011).

5. MGO and insulin resistance

Insulin resistance is clinically defined as the inability of a known quantity of exogenous or endogenous insulin to produce a biological response, as the increase of glucose uptake and utilization (Gisela 2005). A widely accepted theory states that insulin resistance leads to T2DM, metabolic and cardiovascular disease and that MGO may contribute to the pathogenesis of insulin resistance (Nigro et al. 2017). We and others have provided evidence about the role of MGO on insulin-resistance in major target tissues for insulin action (Nigro et al. 2014). For instance, a short exposure of L6 muscle cells to MGO induces an inhibition of insulin-stimulated phosphorylation of protein Kinase B (PKB) and extracellular signal-regulated protein Kinase 1/2 (ERK1/2), without affecting insulin receptor tyrosine phosphorylation (Maessen et al. 2015). Moreover, it has been demonstrated that 3T3-L1 adipocyte treated with MGO, it shown an impairment of the insulin signalling, as indicated by decreased insulin-induced insulin receptor substrate (IRS-1) tyrosine phosphorylation (Jia and Wu 2007). Indeed, the incubation of the pancreatic INS1-E β-cells with MGO results in a glycogen synthase kinase (GSK3) mediated impairment of insulin secretion action (Maessen et al. 2015). In vivo, it has been demonstrated that MGO induces insulin resistance and salt sensitivity by increasing oxidative stress in Sprague–Dawley rats (Guo et al. 2009). In support of animal data and studies in animal models, a very recent human study in healthy overweight individuals demonstrates that with a diet low AGEs reduces the risk of T2DM by improving insulin sensitivity (De Courten et al. 2016). Insulin resistance is typically defined as decreased sensitivity or responsiveness to metabolic actions of insulin. However, diminished sensitivity to the vascular actions of insulin also plays an

important role in the pathophysiology of insulin-resistant states (Baron et al. 1991, Natali et al. 1997). Indeed, endothelial insulin resistance is typically accompanied by reduced phosphatidylinositol 3 kinase (PI3K)/NO pathway and an intact or heightened mitogen-activated protein kinase (MAPK)/ET-1 pathway.
We have shown that MGO alters the sensitivity of the endothelium to insulin action both in vitro and in vivo. In particular, high levels of MGO cause an alteration in the release of two important vasoactive molecules by the endothelium: ET1 (vasoconstrictor action) and NO (vasodilatory action), highlighting MGO as an important culprit of endothelial dysfunction associated with insulin resistance (Nigro et al. 2014). Indeed, insulin resistant states are associated with metabolic abnormalities that include glucotoxicity, lipotoxicity and inflammation, thus contributing to the progression of long term endothelial dysfunction.

6. Effect of MGO accumulation on vascular function

In the last decades, several studies have been focused on the central role of MGO in vascular defects (Shamsaldeen et al 20016), particularly on endothelial dysfunction, which is considered an important factor in the development of cardiovascular disease (Fig. 4).

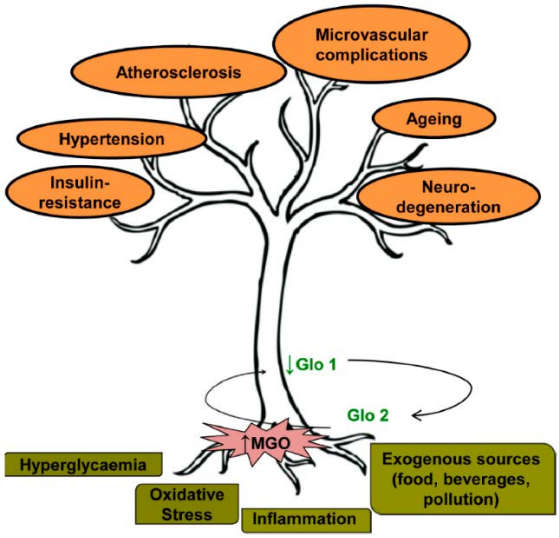

Figure 4. Sources of methylglyoxal (MGO) accumulation contributing to vascular dysfunction*. Hyperglycemia, oxidative stress, inflammation and exogenous sources of MGO contribute both to the increase of MGO levels and the decrease of glyoxalase 1 (Glo1) activity. MGO-Glo1 imbalance leads to vascular dysfunction contributing to endothelial insulin-resistance, hypertension, atherosclerosis, microvascular complications, ageing and neuro-degeneration. (Nigro et al. 2017)*

Brouwers et al. (2010) have demonstrated that Glo1 overexpression improved diabetic-induced impairment of NO-mediated relaxation. In vivo, exogenous administration of MGO to rats induces diabetes-like microvascular changes (Berlanga et al. 2005) and the impairment of endothelial function (Sena et al. 2012). Moreover, recent studies have shown that methylglyoxal induce vascular dysfunction in rat aorta, mesenteric arterial bed (Thilavech et al. 2017) and causes vascular contractile dysfunction in spontaneously hypertensive rats (SHR) (Mukohda et al. 2012). Dhar et al. have demonstrated a novel finding and a probable mechanism of increase in blood pressure, in particular they shown that MGO activates NF-κB through RAGE and thereby increases renin-angiotensin levels (Dhar et al. 2014). The MGO can impair the NO homeostasis and this has been related to endothelial dysfunction via a modulation of eNOS (Su et al 2013 and Turkseven et al 2014). Moreover, MGO and MGO-derived AGEs also play a harmful effect on microvascular function, contributing to the onset of nephropathy and neuropathy. Overexpression of Glo1 enzyme is important in the prevention of early renal impairment in rat models of

diabetes (Brouwers et al. 2014), but also independently of hyperglycemia in apo E-/- mice. This is also confirmed by the evidence that MGO accumulation in Wistar normal rats impairs several renal disease markers progressively observed in diabetic Goto-Kakizaki rats (GK) (Rodrigues et al. 2014). Based on these findings, it became clear that an effective reduction of MGO accumulation is crucial for preserving vascular function.

7. Role of MGO in the development of vascular complications

Hyperglycemia is a common feature in patients with diabetes mellitus (DM). DM is a common disease affecting more than 451 million people worldwide (Cho et al. 2018). One of the major concerns associated with diabetes relates to the development of micro-vascular (diabetic nephropathy, neuropathy, and retinopathy) and macro-vascular complication (coronary artery disease, peripheral arterial disease, and stroke), which greatly contribute to the high morbility and mortality associated with the disease (Fig. 5).

7.1 Microvascular complications

Results from both experimental and clinical studies on diabetes have demonstrated that hyperglycemia-induced MGO accumulation plays an important role in pathogenesis of microvascular complication.

Nephropathy

Diabetic nephropathy is the major cause of kidney disease and is a major risk factor for the development of macrovascular complications in patients effected by diabetic (Maessen et al. 2015). Indeed, it has been demonstrated that in cultured cells and kidneys from diabetic mice, increased glycolytic flux causes methylglyoxal modifications of the corepressor mSin3A, resulting in enhanced angiopoietin-2 expression, sensitizing microvascular endothelial cells to the proinflammatory effects of tumor necrosis factor (TNF-α) (Yao et al. 2007). Moreover, experimental studies in renal cells demonstrated that the MGO-induced inactivation of mitochondrial respiratory, chain may play an important role in renal cellular toxicity and development of diabetic nephropathy (Rosca et al.2002, Maessen et al. 2015).

Retinopathy

Diabetic Retinopathy is a second common microvascular complication of DM, which causes serious damages in the retina, leading to increased vascular permeability, capillary microaneurysms, capillary degeneration and neovascularization (Forbes and Cooper 2013). Many clinical studies have demonstrated that, in both type 1 and type 2 diabetes (Fosmark et al. 2009, Fosmark et al. 2006), increased serum levels of the specific MGO-derived AGEs end product hydroimidazolone, is associated with the development of diabetic retinopathy (Fosmark et al. 2006). Moreover, overexpression of the Glo1 enzyme in diabetic rats prevents hyperglycemia-induced formation of MGO-derived AGEs in the neural retina and protects against retinal capillary degeneration over 6 months of diabetes (Queisser et al. 2010, Berner et al. 2012).

Neuropathy

Diabetic neuropathy is the most common complication of DM affecting as many as 50% of patients with type 1 and type 2 DM. In most cases, it is associated with foot ulcers, gangrene and limb amputation (Costa and Soares 2013, Chawla et al. 2016). The risk of diabetic neuropathy development is directly proportional to both the duration and magnitude of hyperglycemia. Several studies have confirmed the role played by glycation in diabetic neuropathy, however only a few studies focused specially on the importance of MGO and Glo1 (Jack and Wright 2012).

7.2 Macrovascular complications

Atherosclerosis

The atherosclerosis is a major cause of mortality in the people with diabetes (Grundy et al.1999). In most cases, the underlying process is a narrowing of arterial walls throughout the body (Maessen et al. 2015). In detail, it is a result from chronic inflammation and injury to the artery wall in the peripheral or coronary vascular system and of elevated levels of the low-density lipoproteins (LDL). Many studies have demonstrated that LDL can be modified by MGO, resulting in a change in both their physiological and biological properties (Schalkwijk et al 1998, Rabbani and Thornalley 2011, Turk et al. 2011, Brown et al. 2005). LDL play a significant role in the

enhancement, development and progression of atherosclerosis, through a pathway that involves endothelial cell dysfunction.

Hypertension

MGO has been demonstrated to be involved in the development of other different macrovascular disease, such as the hypertension, but the exact mechanism is not yet fully understood. A link between MGO accumulation and hypertension has been demonstrated in rats with increased MGO levels in aortic and renal tissue (Guo et al. 2009, Wu and Juurlink 2002, Wang et al. 2004, Chang et al. 2005). Rats treated with MGO in drinking water show the increase systolic blood pressure and higher plasma levels of aldosterone, renin and catecholamines (Dhar et al. 2014). Similarly, a diet high in fructose, precursor of MGO, induces hypertension and renal injury in rats (Guo et al. 2012, Sánchez-Lozada et al. 2007). Although a dose of 1% MGO in drinking water alone has no effect on blood pressure for up to 4 weeks in Sprague-Dawley rats (Vasdev et al. 1998), surprisingly enough the same dose in combination with high-salt diet induced hypertension and enhances renal oxidative stress (Guo at al. 2009), suggesting that MGO causes hypertension only in rats with enhanced renal oxidative stress (Maessen et al.2015). Moreover, other studies showed that a significant increase in blood pressure coincided with elevated MGO levels in plasma and aorta of SHR in an age-dependent fashion, compared with age-matched Wistar–Kyoto rats (WKY) (Wang et al.2004, Wang et al. 2005). In the last few years, different mechanisms have been suggested as link between MGO and hypertension, as such it is known that MGO causes vascular Ca^{2+} channel alterations, leading to increased cytosolic [Ca^{2+}], peripheral vascular resistance and hypertension (Vasdev et al. 1998). Moreover, another study demonstrated that MGO-induced hypertension takes palace via angiotensin II type 1 receptor-mediates pathway (Chen et al. 2013). An improvement in blood pressure has been observed in SHR after treatment with aminoguanidine, a known scavenger of MGO (Wang et al. 2007, Wang et al. 2008).

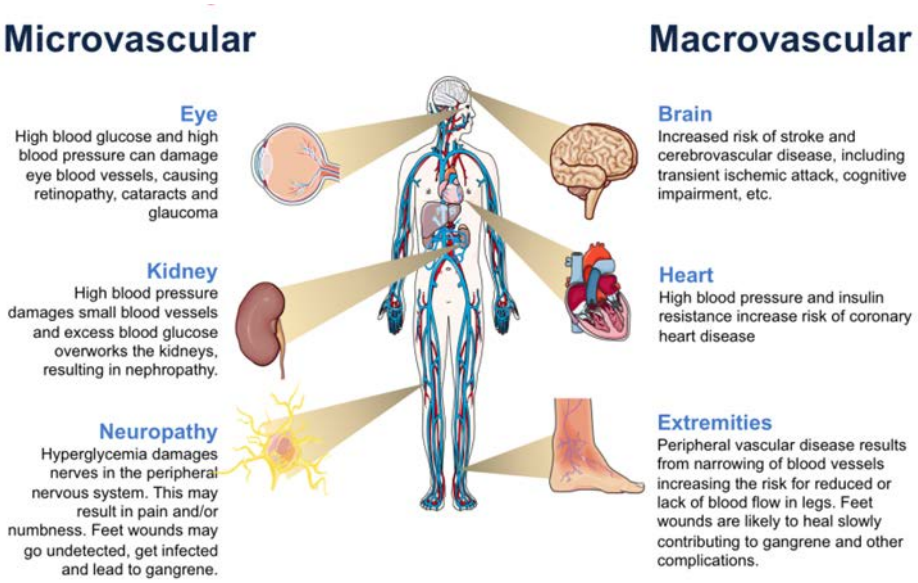

Figure 5. Major microvascular and macrovascular complications associated with diabetes mellitus. *doi: 10.2210/rcsb_pdb/GH/DM/monitoring/complications*

7.3 Bibliography

Addabbo F., Montagnani M., Goligorsky M.S. (2009) Mitochondria and reactive oxygen species. Hypertension. 53(6):885-92. doi: 10.1161/HYPERTENSIONAHA.109.130054

Aronsson A.C., Mannervik E. M. B. (1978) Glyoxalase I, a zinc metalloenzyme of mammals and yeast. Volume 81, Issue 4 Pages 1235-1240 https://doi.org/10.1016/0006-291X(78)91268-8

Baron A.D., Laakso M., Brechtel G., Edelman S.V. (1991) Mechanism of insulin resistance in insulin-dependent diabetes mellitus: a major role for reduced skeletal muscle blood flow. J Clin Endocrinol Metab. ;73(3):637–643

Beisswenger B.G.K, Delucia E.M, Lapoint N., Sanford J. R., Beisswenger P. J. (2006) Ketosis Leads to Increased Methylglyoxal Production on the Atkins Diet. https://doi.org/10.1196/annals.1333.025

Berlanga J., Cibrian D., Guillén I., Freyre F., Alba J.S., Lopez-Saura P., Merino N., Aldama A.., Quintela A.M., Triana M.E., Montequin J.F., Ajamieh H., Urquiza D., Ahmed N. (2005) Methylglyoxal administration induces diabetes-like microvascular changes and perturbs the healing process of cutaneous wounds. JClin Sci (Lond). 109(1):83-95. DOI: 10.1042/CS20050026

Berner A.K., Brouwers O., Pringle R., Klaassen I., Colhoun L., McVicar C., Brockbank S., Curry J.W., Miyata T., Brownlee M., Schlingemann O., Schalkwijk C., Stitt A.W. (2012) Protection against methylglyoxal-derived AGEs by regulation of glyoxalase 1 prevents retinal neuroglial and vasodegenerative pathology. Diabetologia. 55(3):845-54. doi: 10.1007/s00125-011-2393-0

Brouwers O., Niessen P.M., Miyata T., Østergaard J.A., Flyvbjerg A., Peutz-Kootstra C.J., Sieber J., Mundel P.H.., Brownlee M, Janssen B.J., De Mey

J.G., Stehouwer C.D., Schalkwijk C.G. (2014) Glyoxalase-1 overexpression reduces endothelial dysfunction and attenuates early renal impairment in a rat model of diabetes. Diabetologia. 57(1):224-35. doi: 10.1007/s00125-013-3088-5

Brouwers O., Niessen P.M.., Haenen G, Miyata T., Brownlee M., Stehouwer C.D., De Mey J.G., Schalkwijk C.G. (2010) Hyperglycaemia-induced impairment of endothelium-dependent vasorelaxation in rat mesenteric arteries is mediated by intracellular methylglyoxal levels in a pathway dependent on oxidative stress. Diabetologia. 53(5):989-1000. doi: 10.1007/s00125-010-1677-0

Brown B.E., Dean R.T., Davies M.J. **(**2005) Glycation of low-density lipoproteins by methylglyoxal and glycolaldehyde gives rise to the in vitro formation of lipid-laden cells. Diabetologia. 48(2):361-9. DOI:10.1007/s00125-004-1648-4

Brownlee M. (2001) Nature. Dec 13;414(6865):813-20. Biochemistry and molecular cell biology of diabetic complications. DOI:10.1038/414813a

Cai W., Uribarri J., Zhu L., Chen X., Swamy S., Zhao Z., Grosjean F., Simonaro C., Kuchel G.A., Schnaider-Beeri M., Woodward M., Striker G.E., Vlassara H. (2014) Oral glycotoxins are a modifiable cause of dementia and the metabolic syndrome in mice and humans Proc Natl Acad Sci U S A. 1;111(13):4940-5. doi: 10.1073/pnas.1316013111

Chang T., Wang R., Wu L. Methylglyoxal-induced nitric oxide and peroxynitrite production in vascular smooth muscle cells. Free Radical Biology and Medicine Volume 38, Issue 2, 15 January 2005, Pages 286-293https://doi.org/10.1016/j.freeradbiomed.2004.10.034

Chawla A., Chawla R., and Jaggi S. (2016) Microvasular and macrovascular complications in diabetes mellitus: Distinct or continuum? Indian J Endocrinol Metab. 20(4): 546–551. doi: 10.4103/2230-8210.183480

Bibliography

Chen X., Mori T., Guo Q., Hu C., Ohsaki Y., Yoneki Y., Zhu W., Jiang Y., Endo S., Nakayama K., Ogawa S., Nakayama M., Miyata T. & Ito S. (2013). Carbonyl stress induces hypertension and cardio–renal vascular injury in Dahl salt-sensitive rats Hypertension Research volume 36, pages 361–367

Cho N.H., Shaw J.E., Karuranga S., Huang Y., da Rocha Fernandes J.D., Ohlrogge A.W., Malanda B. (2018) IDF Diabetes Atlas: Global estimates of diabetes prevalence for 2017 and projections for 2045. Diabetes Res Clin Pract 138:271-281. doi: 10.1016/j.diabres.02.023

Costa P.Z., Soares R. (2013) Neovascularization in diabetes and its complications. Unraveling the angiogenic paradox. Life SciJun 13;92(22):1037-45. doi: 10.1016/j.lfs.2013.04.001

De Courten B., de Courten M.P., Soldatos G., Dougherty S.L., Straznicky N., Schlaich M., Sourris K.C., Chand V., Scheijen J.L., Kingwell B.A., Cooper M., Schalkwijk C.G., Walker K.Z., Forbes J.M. (2016) Diet low in advanced glycation end products increases insulin sensitivity in healthy overweight individuals: a double-blind, randomized, crossover trial. Am J Clin Nutr. 103(6):1426-33. doi: 10.3945/ajcn.115.125427

Dhananjayan R., Srivani Koundinya K. S, Malati T., Vijay Kumar Kutala. (2016) Endothelial Dysfunction in Type 2 Diabetes Mellitus Indian Journal of Clinical Biochemistry October, Volume 31, Issue 4, pp 372–379 doi: 10.1007/s12291-015-0516-y

Dhar I., Dhar A., Wu L., Desai KM. (2014) Methylglyoxal, a reactive glucose metabolite, increases renin angiotensin aldosterone and blood pressure in male Sprague-Dawley rats. Am J Hypertens. 27(3):308-16. doi: 10.1093/ajh/hpt281

Diabetes Care. 2009 Jan;32 Suppl 1: S62-7. Diagnosis and classification of diabetes mellitus. American Diabetes Association. doi: 10.2337/dc09-S062

Dionne E.M. Maessen, Coen D.A. Stehouwer, Casper G. Schalkwijk. (2015) The role of methylglyoxal and the glyoxalase system in diabetes and other

age-related diseases Clinical Science 128 (12) 839-861; DOI: 10.1042/CS20140683

Du X.L., Edelstein D., Dimmeler S., Ju Q., Sui C., Brownlee M. (2001) Hyperglycemia inhibits endothelial nitric oxide synthase activity by posttranslational modification at the Akt site.J Clin Invest.108(9):1341-8. 10.1172/JCI11235

Fleming T.H., Humpert P.M., Nawroth P.P., Bierhaus A. (2011) Reactive metabolites and AGE/RAGE-mediated cellular dysfunction affect the aging process: a mini-review.Gerontology 57(5):435-43. doi: 10.1159/000322087

Forbes J.M., Cooper M.E. (2013). Mechanisms of diabetic complications.Physiol Rev. Jan;93(1):137-88doi: 10.1152/physrev.00045.2011

Fosmark D.S., Berg J.P., Jensen A.B., Sandvik L.., Agardh E, Agardh C.D., Hanssen K.F. Acta Ophthalmol. (2009) Increased retinopathy occurrence in type 1 diabetes patients with increased serum levels of the advanced glycation endproduct hydroimidazolone. 87(5):498-500. doi: 10.1111/j.1755-3768.2008.01300.x.

Fosmark D.S., Torjesen P.A., Kilhovd B.K., Berg T.J., Sandvik L., Hanssen K.F., Agardh C.D., Agardh E. (2006). Increased serum levels of the specific advanced glycation end product methylglyoxal-derived hydroimidazolone are associated with retinopathy in patients with type 2 diabetes mellitus. Metabolism 55(2):232-6 https://doi.org/10.1016/j.metabol.2005.08.017

Gisela W. (2005) Insulin and Insulin Resistance Clin Biochem Rev. 26(2): 19–39

Groener J.B., Reismann P., Fleming T., Kalscheuer H., Lehnhoff D., Hamann A., Roser P., Bierhaus A., Nawroth P.P., Rudofsky G. (2013) C332C genotype of glyoxalase 1 and its association with late diabetic

complications. Exp Clin Endocrinol Diabetes. 121(7):436-9. doi: 10.1055/s-0033-1345124

Grundy S.M., Benjamin I.J., Burke G.L., Chait A., Eckel R.H., Howard B.V., Mitch W., Smith S.C., Sowers J.R. (1999) Diabetes and cardiovascular disease: a statement for healthcare professionals from the American Heart Association. Circulation. 7;100(10):1134-46.

Guo Q., Mori T., Jiang Y., Hu C., Ohsaki Y., Yoneki Y., Nakamichi T., Ogawa S., Sato H., Ito S. (2012) Losartan modulates muscular capillary density and reverses thiazide diuretic-exacerbated insulin resistance in fructose-fed rats. Hypertens Res. 35(1):48-54. doi: 10.1038/hr.2011.140

Guo Q., Mori T., Jiang Y., Hu C., Osaki Y., Yoneki Y., Sun Y., Hosoya T., Kawamata A., Ogawa S., Nakayama M., Miyata T., Ito S. (2009) Methylglyoxal contributes to the development of insulin resistance and salt sensitivity in Sprague-Dawley rats. J Hypertens. 27(8):1664-71. doi: 10.1097/HJH.0b013e32832c419a

He M.M., Clugston S.L., Honek J.F., Matthews B.W. (2000) Determination of the structure of Escherichia coli glyoxalase I suggests a structural basis for differential metal activation. Biochemistry. 39(30):8719-27. DOI: 10.1021/bi000856g

Igor A., Mireille B. and Pierre J. Magistretti (2015) Methylglyoxal, the dark side of glycolysis Front. Neurosci. https://doi.org/10.3389/fnins.2015.00023

Jack M.M. and Wright D.E. (2012) The Role of Advanced Glycation End products and Glyoxalase I in Diabetic Peripheral Sensory Neuropathy Transl Res. 159(5): 355–365 doi: 10.1016/j.trsl.2011.12.004

Jia X., Wu L. (2007) Accumulation of endogenous methylglyoxal impaired insulin signalling in adipose tissue of fructose-fed rats. Mol Cell Biochem. 306(1-2):133-9. Epub Jul 28. DOI:10.1007/s11010-007-9563-x

Bibliography

Kalapos M.P. (1999) Methylglyoxal in living organisms: chemistry, biochemistry, toxicology and biological implications. Toxicol Lett. 110(3):145-75. https://doi.org/10.1016/S0378-4274(99)00160-5

Lyles G.A., Chalmers J. (1992) The metabolism of aminoacetone to methylglyoxal by semicarbazide-sensitive amine oxidase in human umbilical artery. Biochemical Pharmacology Volume 43, Issue 7, 1 April, Pages 1409-1414 https://doi.org/10.1016/0006-2952(92)90196-P

Maessen D.E., Stehouwer C.D., Schalkwijk C.G. (2015) The role of methylglyoxal and the glyoxalase system in diabetes and other age-related diseases. Clin Sci (Lond). Jun;128(12):839-61. doi: 10.1042/CS20140683

Mukohda M., Okada M., Hara Y., Yamawaki H. (2012) Methylglyoxal accumulation in arterial walls causes vascular contractile dysfunction in spontaneously hypertensive rats. J Pharmacol Sci. 2012;120(1):26-35

Natali A., Taddei S., Quinones G. A., Camastra S., Baldi S., Frascerra S., et al. (1997) Insulin sensitivity, vascular reactivity, and clamp-induced vasodilatation in essential hypertension. Circulation 96(3):849–855

Nigro C., Leone A., Raciti G.A., Longo M., Mirra P., Formisano P., Beguinot F., Miele C. (2017) Methylglyoxal-Glyoxalase 1 Balance: The Root of Vascular Damage. Review. Int J Mol Sci doi: 10.3390/ijms18010188

Nigro C., Raciti G.A., Leone A.., Fleming TH., Longo M,.. Prevenzano I., Fiory F., Mirra P., D'Esposito V., Ulianich L., Nawroth P.P., Formisano P., Beguinot F., Miele C. (2014) Methylglyoxal impairs endothelial insulin sensitivity both in vitro and in vivo. Diabetologia. 57(7):1485-94. doi: 10.1007/s00125-014-3243-7

Queisser M.A., Yao D., Geisler S. et al (2010) Hyperglycemia impairs proteasome function by methylglyoxal. Diabetes 59:670–67. doi: 10.2337/db08-1565

Rabbani N., Thornalley P.J. (2011) Glyoxalase in diabetes, obesity and related disorders. Semin Cell Dev Biol. May;22(3):309-17. doi: 10.1016/j.semcdb.2011.02.015

Rabbani N., Thornalley P.J. (2014) The critical role of methylglyoxal and glyoxalase 1 in diabetic nephropathy. 63(1):50-2. DOI: 10.2337/db13-1606

Rabbani N., Xue M., Thornalley P.J.(2016) Dicarbonyls and glyoxalase in disease mechanisms and clinical therapeutics. Glycoconj J. 33(4):513-25. doi: 10.1007/s10719-016-9705-z

Ranganathan S., Ciaccio P. J., Walsh E. S., Tew K. D. (1999) Genomic sequence of human glyoxalase-I: analysis of promoter activity and its regulation. Gene Volume 240, Issue 1, Pages 149-155 https://doi.org/10.1016/S0378-1119(99)00420-5

Rodrigues L., Matafome P., Crisóstomo J., Santos-Silva D., Sena C., Pereira P., Seiça R. (2014) Advanced glycation end products and diabetic nephropathy: a comparative study using diabetic and normal rats with methylglyoxal-induced glycation. J Physiol Biochem.70(1):173-84. doi: 10.1007/s13105-013-0291-2

Rosca M.G., Monnier V.M., Szweda L.I., Weiss M.F.(2002) Alterations in renal mitochondrial respiration in response to the reactive oxoaldehyde methylglyoxal. Am J Physiol Renal Physiol. 283(1):F52-9 DOI: 10.1152/ajprenal.00302.2001

Sánchez-Lozada L.G., Tapia E., Jiménez A., Bautista P., Cristóbal M., Nepomuceno T., Soto V., Avila-Casado C., Nakagawa T., Johnson R.J., Herrera-Acosta J., Franco M. (2007) Fructose-induced metabolic syndrome is associated with glomerular hypertension and renal microvascular damage in rats. Am J Physiol Renal Physiol. 292(1): F423-9. DOI: 10.1152/ajprenal.00124.2006

Schalkwijk C.G, Stehouwer C.D. (2005) Vascular complications in diabetes mellitus: the role of endothelial dysfunction. Clin Sci (Lond) 109(2):143-59DOI: 10.1042/CS20050025

Schalkwijk C.G., Vermeer M.A., Stehouwer C.D,. te Koppele J., Princen H.M., van Hinsbergh V.W .(1998) Effect of methylglyoxal on the physico-chemical and biological properties of low-density lipoprotein.Biochim Biophys Acta. ;1394(2-3):187-98. https://doi.org/10.1016/S0005-2760(98)00112-X

Sena C.M, Matafome P., Crisóstomo J., Rodrigues L., Fernandes R., Pereira P., Seiça RM. (2012) Methylglyoxal promotes oxidative stress and endothelial dysfunction. Pharmacol Res. 65(5):497-506. doi: 10.1016/j.phrs.2012.03.004

Sena C.M., Pereira A.M., Seiça R. (2013) Endothelial dysfunction - a major mediator of diabetic vascular disease. Biochim Biophys ActaDec 1832(12):2216-31doi: 10.1016/j.bbadis.2013.08.006

Shamsaldeen Y.A., Mackenzie L.S., Lione L.A., Benham C.D. (2016) Methylglyoxal, A Metabolite Increased in Diabetes is Associated with Insulin Resistance, Vascular Dysfunction and Neuropathies. Curr Drug Metab.;17(4):359-67

Sousa S. M, Gomes R.A., Ferreira A.E., Ponces Freire A., Cordeiro C. (2013) The glyoxalase pathway: the first hundred years….and beyond. Biochem J. 453(1):1-15 doi: 10.1042/BJ20121743

Su Y., Qadri S.M.., Hossain M, Wu L., Liu L. (2013) Uncoupling of eNOS contributes to redox-sensitive leukocyte recruitment and microvascular leakage elicited by methylglyoxal. Biochem Pharmacol. 86(12):1762-74. doi: 10.1016/j.bcp.2013.10.008

Taddei S., Ghiadoni L., Virdis A., Versari D., Salvetti A. (2003) Mechanisms of Endothelial Dysfunction: Clinical Significance and Preventive Non-

Pharmacological Therapeutic StrategiesCurrent Pharmaceutical Design Volume 9, Issue 29 DOI: 10.2174/1381612033453866

Thilavech T., Abeywardena M. Y., Adams M., Dallimore J., Adisakwattana S. (2017) Naturally occurring anthocyanin cyanidin-3-rutinoside possesses inherent vasorelaxant actions and prevents methylglyoxal-induced vascular dysfunction in rat aorta and mesenteric arterial bed. Biomedicine and pharmacotherapy volume 95, pages 1251-1259 Doi: 10.1016/j.biopha.2017.09.053

Thornalley P. J., Langborg A., Minhas H. S. (1999) Formation of glyoxal, methylglyoxal and 3-deoxyglucosone in the glycation of proteins by glucose. Biochemical Journal Nov 08, ,344(1)109-116; DOI: 10.1042/bj3440109

Thornalley P.J. (1993) The glyoxalase system in health and disease. Molecular Aspects of Medicine Volume 14, Issue 4, Pages 287-371. https://doi.org/10.1016/0098-2997(93)90002-U

Turk Z., Čavlović-Naglića M., Turk Nikša (2011) Relationship of methylglyoxal-adduct biogenesis to LDL and triglyceride levels in diabetics Turk Life Sciences Volume 89, Issues 13–14, 26 Pages 485-490 https://doi.org/10.1016/j.lfs.2011.07.021

Turkseven S., Ertuna E., Yetik-Anacak G., Yasa M. (2014) Methylglyoxal causes endothelial dysfunction: the role of endothelial nitric oxide synthase and AMP-activated protein kinase α. J Basic Clin Physiol Pharmacol. (1):109-15. doi: 10.1515/jbcpp-2013-0095

Vasdev S., Ford CA.., Longerich L., Parai S., Gadag V., Wadhawan S. (1998) Aldehyde induced hypertension in rats: prevention by N-acetyl cysteine. Artery 1998;23(1):10-36

Wang X., Chang T., Jiang B., Kaushik D., Wu L. (2007) Attenuation of hypertension development by aminoguanidine in spontaneously

hypertensive rats: role of methylglyoxal. Am J Hypertens. 20(6):629-36. DOI:10.1016/j.amjhyper.2006.12.003

Wang X., Desai K., Clausen J. T., and Wu L. (2004) Increased methylglyoxal and advanced glycation end products in kidney from spontaneously hypertensive rats. Kidney International, Vol. 66, pp. 2315–2321 https://doi.org/10.1111/j.1523-1755.2004.66034.x

Wang X., Jia X., Chang T., Kaushik D., Wu L. (2008) Attenuation of hypertension development by scavenging methylglyoxal in fructose-treated rats Journal of Hypertension volume 26 - Issue 4 p 765–772. doi: 10.1097/HJH.0b013e3282f4a13c

Wang X., Kaushik D., Chang T.; Wu L.(2005) Vascular methylglyoxal metabolism and the development of hypertension Journal of Hypertension: Volume 23 - Issue 8 - p 1565–1573 doi: 10.1097/01.hjh.0000173778.85233.1b

Wu L., Juurlink B.H. Hypertension. (2002) Increased methylglyoxal and oxidative stress in hypertensive rat vascular smooth muscle cells. 39(3):809-14

Yao D., Taguchi T., Matsumura T., Pestell R., Edelstein D., Giardino I., Suske G., Rabbani N., Thornalley P. J., Sarthy V. P., Hammes H.Peter and Brownlee M. (2007) High Glucose Increases Angiopoietin-2 Transcription in Microvascular Endothelial Cells Through Methylglyoxal Modification of mSin3A. The Journal of Biological Chemistry 282, 31038-31045. http://www.jbc.org/cgi/doi/10.1074/jbc.M704703200

Chapter 1

Effect of glyoxalase 1 gene deletion on glucose homeostasis and vascular function in mice

Nigro C., Leone A., Longo M., **Prevenzano I**., Fleming T.H., Nicolò A., Parrillo L., Spinelli R., Formisano P., Nawroth P.P., Beguinot F., Miele C. (2018) Methylglyoxal accumulation de-regulates HoxA5 expression, thereby impairing angiogenesis in glyoxalase 1 knock-down mouse aortic endothelial cells. Biochim Biophys Acta Mol Basis Dis. pii: S0925-4439(18)30391-0. doi: 10.1016/j.bbadis.2018.10.014.

1.1 Risk factors for the development of complications in DM

Beyond the classification of DM, the presence of chronically elevated blood glucose levels is implicated in the progression of diabetes complications. For this reason, the primary goal of therapeutic treatment is to reduce hyperglycemia. Nonetheless, while most of the literature claims the benefits of glycemic control in the prevention of vascular complications (Cefalu 2006), additional evidence suggests that the risk of complications may be decreased further if glycated hemoglobin (HbA1c) is reduced below levels currently accepted as clinical goal (Stratton et al. 2000). In support of this possibility, Khaw et al (2001) demonstrated that a reduced HbA1c level is associated with a lower rate of cardiovascular disease, even in non-diabetic subjects. At the same time a clinical study on HbA1c contribution to retinopathy in type 1 diabetic patients shows that lowering HbA1c levels is not enough to prevent the increased incidence of events in the long term (Lind et al. 2010). Moreover, it is known that as blood pressure levels increase in diabetics there is a parallel increase in cardiovascular disease, diabetic retinopathy and nephropathy (Rask-Madsen and King et al. 2013). Many studies have demonstrated clear benefits in lowering blood pressure. Indeed, in the UKPDS trial, tight blood pressure control with angiotensin-converting enzyme (ACE) inhibitors or -blockers significantly reduced diabetes-related events and diabetes-related deaths (U.K Prospective Diabetes Study Group 1998, Katherine L Bate and George Jerums 2003). In addition, other studies demonstrated that it is important to control also the levels of dyslipidemia to reduce the risk of development of diabetic complications. Indeed, two placebo-controlled trials have shown that treatment with statins reduces the risk of a major cardiovascular event by 37% in patients with type 2 diabetes without clinically apparent cardiovascular disease (Heart Protection Study Collaborative Group. 2002, Colhoun et al. 2004, Marshall and Flyvbjerg 2006). A recent study found that the risk of diabetic complication can be reduced through a multifactorial approach, for example reducing the smoke or administration the low-dose of aspirin (Marshall and Flyvbjerg 2006). Therefore, all these studies suggest that other risk factors besides poor glycaemia control may be important for the onset of vascular complications (Bots et al. 2016).

1.2 Rodent Models of DM and its related complications

Studies in animal models have provided significant advances to the knowledge of cardiovascular complications in understanding to which extent insulin resistance, hyperinsulinemia and hyperglycemia may individually contribute to vascular and cardiac dysfunction in diabetes. Among the commonly used models, the ob/ob mouse is a diabetic animal with genetic mutations on the leptin gene. As a consequence of this defect, ob/ob mice develop hyperphagia and obesity, reduced glucose tolerance, severe hyperinsulinemia, insulin resistance and impaired would healing (Potenza et al. 2011). The db/db mice, carrying a mutation on the gene encoding for the leptin receptor in C57b/KsJ strain, show hyperphagia, obesity and early insulin resistance. This model rapidly develop hyperglycemia, diabetic nephropathy and ketosis as their β-cells are unable to maintain high levels of insulin secretion required for survival (Maessen et al. 2015).

In addition, several diabetic models have been utilized to understand the relationship between metabolic control and cardiovascular health. eNOS KO/lepr (db/db) double knockout (DKO) mice develop obesity, hyperglycemia and also hypertension (Potenza et al. 2011). The cp-cp (ceruloplasmin) rats spontaneously develop the pathophysiological characteristic resembling the human metabolic syndrome, for this reason are use as model of diabetes. In detail the cp/cp rats are homozygous for autosomal recessive cp gene and develop atherosclerosis, ischemic myocardial lesions and microvascular renal dysfunction not accompanied by hypertension (Russell et al. 1998). The GK rats show neonatal β-cell mass deficiency, which is responsible for the basal hyperglycemia. Indeed, at 8 weeks of age, sustained hyperglycemia is accompanied by both severely impaired insulin release and insulin resistance (Miralles and Portha 2001). This animal model exhibits endothelial dysfunction as early as 4 months of age and has provided important informations on the relationship between changes in β cells mass and the occurrence of diabetic vascular complications.

Moreover, also the Zucker Diabetic Fatty (ZDF) rats, selectively inbred for hyperglycemia, can be placed in this category. Indeed, at 10 weeks of age, ZDF rats show more than a 4-fold increase in blood glucose levels that

remain high throughout their entire lifespan. They show coronary and aortic endothelial dysfunction that are involved in atherogenesis and vascular alterations occurring in this model (Otlam et al. 2008, Chinen et al. 2007).
SHR rapresent a genetic model of hypertension, in which the defects in endothelial insulin signalling with impaired PI3-Kinase-dependent and augmented MAPK-dependent activities precede several disturbances of the metabolic syndrome (Potenza et al. 2005). For this reason, they are used in the studies of endothelial function.
Further rodent models have been generated to study the role of insulin-signalling mediators in the pathogenesis of DM. In detail, the deletion of IRS-1 in the IRSKO mouse (IRS-1 KO) leads to β-cell hyperplasia and insulin resistance, mainly localized to skeletal muscle tissue. Hypertension onset, secondary to impaired endothelium-dependent relaxation, and hypertriglyceridemia development, secondary to impaired activation of lipoprotein lipase in insulin resistant adipose tissue, have been observed in these mice. Akt2 knockout in mice results in glucose intolerance, hyperinsulinemia, insulin resistance and, under some conditions, overt diabetes. Akt 2 is predominantly expressed in pancreatic β-cells, skeletal muscle and brawn fat, but also in platelets. Indeed, Akt2 knockout mice (Akt 2 KO) display defects in platelet aggregation and thrombus formation (Woulfe et al. 2004). Moreover, liver-specific insulin receptor knockout (LIRKO) mice exhibit a dramatic elevation in blood glucose and the loss of gluconeogenesis regulation. It has been demonstrated that LIRKO mice show marked hypercholesterolemia and develop severe atherosclerosis at 12 weeks, when fed with atherogenic diet (Biddinger et al. 2011).
In the absence of appropriate diabetic/atherosclerotic models, exposure to chemicals (e.g streptozotocin) as well as to diabetogenic or atherogenic diets has been used to evaluate the impact of hyperglycemia, obesity, insulin resistance and hypercholesterolemia on vascular complication development in wild type and genetically modified rodents (Potenza et al. 2011). Schreyer et al. have demonstrated the atherogenic diet containing 1.25% cholesterol, 15% fat, and 0.5% cholic acid induces atherosclerosis. Moreover, also a diabetogenic diet containing 35.5% fat (58% of calories, primarily lard) and 36.6% carbohydrate (primarily sucrose)) may induce vascular lesions by altering both lipid and glucose metabolism, while a high fat/high sucrose diet used to induce obesity and diabetes in C57BL/6 mice, may provide an

important tool for the study of diabetes accelerated atherosclerosis (Schreyer et al. 1998). In rats the administration of streptozotocin (STZ), after a primary administration of nicotinamide adenine dinucleotide (NAD), produces a T2DM model at a rate of 75-80%, which develops a mild and stable hyperglycemia without changes in plasma insulin (Masiello P. et al. 1998). Combination of STZ administration in animals with a genetic insulin resistant background (e.g. in ZFR model) or under a high fat or high fructose diet produces models that develop overt hyperglycemia in the presence of normal blood insulin and, hence, are regarded as more appropriate for T2DM studies (Chatzigeorgiou et al. 2009). Moreover, other studies have shown that the long-term administration of diets containing front 40% to 60% of lipids promotes metabolic disorders in animal models (Flanagan et al., 2008); and induces adipocyte hypertrophy (Barbosa-da-Silva et al. 2012), T2DM, hypertriglyceridemia (Fraulob et al. 2010) and liver steatosis in mice (Aguila et al. 2003, Barbosa-da-Silva et al. 2013).
Therefore, the use of the appropriate animal models can provide interesting data needed to clarify the pathophysiological mechanisms responsible for the onset of diabetic complications.

1.2.1 Mouse models of MGO accumulation

To prove the effect of MGO on vascular function, animal models that allow to observe the systemic implications of an imbalanced accumulation/detoxification ratio of MGO have been generated. Among these, the chronic administration of a MGO solution has been performed in rodents in many studies. Dhar et al (2011) have been demonstrated that chronic MGO infusion by minipumps causes pancreatic β-cell dysfunction and induces DM in Sprague-Dawley rats. Others have been demonstrated that high MGO levels induce vascular contractile dysfunction in arterial wall of SHR (Mukohda et al. 2012). We have previously demonstrated that intraperitoneal administration of MGO to C57BL/6 mice impairs whole-body insulin sensitivity and induced endothelial insulin resistance (Nigro et al. 2014). However, it is important to note that exogenous sources of MGO are only partially absorbed and not completely accumulated in tissues as free MGO, thus limiting the interpretation of these studies. The measurement of tissue and plasma levels of MGO in experimental models is, therefore,

necessary to ensure the patho-physiological relevance of the animal models. To bypass these limitations, a possibility is to modulate Glo1 activity and/or its expression. Indeed, MGO accumulation may be induced by reducing Glo1 activity, through the chemical Glo1 inhibitor "SpBrBzGSHCp2" or silencing Glo1 expression (Nigro et al. 2017). Interestingly, it has been shown that non-diabetic mice knock-down for Glo1 (Glo1 KD) expression show an increase of MGO modified proteins and oxidative stress, causing alteration in kidney indistinguishable from those caused by diabetes (Giacco et al. 2014). Bierhaus et al (2012) demonstrated that this mouse model develops the thermal and medical hyperalgesia, signs of peripheral neuropathy. Moreover, the beneficial effect of MGO detoxification have been proved by studies using Glo1 overexpressing models. Interestingly, Glo1 over-expression in STZ-induced diabetic mice prevents diabetes-induced oxidative stress and the development of kidney pathology, despite unchanged levels of diabetic hyperglycemia (Giacco et al. 2014). Moreover, Glo1 overexpression ameliorates renal ischemia-reperfusion injury (Kumagai et al. 2009), reduces endothelial dysfunction and attenuates early renal impairment in rat model of diabetes (Brouwers et al. 2014).

This is in line with a recent clinical study reporting that pharmacological induction of Glo1 activity improves insulin sensitivity and glycemic control in obese patients (Xue et al. 2016). Furthermore, Glo1 has been linked to coronary artery disease (Makinen et al. 2014) and hypertension (Wilson et al. 1991) in epidemiological studies. A recent study obtained in Glo1-tg mice has shown that Glo1 overexpression is able to prevent the MGO-mediate increase of inflammation in diabetes, which leads to endothelial cell loss and, contributes to the development of diabetic cardiomyopathy (Vulesevic et al. 2016). Moreover, the overexpression of Glo1 reduces age-related glycative and oxidative stress in the vasculature and attenuates endothelial dysfunction through the modulation of eNOS phosphorylation from early aging. This proves that the regulation of glycative stress by enhanced Glo 1 activity counteracts physiological vascular aging. Therefore, the regulation of glycative stress may represent a versatile target for the prevention of vascular aging and its associated complications (Jo-Watanabe et al. 2014, Nigro et al. 2017).

1.3 Aim

DM is a common metabolic disorder that is strongly associated with vascular complications. Several studies demonstrated that diabetes is linked to macro- and microvascular complications, which are responsible for high mortality and morbidity of the disease. For this reason, it is considered an important public health problem.

Hyperglycemia represents the main feature of DM and one of the major cause of plasma and intracellular MGO accumulation. In physiological conditions, MGO is efficiently detoxified by the glyoxalase system, however its levels increase under pathological conditions, such as hyperglycemia contributing to cardiovascular complication associated with diabetes. Indeed, several studies carried out in models of hyperglycemia have proved the toxic effect of MGO and its derived AGEs on micro and macrovascular function (Chinen et al. 2013), on insulin sensitivity of muscle, adipose tissue and β-cells. However, the specific effect of a physiological accumulation of the MGO a tissue damage has not been yet clarified. To this aim, it is necessary to use an optimal experimental model to investigate the pathological processes by which MGO favors the onset of DM and its associated complication.

This work aims to investigate the impact of endogenous MGO accumulation on metabolic and vascular functions in Glo1-knockdown mice ($Glo1^{KD}$).

1.4 Results

1.4.1 Metabolic characterization of Glo1^{KD} mice

Glo1^{KD} mice and their wild type littermates (WT mice) were used to evaluate the effect of MGO accumulation on glucose tolerance. In order to validate this experimental model, the first step was to evalaute the Glo1 expression in different tissues by Real Time-PCR. As expected, Glo1^{KD} mice show a significant reduction in tissue expression of the Glo1 gene compared to WT mice (Figure 1.1A). In detail, the absolute quantification revealed that Glo1^{KD} mRNA levels are reduced from 30% to 50% in vascular tissue, skeletral muscle and adipose tissue isolated from Glo1^{KD} mice compared to WT mice. To test if the partial deletion of Glo1 expression was enough to induce MGO accumulation, endogenous MGO levels were measuread by HPLC and resulted to be increased by 1.5-fold in the serum from Glo1 ^{KD} mice compared to WT mice (figure 1.1 b).

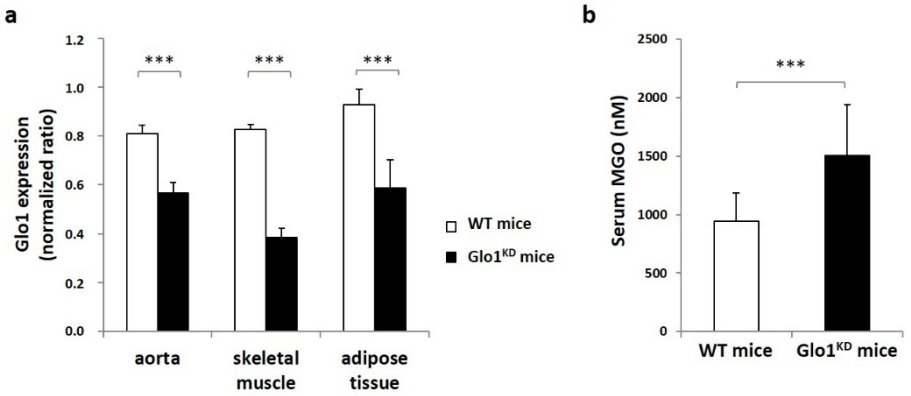

Figure 1.1 Expression levels of the Glo1 gene and serum MGO concentration. *(a) The expression of Glo1 gene was measured in aorta, muscle (quadriceps) and adipose tissue (epididymal fat) of Glo1^{KD} and WT mice. Glo1 expression was normalized on the number of GAPDH molecules, used as a housekeeping gene. (b) Serum MGO concentrations were measured by HPLC. Statistical analysis was performed by Student t-test, where $p \leq 0.05$ was considered statistically significant (*** $p \leq 0.001$).*

Metabolic characterization of Glo1^{KD} mice have been evaluated during lifespan. As shown in table 1.1, the data obtained indicate that Glo1^{KD} mice show no significant variation in body weight, food intake, fasting and fed glycaemia neither at 5 nor at 10 months of age, indicating that Glo1^{KD} mice are normoglycemic and, thus, do not display a diabetic phenotype. Glucose levels have been measured during intraperitoneal Glucose Tolerance Tests (ipGTT) in order to evaluate the ability of the mouse to restore glucose levels at normal values after a bolus of glucose.

Table 1.1. Metabolic parameters

	5 months			10 months		
Variable	**WT mice**	**Glo1^{KD} mice**	**Test T**	**WT mice**	**Glo1^{KD} mice**	**Test-T**
Body weight (g)	25.4±0.8	24.5±0.7	n.s.	32.6±1.5	35.1±1.8	n.s.
Fold intake	2.99±0.04	2.9±0.13	n.s	-	-	n.s
Fasting glycaemia (mg/dl)	105.9±5.3	97.1±3.5	n.s.	114.6±8.4	106.4±6.0	n.s
Fed glycaemia (mg/dl)	138.9±4.1	145.6±6.9	n.s.	143.6±3.1	137.3±4.4	n.s.

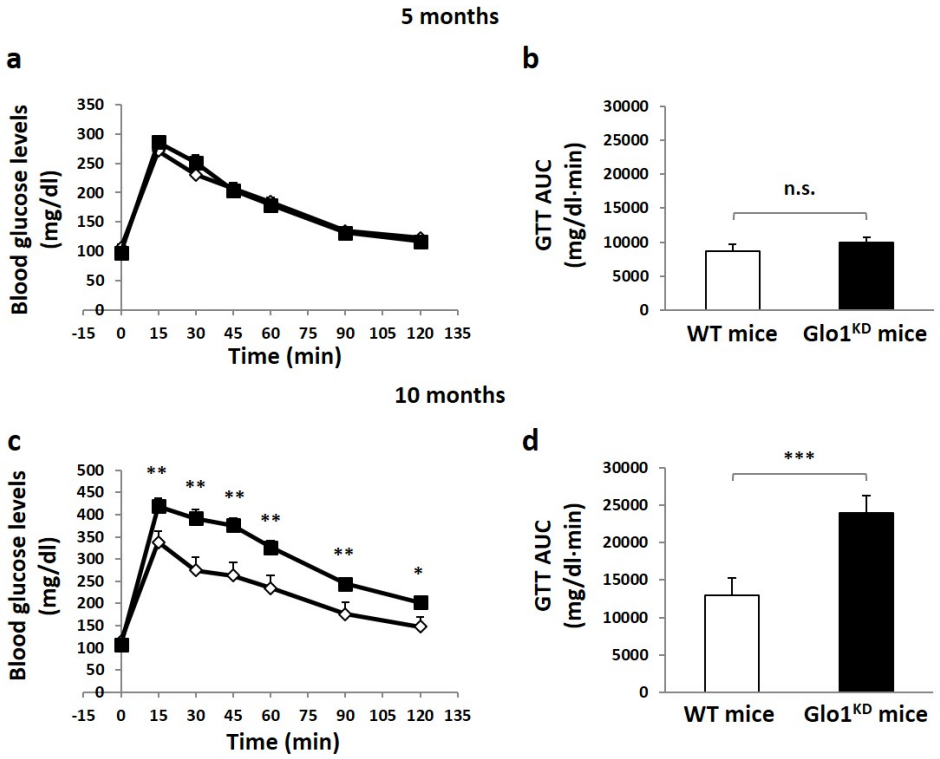

Figure 1.2 Glucose Tolerance Test (ipGTT). *(a, c) The graph shows the curves related to blood glucose levels of WT mice and Glo^{KD} mice within 2 hours after intraperitoneal administration of a glucose bolus (2 g / kg) at 5 and 10 months. Blood glucose was measured by the use of a portable blood glucometer at the indicated times. (b, d) The bars of the graph analyze the area under the glucose curve of Glo1^{KD} and WT mice. Statistical analysis was performed by Student's t-test (* p≤0.05; ** p≤0.01; *** p≤0.001).*

No differences in glucose tolerance have been revealed at 5 months of age. By contrast, Glo1^{KD} mice develop a reduced glucose tolerance at 10 months of age, compared to WT mice. This is indicated by both the calculation of the area under curve (WT 12990±1595 vs KD 23944±2300) and by the single time points of glucose measurements performed during the entire test, when from 15 to 120 minutes following glucose bolus, blood glucose levels are higher in Glo1 ^{KD} mice compared to WT mice (figure 1.2 c).

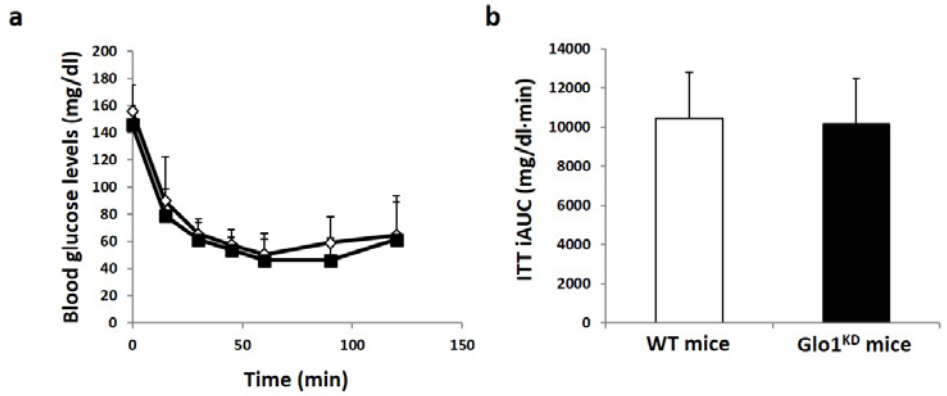

Figure 1.3 Insulin tolerance test (ipITT)
(a) The graph shows the curves related to blood glucose levels of WT mice and Glo^{KD} mice within 2 hours after intraperitoneal administration of a insulin (0,75 U/kg). Blood glucose was measured by the use of a portable blood glucometer at the indicated times. (b) The bars of the graph analyze the area under the glucose curve of Glo1^{KD} and WT mice. Statistical analysis was performed by Student's t-test (p≤0.05; ** p≤0.01; *** p≤0.001).*

Next, insulin sensitivity has been evaluated by means of the insulin tolerance test (ITT). The data obtained show that insulin sensitivity is not affected in Glo1KD mice compared to WT mice (figure 1.3). In light of the impairment of glucose tolerance pancreatic function has been tested by glucose-stimulated insulin secretion (GSIS).

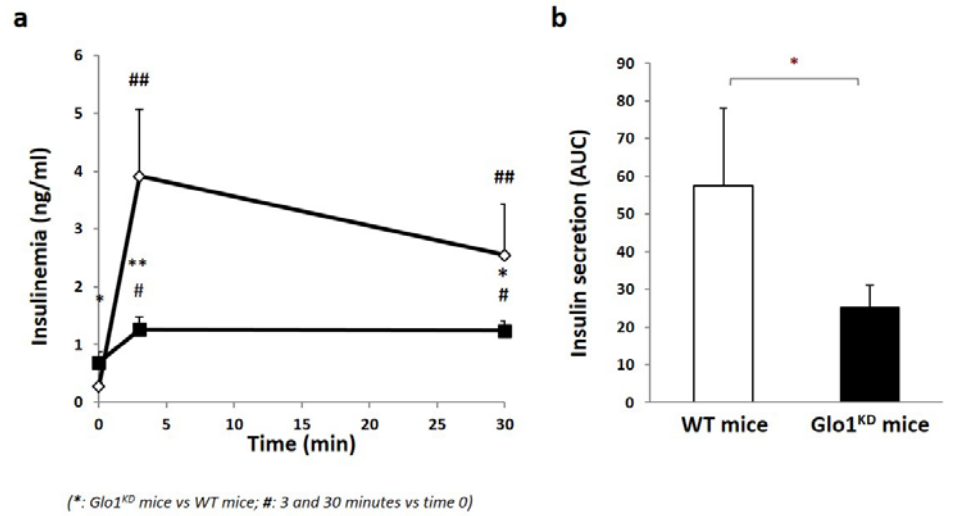

Figure 1.4 Glucose-stimulated insulin secretion (GSIS) and fasting insulinemia *(A) The graph shows the fasting insulinemia values at 3 minutes and 5 minutes after administration of an intraperitoneal glucose (3 g / kg) in Glo1^{KD} and WT mice. Insulin values were measured in serum by RIA test. (B) The bars in the graph represent the calculation of the area under the curve of my insulin values obtained during the insulin secretion test. Statistical analysis was performed by Student's t-test (Glo1^{KD} vs WT mice: * p ≤0.05; ** p≤0.01; 3 and 30 minutes vs. time 0: #p≤0.05; # #p≤0.01)*

The insulin plasma levels have been measured in the fasted state and after 3 and 30 minutes following glucose administration (3 g / kg). As shown in the panel a, the Glo1^{KD} mice have a higher fasting insulinema (KD 0.69±0.18 VS 0.28±0.05 WT) with a reduction in insulin secretion in response to glucose compared to WT mice. Panel b shows the values of the area under the curves of insulinemia levels measured during the GISIS test.

1.4.2 Vascular function of Glo1^{KD} mice

Another objective of this study was to investigate the effect of the inhibition of Glo1 on vascular function of Glo1^{KD} mice and, therefore, on the development of complications associated with diabetes.
Systolic blood pressure was measured during lifespan (at 5, 10 and 15 months of age) and the recorded data show that it is higher in Glo 1^{KD} mice compared to WT mice (figure 1.5), already at 5 months of age, anticipating the physiological increase in blood pressure ad observed in WT mice at the age of 15 months.

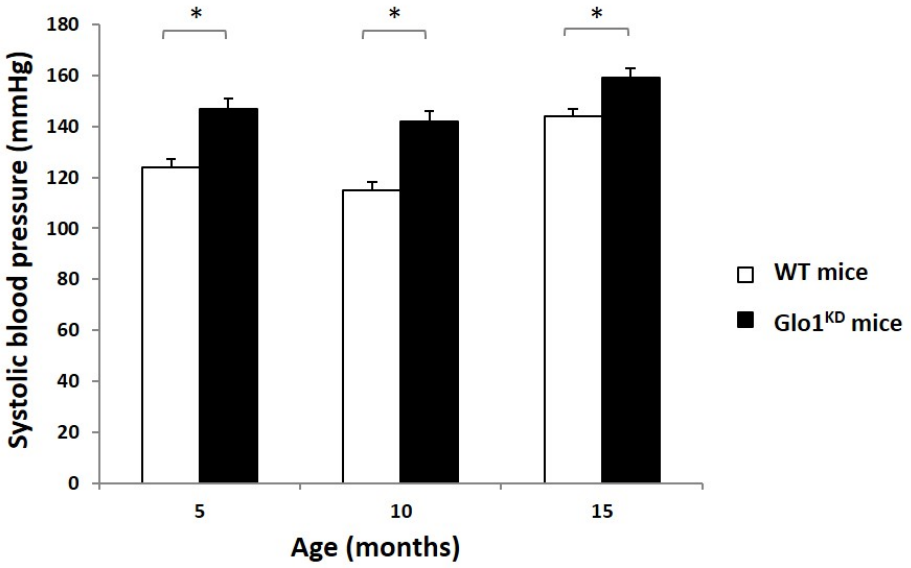

Figure 1.5. Measurement of systolic blood pressure. *Systolic blood pressure is measured in Glo1^{KD} and WT mice by the method CODA. Systolic blood pressure is expressed in mmHg. Statistical analysis was performed using the t-Student * p ≤0.5 and ** p≤0.01 test*

As determination factor in raising blood pressure, vascular resistance was also evaluated. To this aim, the vasodilatory response to increasing concentration of acetylcholine was measured *ex vivo* in the aortae isolated from WT and Glo1^{KD} mice. As shown in the figure 1., the percentage of

residual vasoconstriction, used as a measure of vessel vasodilation, is significantly higher in Glo1^{KD} mice compared to WT mice at 10 months of age. Preliminary data indicate that an impaired endothelial-dependent vasodilation is already observed at 5 months of age in Glo1^{KD} mice, while the same values of residual vasoconstriction is reached by the 2 groups of mice at 18 months (data not shown), suggesting that Glo1 ^{KD} mice anticipate an impairment of vasodilation which is physiologically developed by WT mice with age.

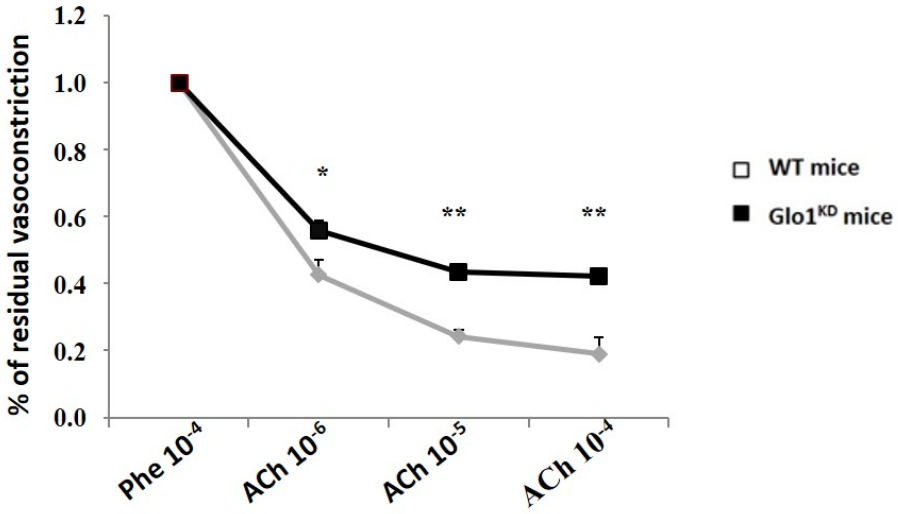

Figure 1.6. Measurement of endothelium-dependent vasodilation. *The % of residual vasoconstriction after vasoconstrictive stimulation (phenylpinephrine) was measured by the detection of vascular tension following stimulation with increasing concentrations of the acetylcholine vasodilator. Statistical analysis was performed using the t-Student * p ≤0.5 and ** p≤0.01 test*

1.5 Discussion

It is known that MGO is increased from 2 to 5- fold in diabetic patients as a consequence of the imbalance between the generation of/exposure to MGO and the impaired activity of its detoxification enzyme, specifically the glyoxalase system (Rabbani and Thornelly 2016). Indeed, MGO accumulation may be the result of the reduced expression or activity of the rate limiting enzyme Glo1 (Maessen et al. 2015). Several studies have demonstrated an association between high MGO and its derived AGEs levels and the increased risk of micro and macrovascular complications (Bourajjai et al 2003). Moreover, a GWAS study identified the decreased Glo1 expression as a driver of coronary artery disease (Makinen et al. 2014). Although chronic hyperglycemia seems to be the leading cause of MGO accumulation, it has also been demonstrated that reducing HbA1c to normal levels, in diabetic patients is not sufficient to prevent the onset of vascular events (Lind et al. 2010), suggesting that hyperglycemia itself is not the only driver of tissue dysfunction and complications progression in diabetes. Moreover, even if normalized on glucose levels, intracellular MGO is higher in diabetic patients (Fleming et al. 2012). Therefore, despite the progress made in the recent years in this field, further research is needed to pinpoint the role played by MGO in the development and progression of DM. To this aim, a promising contribution may be provided by the use of experimental models accumulating MGO. Our previous studies demonstrated that MGO impairs insulin sensitivity by changing the balance of NO and ET-1 release (Nigro 2014). In the chapter 2 of this thesis I have reported our new data showing that MGO induced down-regulation of miR-190a and miR-214 plays a role in endothelial insulin resistance (Mirra et al 2017, Nigro et al. 2018). In this part of the study, we sought to investigate the effect of MGO on glucose homeostasis and vascular function *in vivo*, by the use of a mouse model with a partial deletion of Glo1 gene. The partial reduction of Glo1 expression is associated to 1.5-fold increased levels of MGO in $Glo1^{KD}$ mice. The intracellular accumulation of MGO has been demonstrated by our previous work in $Glo1^{KD}$ MAECs (Nigro et al. 2018) and by Morgenstern et al. in murine Schwann cells ($Glo1^{KO}$) (2016). In line with data obtained by Wortman et al. (2016) in $Glo1^{KD}$ mice, we have not observed significant variation in body weight and food intake. Moreover, fasting and random-fed glycemia in $Glo1^{KD}$ mice is not higher than in WT littermates. Nevertheless,

a glucose intolerance has developed by Glo1^{KD} mice at 10 months. These results suggest the possibility that a reduced insulin sensitivity of target tissues, or an insufficient production of insulin after glucose loading, could be responsible for the phenotype observed. Indeed, data in literature demonstrate that hyperglycemia- dependent MGO accumulation in GK rats associate with peripheral insulin resistance and impaired insulin secretion (Matafone et al. 2011). However, Glo1^{KD} mice do not show systemic insulin resistance as indicated by ITT performed both at 5 and 10 months of age. Conversely, they are characterized by an impaired glucose-stimulated insulin secretion with a basal hyperinsulinemia, compared to WT mice. This important finding is in line with previous research performed by our group demonstrating how MGO impairs GISIS in both INS1-E cells and isolated islets from mice (Fiory et al. 2011). All these data demonstrate for the first time that Glo1^{KD} mice develop an age-dependent glucose intolerance, in the absence of fasting hyperglycemia, and suggest that this is dependent on the impairment of β-cell function, rather than a peripheral insulin resistance. Marow et al. (2018) have very recently demonstrated that the elevation of MGO levels due to Glo1^{KO} in *Drosophila* induces obesity and hyperglycemia. We show here for the first time in a mammalian model that the partial impairment of MGO detoxification system is enough to recapitulate several of the metabolic phenotypes associated to T2DM. We and others have previously provided evidence that MGO accumulation and its derived adducts favor the onset of vascular complications (i.e nephropathy and peripheral neuropathy) in Glo1^{KD} mice and endothelial dysfunction in vitro (Nigro et al. 2014, Nigro et al. 2018). As two mutually related processes in the development of diabetes, together with glucose homeostasis, the hemodynamic function was evaluated in Glo1^{KD} mice, to test the specific contribution of MGO accumulation to the pathogenesis of the diabetes. Therefore, we investigated the effect of Glo1 inhibition on blood pressure, that is known to be increased in the rats with high MGO levels (Wang et al.2006, Maessen et al. 2015). The results show that Glo1^{KD} Glo1 down regulation is sufficient to increase pressure in Glo1^{KD} mice and also to impairs the endothelium-dependent vasodilation. Our hypothesis is that the latter may be the cause of peripheral vascular resistance leading to the increase in blood pressure. Moreover, Giacco et al. (2014) have demonstrated that early signs of kidney damage occur early in life of Glo1^{KD} mice. Differently from our evidence, these signs of nephropathy are not

accompanied by an increase in blood pressure in this paper (Giacco et al. 2014) However, it is important to note that blood pressure was recorded in a much lower age (8week) than in our work (5 months), therefore more than in 2 months of age are necessary, before hypertension is clinical evident in $Glo1^{KD}$ mice.

1.6 Conclusion

The data obtained by this study demonstrate that simply elevating the endogenous MGO levels, which could be due to either evaluated MGO production detoxification, could be the cause of many of the metabolic phenotypes observed in diabetic patients. This evidence places MGO not only downstream the impairment of the glucose metabolism, but also upstream of both glucose and vascular homeostasis, in term of the chain of causality. Therefore, the $Glo1^{KD}$ mouse appears to be a novel and good model for further investigations on the pathogenesis of DM and the development of novel pharmacological interventions to counteract diabetes complications.

1.7 Material and Methods

Mice

Glo1 knockdown mice (Glo 1 KD) were generated and characterized as previously described (Queisser et al. 2010, Bierhaus et al. 2012, Giacco et al. 2014). Mice were housed in a temperature-controlled (22 °C) room with a 12 h light/dark cycle, in accordance with the Guide for the Care and Use of Laboratory Animals published by the National Institutes of Health (publication no. 85-23, revised 1996), and experiments were approved by the ethics committee of the MIUR.

Measurement of MGO

MGO concentration was measured in the serum of WT and Glo1KD mice by HPLC after derivatization with 1,2-diamino-4,5-dimethoxybenzene as previously described (McLellan et al.1992).

Measurement of blood pressure by tail cuff methods

The blood pressure evaluation was performed using the tail-cuff system using the CODA 8-Channel High Throughput instrument. This system allows a non-invasive measurement of blood pressure in mice. The tail-cuff system uses the Volume Pressure Registration (VPR) to measure blood pressure by determining the volume of blood flowing into the tail. The animals, taken from the base of the tail, were placed in the restrainer. Subsequently, the tail that emerges from the restrainer has been connected to the tail-cuff and the VPR detection system for recording the blood pressure values. During the measurement, the body temperature of the animals was constantly monitored by infrared thermometer.

Reverse transcription and Real Time-PCR

RNA was isolated from aorta, skeletal muscle and adipose tissues using miRNeasy mini kit (QIAGEN) according to the manufacture's instructions. Reverse transcription of 1 μg of total RNA was performed using Super Script III (Life Technologies, Carlsbad, CA, USA), according to the

manufacturer's instructions. Quantitative real-time PCR was performed in triplicate by using iQ SYBR Green Super mix on iCycler Real-Time Detection System (Bio-Rad Laboratories, Hercules, CA, USA). The GAPDH gene was used as internal control and the results of Real time analysis are expressed as the ratio between the copy number variation (CNV) of Glo1 and that of the reference gene. Primer-Blast (http://www.ncbi.nlm.nih.gov/tools/primer-blast/) was used to design primers specific, which were then purchased from Sigma-Aldrich (St Louis, MO, USA). Primers used for real-time Real-time-PCR are as follow:

GAPDH	*Forward 5'-AAGGCGGGGGCCCACTTGAA-3'*
	Reverse 5'-TGGGTGGCAGTGATGGCATGG-3'
Glo1	*Forward 5'-CCCTCGTGGATTTGGTCACA-3'*
	Reverse 5'-AGCCGTCAGGGTCTTGAATG-3'

Glucose tolerance test (GTT)

Mice were fasted overnight. Glucose levels were determined at 0, 15, 30, 45, 60, 90, 120 min after the administration of a 20% w/vol D-glucose solution (2g/kg body weight) by intraperitoneal injection. Blood was obtained from the tail vein. Blood glucose was assessed using a the glucometer One Touch® Ultra Lifescan (Johnson & Johnson, Milpitas, Italy).

Insulin tolerance test (ITT)

Mice were fasted for 4 h, then they are injected with insulin. The human insulin used WAS injected at the concentration of 0.25 UI/kg (Actrapid®, Novo Nordisk, Boulogne-Billancourt, France). Blood samples were taken from mice tail and glycaemia was analyzed by using a glucose analyzer (LifeScan). Glucose levels were determined at the following time points: 0, 15, 30, 45, 60, 90, 120 min after insulin injection.

Glucose-Stimulated Insulin Secretion (GSIS)

Animals were intraperitoneally injected with 3g/kg body weight of glucose. In parallel, blood samples were taken from mice tail, to assess glycaemia, and from orbital sinus in order to collect large volumes of blood to further measure serum insulin. Blood samples were collected 0, 3, 30 min after glucose injection. Blood samples were centrifuged at 1500 rpm for 20 min at room temperature and serum collected. Insulin levels were measured with radioimmunoassay (RIA) kit (#RI-13K, Millipore), according to the manufacturer's protocol.

Statistic Procedures

Data are expressed as means ± SD, as indicated in figure legends. Comparison between groups was performed using Student's t-test. A p-value of less than 0.05 was considered statistically significant.

1.8 Bibliography

Aguila M. B., Pinheiro A. R., Parente L. B., Mandarimde-Lacerda C. A. (2003) Dietary effect of different high-fat diet on rat liver stereology. Liver Int., 23(5):363-70

Barbosa-da-Silva S., da Silva N. C., Aguila M. B., Mandarim- de-Lacerda C. A. (2013). Liver damage is not reversed during the lean period in diet-induced weight cycling in mice. Hepatol Res. doi:10.1111/hepr.12138

Barbosa-da-Silva S., Fraulob-Aquino J. C., Lopes J. R., Mandarim-de-Lacerda C. A., Aguila, M. B. (2012) Weight cyclingenhances adipose tissue inflammatory responses in male mice. PLoS One, 7(7): e39837

Bate K. L. and Jerums G. (2003) Preventing complications of diabetes Med J Aust; 179 (9): 498-503

Biddinger S.B., Hernandez-Ono A., Rask-Madsen C., Haas J.T., Alemán J.O., Suzuki R., Scapa E.F., Agarwal C., Carey M.C., Stephanopoulos G., Cohen D.E., King G.L., Ginsberg H.N., Kahn C.R. (2008) Hepatic insulin resistance is sufficient to produce dyslipidemia and susceptibility to atherosclerosis. Cell Metab.7(2):125-34. doi: 10.1016/j.cmet.2007.11.013

Bierhaus A., Fleming T., Stoyanov S., et al. (2012) Methylglyoxal modification of Nav1.8 facilitates nociceptive neuron firing and causes hyperalgesia in diabetic neuropathy. Nat Med. (6):926-33. doi: 10.1038/nm.2750

Bots Sophie H. , van der Graaf Y. , Nathoe Hendrik M. W. , Jan de Borst Gert, Kappelle Jaap L. , Visseren Frank L. J. , Westerink Jan , and on behalf of the SMART Study Group. (2016) The influence of baseline risk on the relation between HbA1c and risk for new cardiovascular events and mortality in patients with type 2 diabetes and symptomatic cardiovascular disease. Cardiovasc Diabetol. 15: 101 doi: 10.1186/s12933-016-0418-1

Bourajjaj M., Stehouwer C.D., van Hinsbergh V.W., Schalkwijk G. (2003) Role of methylglyoxal adducts in the development of vascular

complications in diabetes mellitus. Biochem Soc Trans. Dec;31(Pt 6):1400-2

Brouwers O., Niessen P.M., Miyata T., Østergaard J.A., Flyvbjerg A., Peutz-Kootstra C.J., Sieber J., Mundel P.H., Brownlee M., Janssen B.J., De Mey J.G., Stehouwer C.D., Schalkwijk C.G. (2014) Glyoxalase-1 overexpression reduces endothelial dysfunction and attenuates early renal impairment in a rat model of diabetes. Diabetologia. 57(1):224-35. doi: 10.1007/s00125-013-3088-5

Cefalu W.T. (2006) Animal models of type 2 diabetes: clinical presentation and pathophysiological relevance to the human condition. ILAR J.;47(3):186-98

Chatzigeorgiou A., Halapas A., Kalafatakis K., Kamper E. (2009) The use of animal models in the study of diabetes mellitus. In Vivo. (2):245-58

Chinen I., Shimabukuro M., Yamakawa K., Higa N., Matsuzaki T., Noguchi K., Ueda S., Sakanashi M., Takasu N. (2007) Vascular lipotoxicity: endothelial dysfunction via fatty-acid-induced reactive oxygen species overproduction in obese Zucker diabetic fatty rats. 148(1):160-5 DOI: 10.1210/en.2006-1132

Colhoun H.M, Betteridge D.J, Durrington P.N, et al (2004) Primary prevention of cardiovascular disease with atorvastatin in type 2 diabetes in the Collaborative Atorvastatin Diabetes Study (CARDS): multicentre randomised placebo-controlled trial Lancet 364: 685–96.DOI: 10.1016/S0140- 6736(04)16895-5

Dhar A, Dhar I, Jiang B, Desai KM, Wu L. (2011) Chronic methylglyoxal infusion by minipump causes pancreatic beta-cell dysfunction and induces type 2 diabetes in Sprague-Dawley rats. Diabetes. 60(3):899-908. doi: 10.2337/db10-0627

Fiory F., Lombardi A., Miele C., Giudicelli J., Beguinot F., Van Obberghen E. (2011) Methylglyoxal impairs insulin signalling and insulin action on glucose-induced insulin secretion in the pancreatic beta cell line INS-1E. Diabetologia.;54(11):2941-52. doi: 10.1007/s00125-011-2280-8.

Flanagan A. M., Brown J. L., Santiago C. A., Aad P. Y., Spicer L. J., Spicer M. T. (2008) High-fat diets promote insulin resistancethrough cytokine gene expression in growing female rats. J. Nutr. Biochem., 19(8):505-13

Fleming T., CunyJ., Nawroth G., Djuric Z., Humpert P. M., Zeier M. Bierhaus A., Nawroth P. P. (2012) Is diabetes an acquired disorder of reactive glucose metabolites and their intermediates? Volume 55, Issue 4, pp 1151–1155

Fraulob J. C., Ogg-Diamantino R., Fernandes-Santos C., Agui-la M. B., Mandarim-de-Lacerda C. A. (2010) A Mouse Model of Metabolic Syndrome: Insulin Resistance, Fatty Liver and Non- Alcoholic Fatty Pancreas Disease (NAFPD) in C57BL/6 Mice Fed a High Fat Diet. J. Clin. Biochem. Nutr., 46(3):212-23

Giacco F., Du X., D'Agati V.D., Milne R., Sui G., Geoffrion M., Brownlee M. (2014) Knockdown of glyoxalase 1 mimics diabetic nephropathy in nondiabetic mice. Diabetes 63(1):291-9. doi: 10.2337/db13-0316. DOI: 10.2337/db13-0316

Heart Protection Study Collaborative Group. (2002) MRC/BHF Heart Protection Study of cholesterol lowering with simvastatin in 20 536 high-risk individuals: a randomised placebo-controlled trial. Lancet. 360: 7-22

Khaw K.T., Wareham N., Luben R., Bingham S., Oakes S., et al. (2001) Glycated hemoglobin, diabetes and mortality in men in Norfolk cohort of European Prospective Investigation of Cancer and Nutrition EPIC-Norfolk. BMJ 322(7277): 15-18

Kumagai T., Nangaku M., Kojima I., Nagai R., Ingelfinger J.R., Miyata T., Fujita T., Inagi R. (2009) Glyoxalase I overexpression ameliorates renal ischemia-reperfusion injury in rats. Am J Physiol Renal Physiol. 296(4): F912-21. doi: 10.1152/ajprenal.90575.2008

Lind M., Odén A., Fahlén M., Eliasson B. (2010) The shape of the metabolic memory of HbA1c: re-analysing the DCCT with respect to time-dependent effects. Diabetologia. 53(6):1093-8. doi: 10.1007/s00125-010-1706-z

Maessen D.E., Stehouwer C.D., Schalkwijk C.G. (2015) The role of methylglyoxal and the glyoxalase system in diabetes and other age-related diseases. Clin Sci (Lond). Jun;128(12):839-61. doi: 10.1042/CS20140683

Mäkinen V.P., Civelek M., Meng Q. et al, (2014) Integrative Genomics Reveals Novel Molecular Pathways and Gene Networks for Coronary Artery Disease PLoS Genet10(7): e1004502 doi: 10.1371/journal.pgen.1004502

Marshall S. M., Flyvbjerg A. (2006) Prevention and early detection of vascular complications of diabetes. BMJ. 333(7566): 475–480 doi: 10.1136/bmj.38922.650521.80

Masiello P., Broca C., Gross R., Roye M., Manteghetti M., Hillaire-Buys D., Novelli M. and Ribes G. (1998) Development of a new model in adult rats administered streptozotocin and nicotinamide. Diabetes 47: 224-229

Matafome P., Santos-Silva D., Crisóstomo J., Rodrigues T.,Rodrigues L., Sena C. M. (2011) Methylglyoxal causes structural and functional alterations in adipose tissue independently of obesity. Pages 58-68 https://doi.org0.3109/13813455.2012.658065

McLellan A.C., Phillips S.A., Thornalley P.J. (1992) The assay of methylglyoxal in biological systems by derivatization with 1,2-diamino-4,5-dimethoxybenzene. Anal Biochem. 206(1):17-23.

Miralles F., Portha B. (2001) Early development of beta-cells is impaired in the GK rat model of type 2 diabetes. Diabetes. 50 Suppl 1: S84-8

Morgenstern J., Fleming T., Schumacher D., Eckstein V., Freichel M., Herzig S., Nawroth P. (2017) Loss of Glyoxalase 1 Induces Compensatory Mechanism to Achieve Dicarbonyl Detoxification in Mammalian Schwann Cells. J Biol Chem. Feb 24;292(8):3224-3238. doi: 10.1074/jbc.M116.760132

Mukohda M., Okada M., Hara Y., Yamawaki H. (2012) Methylglyoxal accumulation in arterial walls causes vascular contractile dysfunction in spontaneously hypertensive rats. J Pharmacol Sci. 120(1):26-35

Nigro C., Leone A., Longo M., Prevenzano I., Fleming T.H., Nicolò A., Parrillo L., Spinelli R., Formisano P., Nawroth P.P., Beguinot F., Miele C. (2018) Methylglyoxal accumulation de-regulates HoxA5 expression, thereby impairing angiogenesis in glyoxalase 1 knock-down mouse aortic endothelial cells. Biochim Biophys Acta Mol Basis Dis. pii: S0925-4439(18)30391-0. doi: 10.1016/j.bbadis.2018.10.014

Nigro C., Leone A., Raciti G.A., Longo M., Mirra P., Formisano P., Beguinot F., Miele C. (2017) Methylglyoxal-Glyoxalase 1 Balance: The Root of Vascular Damage. doi: 10.3390/ijms18010188. Review. Int J Mol Sci

Nigro C., Raciti G.A., Leone A., Fleming T.H., Longo M., Prevenzano I., Fiory F., Mirra P., D'Esposito V., Ulianich L., Nawroth P.P., Formisano P., Beguinot F., Miele C. (2014) Methylglyoxal impairs endothelial insulin sensitivity both in vitro and in vivo. Diabetologia. 57(7):1485-94. doi: 10.1007/s00125-014-3243-7

Oltman C. L., Davidson E.P., Coppey L. J., Kleinschmidt T. L., Lund D. D., Adebara E. T, Yorek M. A. (2008) Vascular and neural dysfunction in Zucker diabetic fatty rats: a difficult condition to reverse. Diabetes Obes. Metab. Volume10, Issue1 Pages 64-74 https://doi.org/10.1111/j.1463-1326.2007.00814.x

Potenza M.A., Marasciulo F.L., Chieppa D.M., Brigiani G.S., Formoso G., Quon M.J., Montagnani M. (2005) Insulin resistance in spontaneously hypertensive rats is associated with endothelial dysfunction characterized by imbalance between NO and ET-1 production. Am J Physiol Heart Circ Physiol. 289(2):H813-22. DOI:10.1152/ajpheart.00092.2005

Potenza M.A., Nacci C., Gagliardi S., Montagnani M. (2011) Cardiovascular complications in diabetes: lessons from animal models. Curr Med Chem.;18(12):1806-19

Queisser M. A., Y. Dachun, Geisler S., Hammes H., Lochnit G., Schleicher E. D., Brownlee M., Preissner K. T. (2010) Hyperglycemia Impairs Proteasome Function by Methylglyoxal. Diabetes 59(3): 670-678. https://doi.org/10.2337/db08-1565

Rabbani N., Xue M., Thornalley P.J. (2016) Methylglyoxal-induced dicarbonyl stress in aging and disease: first steps towards glyoxalase 1-based treatments. Clin Sci (Lond). 130(19):1677-96. doi: 10.1042/CS20160025

Rask-Madsen C., King G.L. (2013) Vascular complications of diabetes: mechanisms of injury and protective factors. Cell Metab. 17(1):20-33. doi: 10.1016/j.cmet.2012.11.012

Robert Turner, Rury Holman, Irene Stratton, Carole Cull, Valeria Frighi, Susan Manley, David Matthews, Andrew Neil, Heather McElroy, Eva Kohner, Charles Fox, David Hadden, and David Wright. (1998) Tight blood pressure control and risk of macrovascular and microvascular complications in type 2 diabetes: UKPDS 38 BMJ. 317(7160): 703–713

Russell J.C., Graham S.E., Richardson M. (1998) Cardiovascular disease in the JCR:LA-cp rat. Mol Cell Biochem (1-2):113-26

Schreyer A S., Wilson D. L., LeBoeuf R. C. (1998) C57BL/6 mice fed high fat diets as models for diabetes-accelerated atherosclerosis. Atherosclerosis Volume 136, Issue 1, 1 January, Pages 17-24 https://doi.org/10.1016/S0021-9150(97)00165-2

Stratton I.M., Adler A.I., Neil H.A., Matthews D.R., Manley S.E., Cull C.A., Hadden D., Turner R.C., Holman R.R. (2000) Association of glycaemia with macrovascular and microvascular complications of type 2 diabetes (UKPDS 35): prospective observational study. BMJ. 12;321(7258):405-12

UK Prospective Diabetes Study Group. (1998) Tight blood pressure control and risk of macrovascular and microvascular complications in type 2 diabetes: UKPDS 38 doi: https://doi.org/10.1136/bmj.317.7160.703

Vulesevic B., McNeill B., Giacco F., Maeda K., Blackburn N.J., Brownlee M., Milne R.W., Suuronen E.J. (2016) Methylglyoxal-Induced

Endothelial Cell Loss and Inflammation Contribute to the Development of Diabetic Cardiomyopathy. DiabetesJun;65(6):1699-713. doi: 10.2337/db15-0568

Wang X., Kaushik D., Chang T.; Wu L. (2005) Vascular methylglyoxal metabolism and the development of hypertension Journal of Hypertension: Volume 23 - Issue 8 - p 1565–1573 doi: 10.1097/01.hjh.0000173778.85233.1b

Wilson A.F., Elston R.C., Tran L.D., Siervogel. RM (1991) Use of the robust sib-pair method to screen for single-locus, multiple-locus, and pleiotropic effects: application to traits related to hypertension. Am J Hum Genet; 48:862–872

Xue M, Weickert M.O., Qureshi S., Kandala N.B., Anwar A., Waldron M., Shafie A., Messenger D.., Fowler M, Jenkins G., Rabbani N., Thornalley P.J. (2016) Improved Glycemic Control and Vascular Function in Overweight and Obese Subjects by Glyoxalase 1 Inducer Formulation. Diabetes. Aug;65(8):2282-94. doi: 10.2337/db16-0153

Chapter 2

The role of miRNAs in MGO-induced insulin resistance in mouse aortic endothelial cells

Mirra P, Nigro C, **Prevenzano I**, Procopio T, Leone A, Raciti GA, Andreozzi F, Longo M, Fiory F, Beguinot F, Miele C.
The role of miR-190a in methylglyoxal-induced insulin resistance in endothelial cells. Biochim Biophys Acta Mol Basis Dis. **2017** *Feb;1863(2):440-449.*

Nigro C, Mirra P, **Prevenzano I**, Leone A, Fiory F, Longo M, Cabaro S, Oriente F, Beguinot F, Miele C.
miR-214-Dependent Increase of PHLPP2 Levels Mediates the Impairment of Insulin-Stimulated Akt Activation in Mouse Aortic Endothelial Cells Exposed to Methylglyoxal. *Int. J. Mol. Sci.* **2018**, *19*(2), 522.

Mirra P, Nigro C, **Prevenzano I**, Leone A, Raciti GA, Formisano P, Beguinot F, Miele C. *The Destiny of Glucose from a MicroRNA Perspective.* Front Endocrinol (Lausanne). **2018** Feb 26;9:46.

2.1 Insulin action

Insulin is a hormone which plays a key role in the regulation of blood glucose levels and in the carbohydrate and lipid metabolism, and it has significant influences on protein and mineral metabolism. The effects of insulin on glucose metabolism vary depending on the target tissue. In particular, insulin inhibits gluconeogenesis and glycogenolysis and promoting the glycolysis and glycogenesis. Moreover, insulin stimulates the uptake and incorporation of amino acids into proteins, inhibits protein degradation, stimulates lipogenesis, and suppresses lipolysis (Qaid and Abdelrahman 2016). Insulin exerts its action by binding to its receptor (IR), a transmembrane glycoprotein with intrinsic protein tyrosine kinase activity. This receptor consists of an α-subunit, which binds the hormone, and a β-subunit, which is a tyrosine protein kinase.
Once activated, the receptor triggers a complex intracellular signalling network. IRS-1 binds PI3K that causes phosphorylation of the 3'OH on phosphatidyl inositol (PI) in the inner leaflet of the membrane to form PI (3) P. PI3K is a heterodimeric molecule composed of a regulatory (p85) and a catalytic subunit (p110). It is known that targeted deletion of the PI3K regulatory subunit in mice results in increased insulin sensitivity. Conversely, gene knockout of the catalytic subunit results in insulin resistance and glucose intolerance (Chang et al. 2004). In absence of insulin stimulation, the p110 subunit is constrained and inhibited by the p85 adaptive subunit; when appropriate cell stimuli are present, the catalytic subunit p110 of PI3K phosphorylates the PI (4,5) P2 molecule (phosphatidyl-inositol (4,5) bisphosphate), leading to the formation of PI (3,4,5) P3. In turn, PI (3,4,5) P3 active the AKT molecule (also known as protein kinase B or PKB) and is recruited from the plasma membrane. This lipid is very important because serve as plasma membrane docking sites for proteins that harbor pleckstrin-homology (PH) domains, including AKT and phosphoinositide-dependent kinase 1 (PDK1). The latter phosphorylates and activates Akt (Alessi et al. 1997). Akt has a pivotal role in the transmission of the insulin signal, by phosphorylating the enzyme GSK3, the forkhead transcription factors and cAMP response element-binding protein. As is the case for other growth factors insulin stimulates the extracellular signal-regulated kinases/mitogen-activated protein Kinases (ERK/MAPK) pathway. This pathway involves the tyrosine phosphorylation of IRS proteins and/or Shc, which in turn interact with the adapter protein Grb2. Grb2 constitutively associates with Sos, the guanine nucleotide exchange

factor for plasma membrane–bound Ras. Docking of Grb2 to IRS proteins recruits Sos to Ras, resulting in the activation of its GTPase. This leads to the subsequent activation of the serine/threonine kinase cascade known as the MAPK cascade. This cascade relays the signal from the plasma membrane to the nucleus and is the essential signalling pathway for mitogenesis (Virkamäki et al. 1999). It has recently become evident that insulin also acts on endothelium where, through the activation of its own receptor, regulates the vascular tone (Scherrer et al. 1994).

2.2 Insulin action on endothelium

In the last years, endothelium is a considerate a new target of insulin action. One of the key vascular actions of insulin is to modulate vascular tone. To carry out its functions, the endothelium promotes the release of the vasodilator NO and the vasoconstrictor ET-1 (Sandoo et al. 2010). Insulin binding to its receptor on the endothelial cells activates the insulin receptor substrates: IRS-1 and IRS-2, thereby activating two different branches of insulin signalling. On one side, insulin binding to its receptor results in phosphorylation of insulin receptor substrate IRS-1, which then binds and activates PI3K, leading to phosphorylation and activation of PDK-1 via increases in PI (3,4,5)3P. PDK-1, in turn, phosphorylates and activates Akt, which then directly phosphorylates endothelial eNOS at Ser1177, resulting in increased eNOS activity and subsequent NO production (Muniyappa et al. 2007). The eNOS dimer generates NO by means of the conversion of arginine in(to) NO and L-cytrulline by a ratio of 1 to 1. This is an oxygen and NADPH-dependent reaction. eNOS is a central regulator of cellular function that is important to maintain endothelial homeostasis. On the other side, through the activation of IRS-2, insulin activates the proatherogenic Ras-Raf-MAPK pathway, resulting in secretion on ET-1.
Insulin action in EC maintain the balance between the production of the vasodilator NO and the vasoconstrictor ET-1, with vasodilatation representing the normal response and impaired vasodilatation, or even net vasoconstriction, representing the abnormal responses associated with endothelial dysfunction (Eringa et al. 2004). We have recently demonstrated that MGO induces endothelial insulin-sensitivity by impairing the insulin-mediated activation of PI3K/Akt/eNOS pathway and increasing the phosphorylation of Extracellular Signal-Regulated Kinase 1/2 (ERK 1/2). On the others side, thus leading to an imbalance between the production of NO and ET-1 by MAECs (NIGRO et al. 2014).

2.3 Biogenesis of miRNAs

MicroRNAs (miRNAs) are small (20–22 nucleotides), non-coding RNAs, characterized by an evolutionary conservation and able to regulate gene expression at the posttranscriptional level. In more detail, the miRNA seed region interacts with the complementary sequence in at 3′ untranslated region (UTR) of target messenger RNAs (mRNAs) and, subsequently, inhibits the translation or targets the degradation of the bound mRNAs (Mirra et al. 2018).

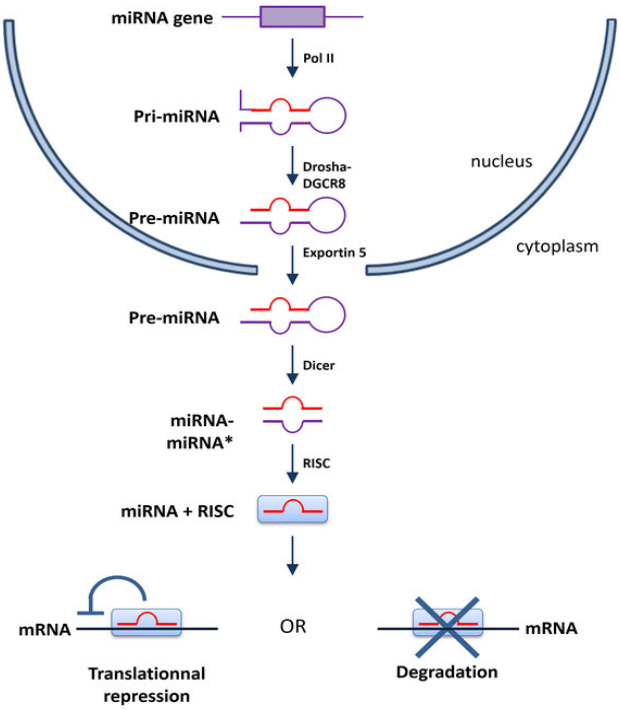

Figure 2.1 Biogenesis of miRNA (Devaux et al. 2015).

The nascent transcript, referred to as the pri-miRNA, is usually several hundred nucleotides in length and contains one or more hairpin structures. The miRNA-specific processing begins in the nucleus with the cleavage at the stem-loop formations by an RNase III-like enzyme, known as Drosha, which acts in concert with co-factors, including DiGeorge syndrome critical region 8 (also known as Pasha in flies and nematodes), at the level of the

microprocessor complex. The result is a 70-nucleotide long stem loop precursor, known as the pre-miRNA, which is then exported to the cytosol by exportin 5 and Ran-GTP through nuclear pores. Once in the cytoplasm, Dicer, another RNase III-like endonuclease, recognizes the hairpin-shaped pre-miRNA hairpin and cuts the terminal-loop to generate a RNA duplex, 20–22 nucleotides in length. To stabilize the interaction of Dicer with the pre-miRNA, the Dicer cleavage takes place in a large complex, which includes TRBP or TARBP2 (the human immunodeficiency virus transactivating response RNA-binding protein). The resulting miRNA duplex is composed of the mature miRNA and the base-paired passenger strand, sometimes indicated as the miRNA* strand. The final step consists in the incorporation of the miRNA duplex into the final effector complex, namely the RNA-induced silencing complex (RISC), where it is loaded onto an Argonaute (Ago) protein. At this point, the strand that exhibits less stable base pairing at the 5′ end remains associated with the Ago protein (mature miRNA), while the other is unwound from the duplex and typically degraded by the RISC (miRNA* strand), although some miRNAs* are thought to regulate gene expression like mature miRNAs (Fig.2.1).

2.4 Influence of miRNAs in insulin signalling pathway and insulin resistance

Recent studies have highlighted the role of miRNAs in the regulating the expression of endothelial genes involved in angiogenesis, EC proliferation and function. In increasing number of studies on miRNAs related to human diseases has pointed out that these molecules play a significant role in controlling insulin pathway beside other cellular pathways. The involvement of miRNAs in T2DM was first confirmed by Poy et al. (2007), who have demonstrated the role of miR-375 in the control of insulin secretion. Up to date, a large number of miRNAs is known to be connected with the cascade of pathways related to T2DM. Among these miR-33a and miR-33b have a role in the insulin signalling by controlling AKT phosphorylation and they also target the IRS-2 and insulin signalling pathways in the liver (Dávalos et al. 2011). There are other evidence demonstrating that miR-144 directly inhibits IRS1 (a key molecule in insulin signalling), Moreover, the miR-322 regulates insulin signalling pathway and protects against metabolic syndrome-induced cardiac dysfunction in mice (Marchand et al. 2016), while miR-320 favors insulin sensitivity in insulin resistant conditions by regulating the insulin-IGF-1 signalling pathways. Different are the miRNAs expressed in the ECs. miR-126 is involved in the inflammatory response, and it has an essential role in the maintaining vascular integrity and homeostasis after tissue damage, by enhancing endothelial repair capacity. The endothelium-specific miRNA, miR-92a, negatively regulates EC-derived production of NO and its upregulation has been associated with atherosclerosis and myocardial injury. On the contrary, miR-92a inhibition may play an important role in preventing neointimal hyperplasia since NO production by ECs inhibits VSMCs proliferation (Pujol-López et al. 2017). Hence, normalizing the expression of the dysregulated miRNAs may serve as a therapeutic approach in controlling the development and/or progression of insulin resistance and endothelial dysfunction thus preventing cardiovascular disease (Fig. 2.2)

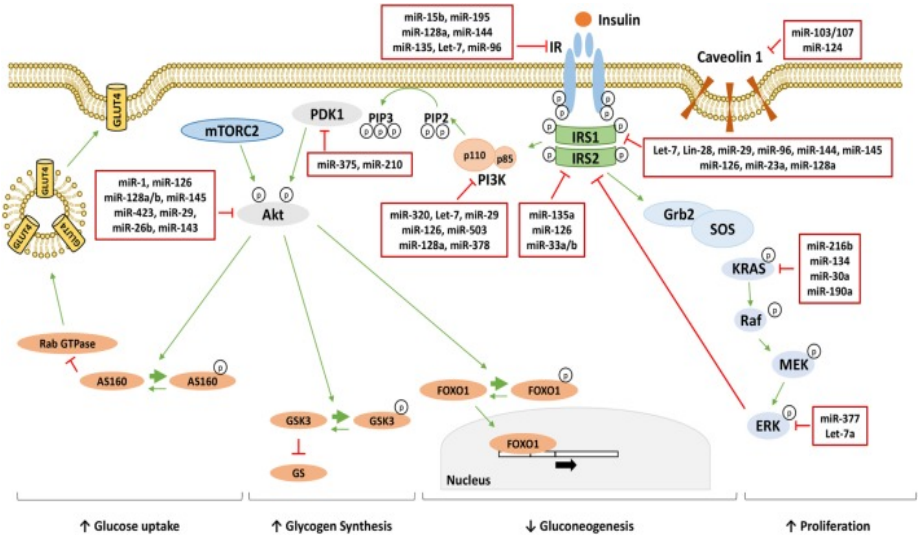

Figure 2.2 MicroRNAs (miRNAs) targeting insulin signalling mediators. *Following the binding to insulin receptor (IR), insulin induces the activation of phosphatidylinositol 3-kinase (PI3K)/AKT pathway responsible for the metabolic effect of insulin through the increase of glucose uptake, the increase of glycogen synthesis and the reduction of gluconeogenesis. On the other hand, insulin activates the mitogen-activated protein kinase (MAPK) pathway increasing cellular proliferation. miRNAs directly targeting critical nodes of insulin signalling are reported in the red boxes in figure. Thin green arrows indicate activation, while red T arrows indicate direct inhibition. Thick green arrows indicate inhibitory phosphorylation. (p) Indicates a phosphate group. Abbreviations: IRS1/2, insulin receptor substrate 1/2; PIP3, phosphatidylinositol 3,4,5-triphoshate; PIP2, phosphatidylinositol 4,5-bisphoshate; PDK1, phosphoinositide-dependent kinase 1; mTORC2, mammalian target of rapamycin complex 2; FOXO1, forkhead box protein O1; GSK3, glycogen synthase kinase 3; GS, glycogen synthase; AS160, AKT substrate of 160 kDa; GLUT4, glucose transporter 4; Grb2, growth factor receptor-bound protein 2; SOS, son of seven less; KRAS, Kirsten rat sarcoma viral oncogene homolog (proto-oncogene); RAF, RAF proto-oncogene serine/threonine-protein kinase; MEK, mitogen-activated protein kinase kinase; ERK, extracellular signal-regulated kinase (Mirra et al.2017).*

2.5 Aim

The increased formation of MGO is one of the mechanisms proposed as the cause of insulin resistance and an important contributor to the development of vascular complications in chronic hyperglycemia. An interesting new concept concerns the possibility that MGO may also affect gene expression through mediating epigenetic changes including miRNAs modulation. We and others have demonstrated that MGO leads to endothelial insulin resistance. In light of these recent findings, we have examined here the involvement of miRNAs as potential culprits behind the action of MGO on the endothelium, in order to explain the molecular mechanisms responsible for the MGO-dependent impairment of the endothelial insulin sensitivity previously demonstrated (Nigro et al. 2014).

2.6 Results

2.6.1 Effect of MGO accumulation on miRNAs expression in endothelial cells.

Insulin resistance is a major risk factor for type 2 diabetes (Zang et al. 2017), which promotes endothelial dysfunction, in the long term. It is known that increased MGO levels impair the endothelial function in various ways and in different body districts, (Nigro et al. 2017), leading to the development of endothelial dysfunction, principal cause of the cardiovascular diseases (Stehouwer et al. 1997, De Caterina 2000, Schalkwijk et al. 2005). Nevertheless, the underlying molecular mechanisms are not fully understood yet. In order to evaluate the MGO effect on miRNAs and their impact on pathophysiological pathways of insulin action, we have analyzed the expression profile of 84 miRNAs experimentally identified and/or bioinformatically predicted to be involved in diabetes-related biological processes, by the use of a miRNA PCR Array. Mouse aortic endothelial cells (MAECs) have been treated with MGO 500 μmol/l for 16 hours and 12 of 84 tested miRNAs resulted to be over or under the arbitrary chosen cut-off (± log 0.5-fold changes vs untreated cells). Among these, 5 miRNAs are up-regulated and 7 are down-regulated in MGO treated MAECs compared to control untreated cells. To validate these data, the expression of these 12 miRNAs was then tested by Real Time-PCR and the differential expression of miR-126, miR-190a, miR-214 and miR-450a was confirmed (figure 2.3). It is following described the study we have performed on the role of these differently expressed miRNAs on insulin signal transduction in endothelial cells.

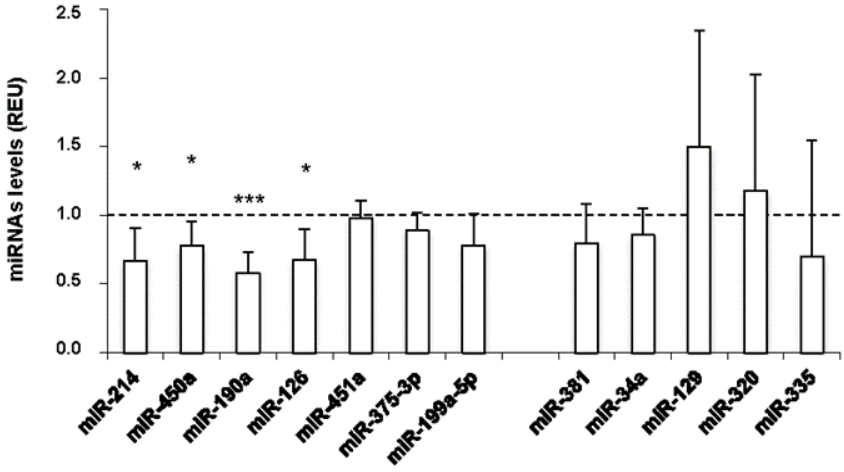

Figure 2.3 MGO effect on miRNAs expression. *The expression of miRNAs resulted to be differentially expressed in the PCR array was tested by Real Time-PCR in MAECs treated with 500 µmol/lMGO. The bars in the graph represent the mean ± SD of the expression units relative to U6 snRNA levels, used as housekeeping gene. Control levels of miRNAs in not treated MAECs are referred as 1 (dotted line). Statistical significance was evaluated using the Student's t-test; *p≤0.05, ***p≤0.001.*

2.6.2 The role of miR-190a on MGO-mediated insulin-resistance in endothelial cells.

To demonstrate the role of miR-190a in endothelial insulin signalling, its expression was antagonized by transfecting the miR-190a inhibitor in MAECs cells stimulated or not with insulin. Interestingly, similarly to MGO-treated cells, the inhibition of miR-190a significantly decreases the insulin-induced tyrosine phosphorylation of IRS1 (Fig. 2.4 a) and Akt phosphorylation, both on ser473 and thr308 (Fig. 2.4 b), compared to control MAECs transfected with a scramble miRNA, without affecting the insulin-receptor (IR) phosphorylation (Fig. 2.4 a). In addition, as shown in figure 2c, insulin-dependent eNOS activation is impaired by the inhibition of miR-190a. Indeed, we have seen a reduction of phosphorylation on ser1177 and a loss of de-phosphorylation in thr497 in MAEC cells treated with insulin, compared to scramble treated cells. Consistent with eNOS activation,

insulin stimulation induces a ~1.4- fold increase of NO release in scramble-treated cells, as expected, while no increase of NO levels is revealed in the culture medium from MAECs transfected with miR-190a inhibitor (Fig.1d). Furthermore, as in MGO-treated cells, the inhibition of miR-190a increases basal ERK 1/2 phosphorylation (Fig. 2.4 e). Thus, these data demonstrate that, independently from MGO exposure, the reduction of miR-190a levels is sufficient to affect ERK 1/2 activation and insulin-dependent IRS1/Akt/eNOS pathway in MAECs.

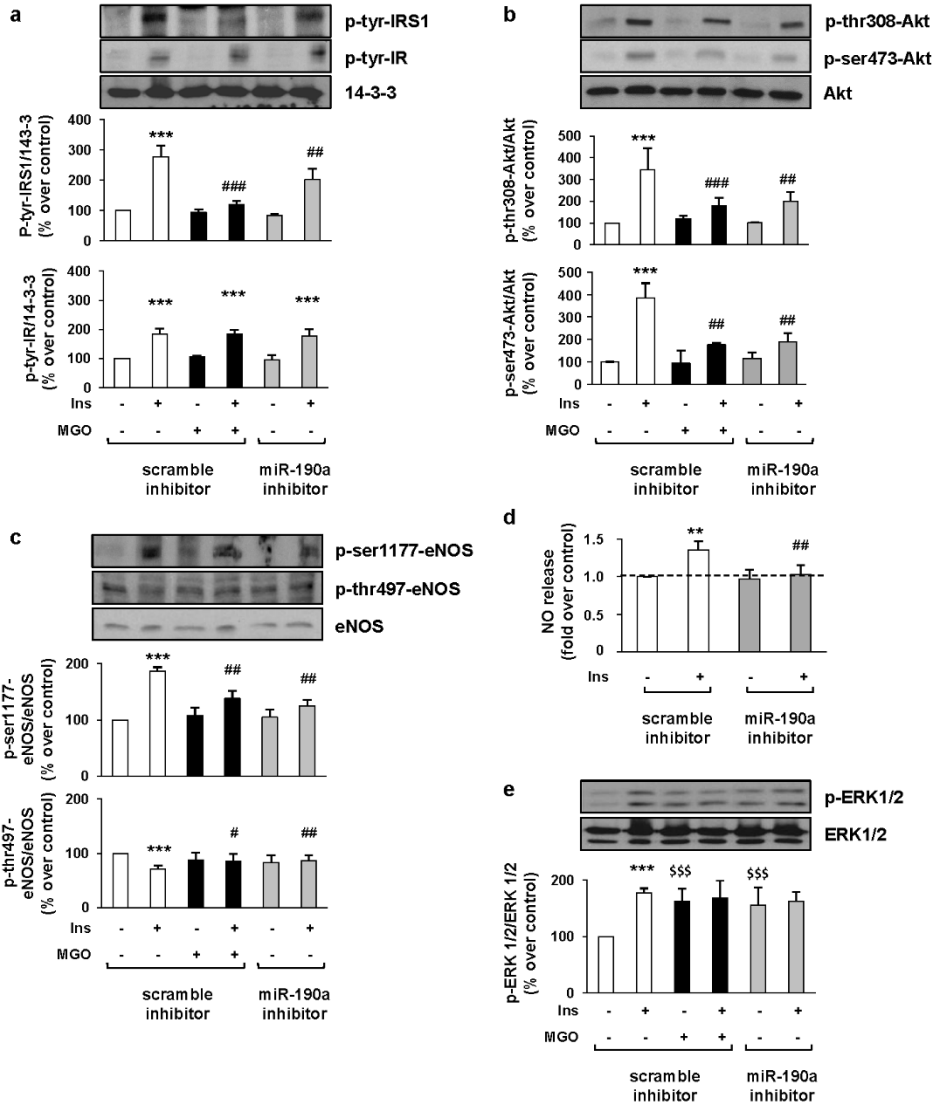

Figure 2.4 Effect of miR-190a inhibitor on insulin sensitivity in MAECs. *MAECs were transfected with a negative control (scramble; white and black bars) or with the inhibitor of miR-190a (gray bars) and incubated with 500 µmol/l MGO (black bars) where indicated. They were then stimulated or not with 100 nmol/l insulin (Ins) for 10 min. Protein lysates obtained from these cells were analyzed by Western Blot with anti-p-tyr-IR, anti-p-tyr-IRS1, anti 14-3-3 (a), anti-p-ser473-Akt, anti-p-thr308-Akt, anti-Akt (b), anti-p-ser1177-eNOS, anti-p-thr497-eNOS, anti-eNOS (c), anti-p-ERK1/2 and anti-ERK1/2 antibodies (e).*

Protein levels were quantified by the densitometric analysis of at least 3 independent experiments. The bars in the graph represent the means ± SEM of the percent (%) over control. (d) The culture medium was collected and tested for NO concentration by a colorimetric kit assay. The bars in the graph represent the increase of NO medium content after insulin stimulation over the control. The basal NO medium concentration is referred as 1.0 (dotted line). Values are expressed as means ± SD of triplicate determinations. Statistical analysis was evaluated using the Student's t-test; $^{**}p \leq 0.01$ $^{***}p \leq 0.001$ (+insulin vs − insulin); $^{\#\#}p \leq 0.01$(MGO scramble +insulin and miR-190a inhibitor +insulin vs scramble untreated +insulin); $^{\$\$\$}p \leq 0.001$ (MGO scramble − insulin and miR-190a inhibitor − insulin vs scramble untreated − insulin).

Next, wondering how the reduced expression of miR-190a may be crucial in mediating the MGO effect on endothelial insulin-sensitivity, miR-190a levels were increased by transfecting cells with a miR-190a mimic. As previously demonstrated by our group (Nigro et al. 2014), insulin-induced IRS1, but not IR, phosphorylation (Fig. 2.5a), ser473 and thr308-Akt phosphorylation (Fig. 2.5b) and the downstream ser1177-eNOS phosphorylation (Fig. 2.5c) are impaired in MAECs treated with MGO. Interesting, the overexpression of miR-190a in MGO-treated cells, at least partly, prevents the MGO deleterious effects on the insulin-stimulated activation of IRS1/Akt/eNOS (Fig. 2.5a–c). Interestingly, the overexpression of miR-190a also rescues the insulin-induced NO release in MGO-treated MAECs. Moreover, the MGO-induced ERK 1/2 hyperactivation is prevented by the transfection of the miR-190a mimic (Fig. 2.5e).

The data described so far show that miR-190a is a key player in the MGO-dependent impairment of insulin sensitivity in MAECs.

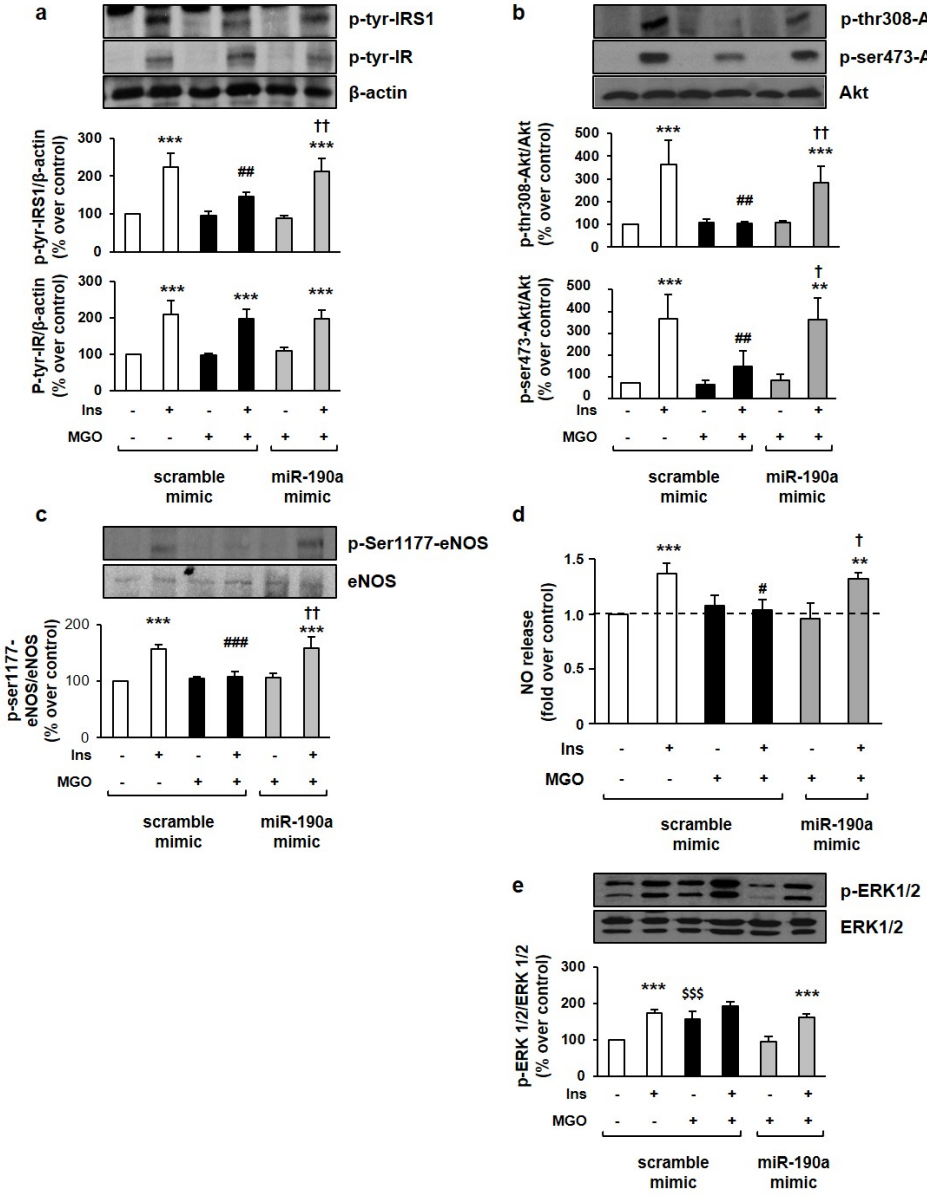

Fig. 2.5. Effect of miR-190a mimic on insulin sensitivity in MAECs. *MAECs were transfected with a negative control (scramble; white and black bars) or with the mimic of miR-190a (gray bars), and incubated with 500 µmol/l MGO, where indicated. They were then stimulated or not with 100 nmol/l insulin for 10 min. (a, b, c and e) Protein lysates obtained from these cells were analyzed by Western Blot as described in figure legend 2. The bars in the graph represent the means ± SEM of the percent (%) over control. (d) NO*

production was evaluated as reported in figure legend 2. The bars in the graph represent the increase of NO medium content after insulin stimulation over the control. The basal NO medium concentration is referred as 1.0 (dotted line). Values are expressed as means ± SD of triplicate determinations. Statistical analysis was evaluated using the Student's t-test;$^{**}p \leq 0.01$,$^{***}p \leq 0.001$ (+insulin vs − insulin);$^{\#}p \leq 0.05$,$^{\#\#}p \leq 0.01$,$^{\#\#\#}p \leq 0.001$ (MGO scramble +insulin vs scramble untreated +insulin);$^{\dagger}p \leq 0.05$,$^{\dagger\dagger}p \leq 0.01$ (miR-190a mimic +insulin vs MGO scramble +insulin);$^{\$\$\$}p \leq 0.001$ (MGO scramble − insulin vs scramble untreated − insulin).

2.6.3 miR-190a down-regulation plays a role in MGO-induced endothelial insulin resistance by increasing KRAS protein levels.

We have previously published that MGO exposure affects insulin sensitivity in MAECs through the hyperactivation of ERK1/2 (Nigro 2014). Thus, in order to establish whether ERK 1/2 activation could be up- or down-stream the MGO-induced miR-190a down-regulation, ERK 1/2 phosphorylation was prevented by the chemical inhibitor UO126.
Pre-treatment with the MAPK ERK Kinase (MEK) inhibitor U0126 does not affect the MGO-induced miR-190a reduced expression (Fig. 2.6a). Interestingly, the protein protein levels of GTPase Kirsten Rat Sarcoma Viral Oncogene Homolog (KRAS), which is one of the validated targets of miR-190a are increased by both MGO exposure and miR-190a inhibitor transfection (Fig. 2.6 b). Conversely, reduced levels of KRAS are shown, when miR-190a expression is increased by miR-190a mimic transfection, even in presence of MGO (Fig. 2.6 c). Furthermore, the role of KRAS in the MGO effect on insulin signalling was evaluated by transfecting MAECs with a specific siRNA for KRAS. KRAS protein levels are reduced by siKRAS compared to MGO-treated cells transfected with a scramble siRNA, used as negative control (Fig. 2.6d). Silencing of KRAS prevents ERK 1/2 basal activation as well as IRS1 phosphorylation on ser616 (Fig. 2.6 d), also rescuing the insulin-dependent Akt and eNOS activation (Fig. 2.6e). Together, these results indicate that miR-190a down-regulation mediates the MGO effect on endothelial insulin sensitivity, at least in part, by increasing the levels of its target KRAS.

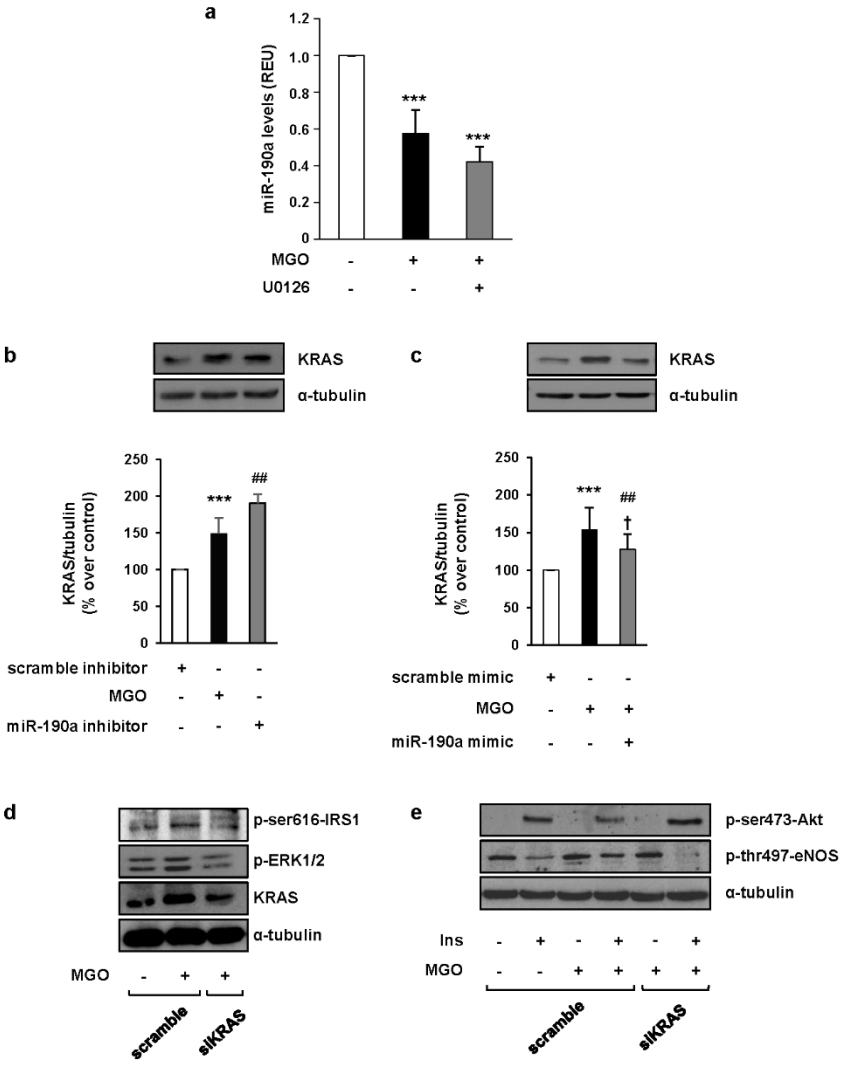

Fig. 2.6. The role of KRAS in MGO-mediated effect. *(a) MAECs were pre-treated with the MEK inhibitor U0126 15 µmol/l and then treated with MGO 500 µmol/l. Total RNA was extracted from these cells and analyzed by Real Time-PCR. The bars in panel a represent the means ± SD of miR-190a expression units relative to U6 snRNA levels. (b, c) MAECs were transfected with a negative control (scramble inhibitor or scramble mimic; white bars) or treated with 500 µmol/l MGO (black bars) and transfected with the inhibitor (b) and the mimic (c) of miR-190a (gray bars), were indicated. Protein lysates obtained from these cells were analyzed by Western Blot with anti-KRAS and anti-α-tubulin antibodies. Protein levels were quantified by the densitometric analysis of at least 3 independent experiments. The bars in the graph represent the means ± SEM of the percent (%) over*

control. (d, e) MAECs were transfected with a negative control, treated or not with MGO 500 µmol/l, or transfected with an interfering RNA specific for KRAS, as indicated. Protein lysates obtained from these cells were analyzed by Western Blot with anti-p-ser616-IRS1, anti-p-ERK1/2, anti-KRAS (d), anti-p-ser473-Akt, anti-p-thr497-eNOS antibodies (e). Anti-α-tubulin antibody was used as loading control. Statistical analysis was evaluated using the Student's t-test; $^{***}p\leq0.001$ (MGO vs control untreated or scramble); $^{\#\#}p\leq0.01$ (miR-190a inhibitor and mimic vs scramble); $^{\dagger}p\leq0.05$(MGO + miR190a mimic vs MGO).

2.6.4 Effect of MGO on insulin pathway phosphatases, targets of miRNAs down-regulated by MGO.

Besides miR-190a, we evaluated the possible contribution of other differently expressed miRNAs in the insulin signalling alteration in MAECs exposed to MGO. To this aim, the putative targets have been checked by the use of mirWalk database (http://zmf.umm.uni-heidelberg.de/apps/zmf/mirwalk/). Among these, the phosphatase and tensin homolog (PTEN), protein tyrosine phosphatase 1B (PTP1B), PH domain leucine-rich repeat protein phosphatase 1 and 2 (PHLPP1 and PHLPP2) play an important role in the regulation of insulin signalling. As shown in Figure 2.7, treatment of MAECs with MGO has no effect on the protein levels of PTEN (Fig. 2.7a), PTP1B (Fig. 2.7 b) and PHLPP1 (Fig. 2.7c). By contrast, protein levels of PHLPP2 are 4-fold increase in MGO-treated MAECs compared to the untreated control cells (Fig. 2. 7d).

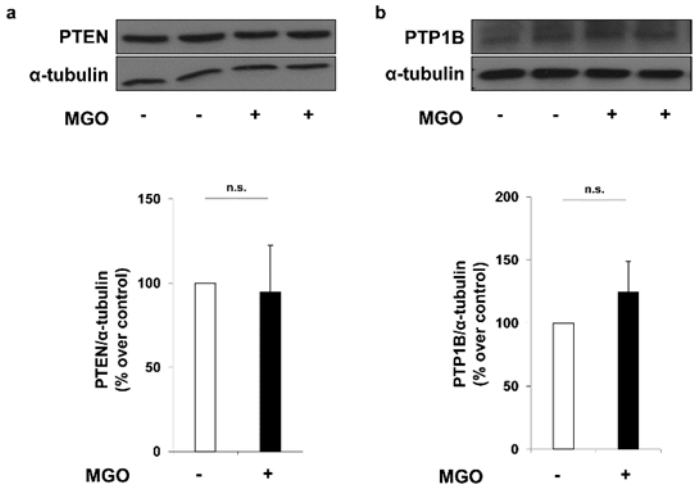

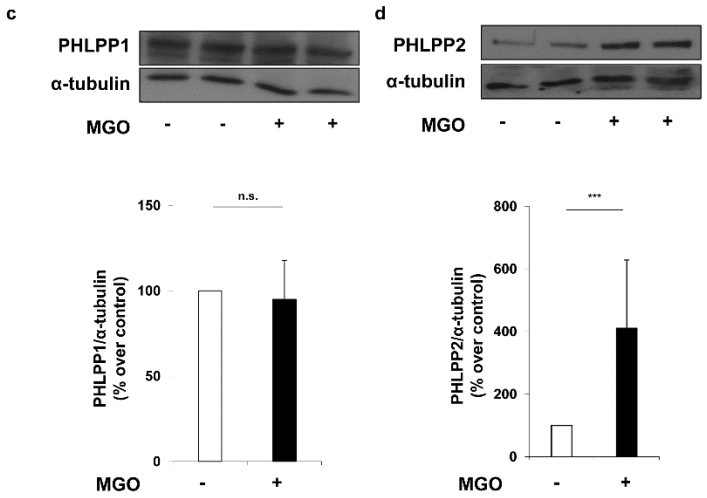

Figure 2.7 Effect of methylglyoxal (MGO) on miR-214 and miR-126 target phosphatases of insulin signalling mediators. *Mouse aortic endothelial cells (MAECs) were treated with 500 µmol/L MGO for 16 h. Protein lysates obtained from these cells were analyzed by Western blot with anti-PTEN (a) anti-PTP1B (b) anti-PHLPP1 (c) and anti-PHLPP2 antibodies (d). Protein normalization was performed using α-tubulin antibody. Exposure timing was of 1 min for blots in panels (a, c, d), and 2 min for blots in panel (b). Protein levels were quantified by the densitometric analysis of at least three independent experiments. Bars in the graphs represent the mean ± SD of the percent (%) over control (−MGO). Statistical analysis was evaluated using the Student's* t-test; *** $p \leq 0.001$.

2.6.5 Effect of the modulation of the miR-214 and miR-126 on PHLPP2 protein levels in MAECs.

The preliminary bioinformatic analysis indicated PHLPP2 as a potential target of both miR-214 AND Mir-126. In the light of these informations, we have modulated the expression of both miR-214 and miR-126 in MAECs. We have first transfected MAECs with a specific antisense inhibitor for miR-214 (miR-214 inhibitor) and surprisingly, as shown in figure 8a, the reduction of miR-214 induces a dose-dependent increase of PHLPP2 protein levels. Differently, we have not observed any significant difference between MAECs transfected with a specific antisense inhibitor for miR-126 (miR-126 inhibitor) and MAECs transfected with a non-targeting antisense inhibitor (control inhibitor) (Figure 8b). In accordance with the previous results, a significant reduction in PHLPP2 levels is observed in MAECs

overexpressing miR-214, when transfected with 50 nmol/L of a RNA oligonucleotide which specifically mimics miR-214 (miR-214 mimic) (figure 8c). Conversely, the MAEC cells transfected with a RNA oligonucleotide mimicking miR-126 (miR-126 mimic) did not show any difference in levels PHLPP2 compared with cells transfected with a non-targeting control oligonucleotide (control mimic). Taken together, these results show that miR-214, but not miR-126, is able to modulate the protein levels of PHLPP2 in MAECs.

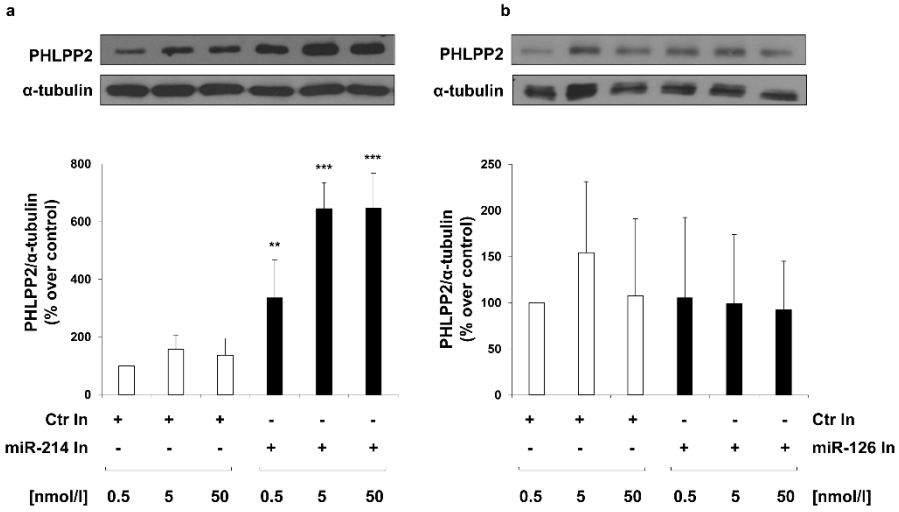

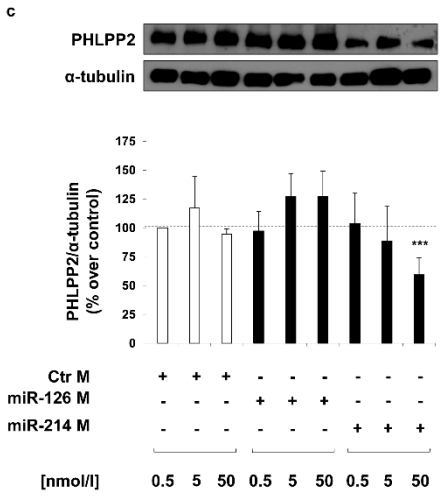

FIGURE 2.8 Effect of miR-214 and miR-126 modulation on PHLPP2 protein levels in MAECs. *MAECs were transfected with different concentrations (0.5, 5, and 50 nmol/L) of miR-214 (a) and miR-126 (b) inhibitor (miR-214 In and miR-126 In), or miR-214 and miR-126 mimic (miR-214 M and miR-126 M) (c). Transfection with a non-targeting antisense inhibitor (Ctr In; (a, b)), and a non-targeting control oligonucleotide (Ctr M; (c)) were used as negative controls. Forty-eight hours after transfection, cells were collected, and protein lysates were analyzed by Western blot with anti-PHLPP2 and anti-α-tubulin antibodies. Exposure timing was 4 min for blots in panels (a), 2 min for blots in panels (b) and 20 min for blots in panel (**c**). Protein levels were quantified by the densitometric analysis of at least three independent experiments. Bars in the graphs represent the mean ± SD of the percent (%) over control (Ctr In or Ctr M) 0.5 nmol/L. Statistical analysis was evaluated using Student's* t-*test; ** $p \leq 0.01$; *** $p \leq 0.001$.*

2.6.6 Effect of the modulation of miR-214 on PHLPP2 levels in MAECs.

As shown in the figure 9, MAECs transfected with the miR-214 inhibitor show an increase of PHLPP2 levels by about 4-fold, similarly to that observed in both MGO-treated control cells and miR-214 inhibitor plus MGO co-treated cells. In addition, in the presence of MGO, the transfection of MAECs with the miR-214 mimic reverses the effect due to MGO, leading to a 2.5-fold reduction of PHLPP2 levels. Therefore, these data demonstrate that miR-214 mediates the effect of MGO on the PHLPP2 expression.

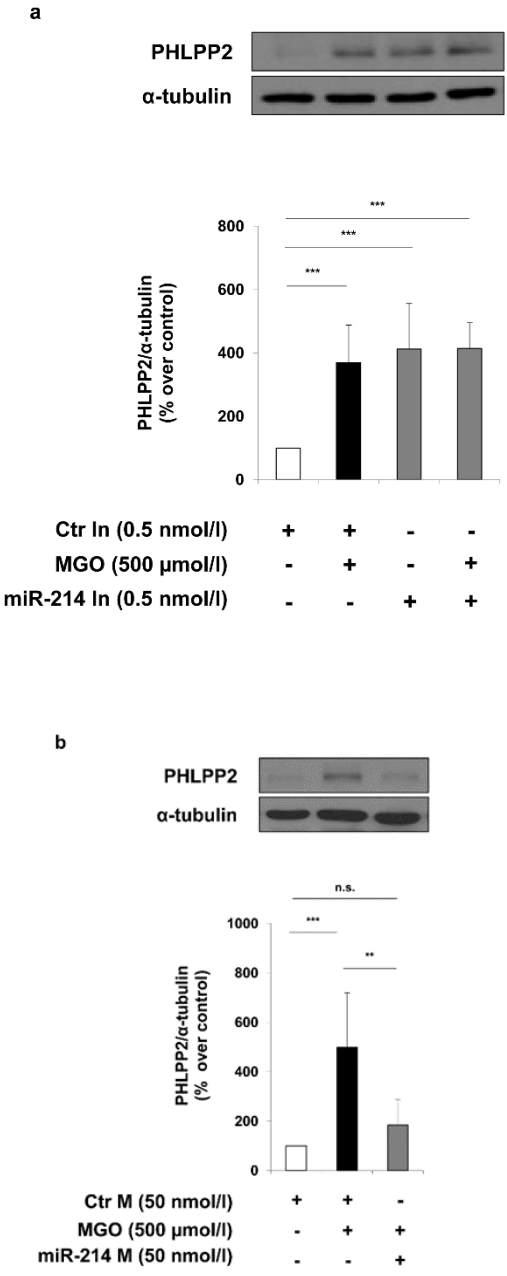

Figure 2.9. Effect of miR-214 mimic and miR-214 inhibitor on PHLPP2 levels in MAECs with or without MGO*. MAECs were transfected with a non-targeting antisense inhibitor (Ctr In 0.5 nmol/L; (a)) and a non-targeting control oligonucleotide (Ctr M 50 nmol/L; (b))*

*(white and black bars), with miR-214inhibitor (miR-214 In 0.5 nmol/L; (a)) or miR-214 mimic (miR-214 M 50 nmol/L; (b)) (gray bars). Where indicated, MAECs were treated with MGO for 16 h. Protein lysates obtained from these cells 48 h after transfection were analyzed by Western blot with anti-PHLPP2 and anti--tubulin antibodies. Exposure timing was of 2 min for PHLPP2 blots and 10 min for -tubulin blots. Protein levels were quantified by the densitometric analysis of at least three independent experiments. Bars in the graphs represent the mean ± SD of the percent (%) over control (Ctr M and Ctr In). Statistical analysis was evaluated using the Student's t-test; ** $p \leq 0.01$; *** $p \leq 0.001$.*

In order to prove a direct regulation of PHLPP2 expression by miR-214, a mi Script Target Protector (TP) specific for the binding site of miR-214 on the 3′ untranslated region (UTR) of the mouse PHLPP2 has been used to treat MAECs. The data obtained demonstrate that the decrease of PHLPP2 protein levels in MAECs transfected with miR-214 mimic, is no longer observed in MAECs transfected with both the mi Script Target Protector (TP) and miR-214 mimic (Figure 10a). In line with this, the luciferase reporter assay performed in MAECs using a construct in which the PHLPP2-3'UTR is cloned immediately downstream of the Firefly luciferase confirms a miR-214-dependent regulation of PHLPP2. Indeed, the transfection of miR-214 mimic induces a 25% reduction of luciferase activity driven by the PHLPP2-3'UTR, while no effect on luciferase activity is induced by miR-214 mimic in the empty control vector-transfected cells (figure 10b). Together this data, demonstrate that miR-214 binds the PHLPP2-3'UTR region and, therefore, regulates its expression.

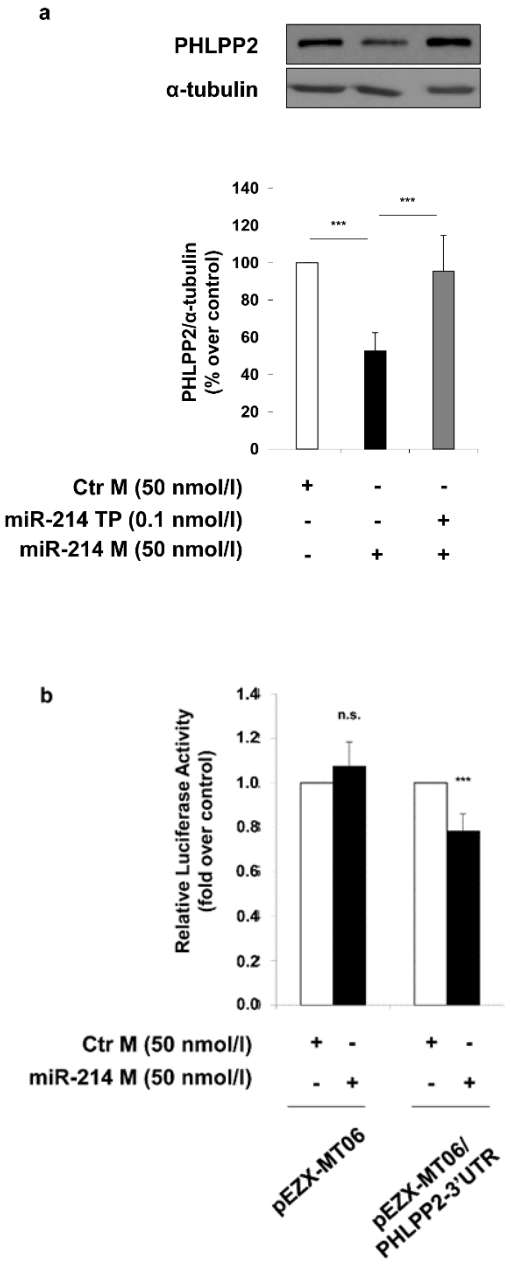

Figure 2.10. Effect of miR-214 on PHLPP2 regulation. *(a) MAECs were transfected with a non-targeting control oligonucleotide (Ctr M; white bars) or miR-214 mimic (miR-214 M 50 nmol/L; black bars). Where indicated, MAECs were co-transfected with mi Script miR-214 Target Protector (miR-214 TP 0.1 nmol/L). Protein lysates obtained from 48 h*

*transfected MAECs were analyzed by Western blot with anti-PHLPP2 and anti-α-tubulin antibodies. Exposure timing of blots was of 2 min. Protein levels were quantified by the densitometric analysis of at least three independent experiments. Bars in the graphs represent the mean ± SD of the percent (%) over control (Ctr M). (b) MAECs were transfected for 24 h with non-targeting control oligonucleotide (Ctr M 50 nmol/L; white bars) or miR-214 mimic (miR-214 M 50 nmol/L; black bars) in the presence of the pEZX-MT06 control reporter vector or the pEZX-MT06/PHLPP2-30UTR reporter vector. Firefly and Renilla luciferase activities were determined in cell lysates under each experimental condition. Results are normalized to Renilla activity. Bars in the graphs represent the mean ± SD of the fold over control (Ctr M). Statistical analysis was evaluated using Student's t-test; *** $p \leq 0.001$.*

2.6.7 Role of miR-214 on MGO-mediated endothelial insulin-resistance.

Once demonstrated the regulation of PHLPP2 by miR-214, to prove a role of miR-214 on MGO-mediated endothelial insulin-resistance, we analyzed the effect of miR-214 inhibitor and miR-214 mimic on insulin-dependent phosphorylation of Akt. As shown figure 11, MGO induces a reduction of insulin-induced Akt phosphorylation, in MAECs transfected with the control inhibitor, compared to the control cells not exposed to MGO. Similarly, the transfection of MAECs with miR-214 inhibitor significantly decreases the insulin-stimulated Akt phosphorylation compared to control cells. Differently, the transfection the MAEC with a miR-214 mimic prevents the MGO deleterious effect on the insulin-dependent Akt phosphorylation (figure 11 b).

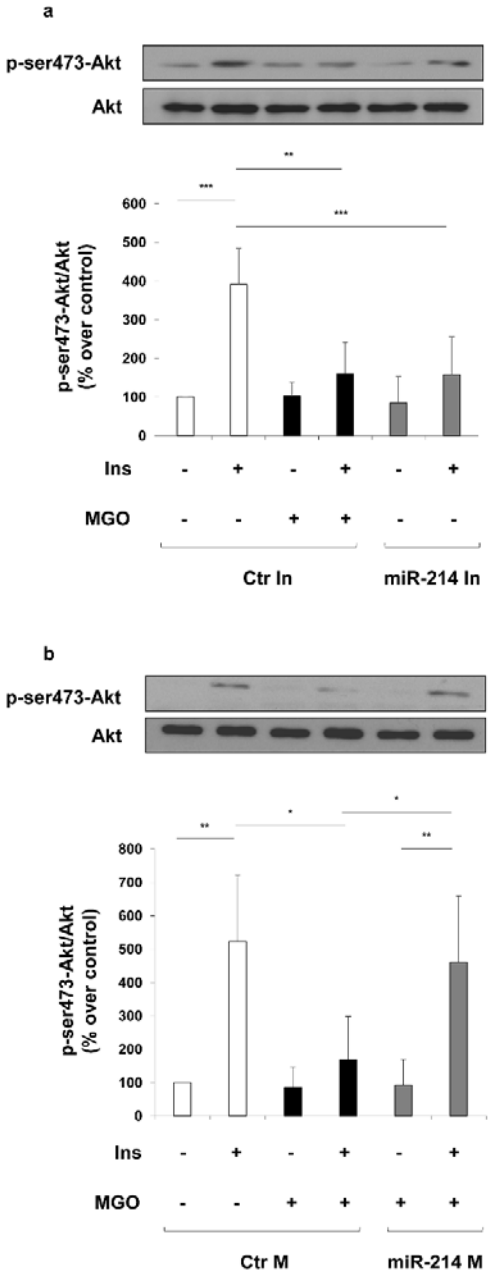

Figure 2.11. Effect of miR-214 modulation on insulin-dependent Akt activation in MAECs. *MAECs were transfected with a non-targeting antisense inhibitor (Ctr In 0.5 nmol/L; (a)) or a non-targeting control oligonucleotide (Ctr M 50 nmol/L; (b)) (white and*

*black bars), with miR-214 inhibitor (a) or miR-214 mimic (b) (miR-214 In 0.5 nmol/L or miR-214 M 50 nmol/L; gray bars). Where indicated, MAECs were treated with 500 _mol/L MGO (black bars) for 16 h before harvesting. After 48 h of transfection, cells were stimulated or not with 100 nmol/L insulin for 10 min. Protein lysates were analyzed by Western blot with p-ser473-Akt and Akt antibodies. Exposure timing was of 30 seconds. Protein levels were quantified by the densitometric analysis of at least three independent experiments. p-ser473-Akt levels were normalized to Akt total levels. Bars in the graphs represent the mean _ SD of the percent (%) over control (Ctr In and Ctr M). Statistical analysis was evaluated using the Student's t-test; * $p \leq 0.05$; ** $p \leq 0.01$; *** $p \leq 0.001$*

Finally, in addition to the above reported experiments carried out in vitro in MAECs, we have also validated the effect of MGO on miR-190a and miR-214 in vivo. To this aim, aortae were isolated from non-diabetic Glo1-KD mice, described to have high levels of MGO-modified proteins (Queisser et al. 2010, Giacco et al. 2014), and miR-190a and miR-214 levels were analyzed by Real Time-PCR. As shown in figure 2.12, the vascular expression of the both miR-190a and miR-214 are reduced by 60% and 45% respectively in Glo1-KD mice compared to their WT littermates. Moreover, we performed Western Blot analysis with the proteins isolated from both WT and Glo1-KD mice, stimulated or not with insulin. The data obtained show that insulin stimulation induces an 8- and 3-fold increase of ser473-Akt and ser1177-eNOS phosphorylation, respectively, in the aortae from WT mice. Conversely, the aortae from Glo1-KD mice show a 60% decrease of insulin-dependent Akt activation and a 50% decrease of eNOS activation, compared to WT mice (Fig. 5b).
This is an interesting result, showing that a mouse model, which is prone to accumulate MGO-modified proteins (Queisser et al. 2010), also shows reduced levels of miR-190a, miR-214 and vascular insulin sensitivity.

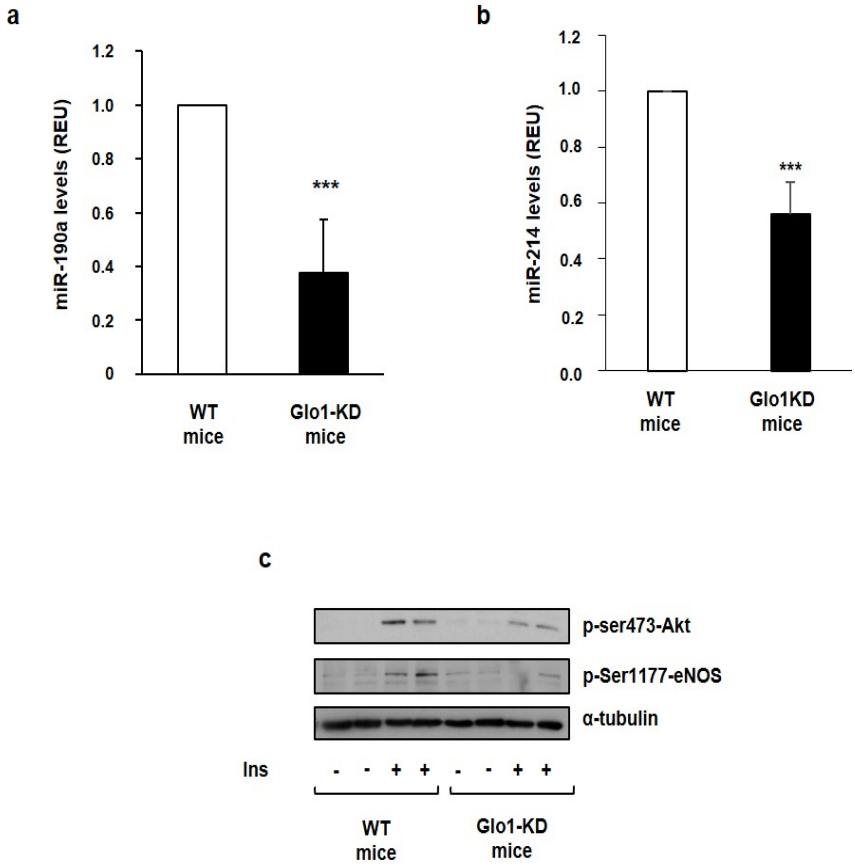

Fig. 2.12 Effect of MGO and vascular insulin sensitivity in vivo. *(a) miR-190a expression and miR-214 (b) were measured by Real Time-PCR in aortae from Glo1-KD and WT mice. The bars in the graphs represent the mean ± SD of the expression units relative to U6 snRNA levels, used as housekeeping gene. Statistical significance was evaluated using the Student's t-test; ∗∗∗$p \leq 0.001$. (c) Proteins were isolated from aortae of Glo1-KD and WT mice, receiving or not an i.p. bolus of insulin, and then analyzed by Western Blot with anti-p-ser473-Akt, anti-p-ser1177-eNOS and anti-α-tubulin. Blots are representative of at least four mice.*

2.7 Discussion

MGO is a highly reactive dicarbonyl compound which is formed as a by-product of glycolysis (Rabbani et al 2014). It is a major precursor of AGEs, reacting non-enzymatically with amino acid residues (e.g., Lys and Arg) located in the active sites of proteins and thereby causing their loss of function. (Ahmed and Thornalley 2006, Mirra et al. 2017) MGO levels increase in condition of hyperglycemia and reduced activity of the glyoxalase system. Plasma levels of MGO are increased in patients with DM (Beisswenger et al. 2001) and its abnormal accumulation contributes to the damage of various tissues. (Mirra et al 2017, Beisswenger 2014), also disturbing the insulin signalling pathway (Fiory et al 2011, Guo et al.2009 Riboulet-Chavey et al.2006). Emerging evidence have highlighted the harmful effect of MGO on the pathogenesis of insulin resistance by means of direct functional modifications in the molecular components of the insulin signalling pathway. For instance, an impairment in the insulin-stimulated activation of IRS-1 has been observed in the adipose tissue of fructose fed rats and in 3T3-L1 adipocytes (Jia and Wu 2007), in L6 muscle cells (Riboulet-Chavey) and in INS-1E β-cells treated with MGO (Fiory et al. 2011). Moreover, we have previously demonstrated that the exposure of both endothelial cells in vitro and mice to MGO impairs the insulin-dependent IRS-1/Akt/eNOS pathway and the consequent release of NO. In addition, we demonstrated that the MGO-dependent ERK 1/2 hyper-activation is responsible, at least in part, for the negative effect of MGO on the IRS-1/Akt/eNOS signalling pathway (Nigro et al. 2014). More recently, several studies, demonstrated that MGO alters gene expression by modifying transcription factors (Yao et al. 2007, Thangarajah et al 2009, Laga et al. 2007). An interesting new concept concerns the possibility that MGO may also affect gene expression through changes in DNA methylation (Palsamy et al. 2014), histone modifications (El-Osta et al. 2008) and miRNA expression (Liu H et al 2014, Shan-Shan et al. 2015). In particular, we have focused our attention on miRNAs as potential culprits behind the action of MGO on the endothelium in order to identify the molecular mechanisms responsible for the MGO-dependent impairment of the endothelial insulin sensitivity previously demonstrated (Nigro et al. 2014). To this aim, the expression profile of 84 diabetes-associated miRNAs were evaluated through a diabetic-specific array platform. Among these, we validated the reduced expression of 4 miRNAs in MGO-treated MAECs: miR-126, miR-190a, miR-214 and miR450a. We have provided the first

evidence that MGO down-regulates the expression of miR-190a and miR-214 both in MAECs, and in the vascular tissue of mouse model of MGO accumulation. Glo1-KD mice, represent a suitable animal model to study the effects of MGO accumulation. They develop signs of diabetic complications and, besides the impaired endothelium-dependent vasodilation described in the chapter 1 of this thesis, we have found an impaired insulin sensitivity in the aortae tissue of Glo 1 KD mice compared to WT mice. Therefore, a vascular insulin-resistance associates with reduced levels of miR-190a and miR-214 in vivo, as well. We proved the identified miRNAs in the impaired endothelial insulin-sensitivity by gain and loss of function experiments. Interestingly, the inhibition of miR-190a, mimicks the MGO-dependent effect on the insulin sensitivity in the endothelial cells, as it is sufficient to cause insulin resistance and impair the insulin-induced NO secretion. In a previous study, we have demonstrated that the MGO-dependent ERK 1/2 hyperactivation is responsible, at least partly, for the negative effect of MGO on the IRS1/Akt/eNOS transduction. Therefore, to the aim of establishing how MGO mediates the miR-190a down-regulation in MAECs, we have investigated the ERK 1/2 pathway. Moreover, a decreased transcription of miR-190a has recently been described to be dependent on ERK 1/2 nuclear activity in rat primary hippocampal neuron cultures and in mouse hippocampi (Zheng et al 2010, Zheng, Chu et al. 2010) However, in MAECs cells treated with UO126, a highly selective inhibitor of MEK Kinase, MGO still affected the miR-190a expression in MAECs, thus indicating that MGO modulates the miR-190a expression independently of ERK 1/2 in the endothelial cells. By contrast, when we induced alterations in the miR-190a levels, an inverse correlation between the miR-190a and ERK 1/2 phosphorylation levels was observed. This result suggests that the MGO-dependent hyper-activation of ERK 1/2 might be mediated by miR-190a. In order to clarify how miR-190a mediates the hyper-activation of ERK 1/2 we first tested whether alterations in the miR-190a levels were able to modulate the expression of miR-190a. However, we did not observe any difference in the protein levels of ERK 1/2 in MAECs when alterations in the miR-190a levels were induced. Afterwards, we identified the MAPK signalling pathway as one of the most enriched molecular pathways in the miR-190a target set, achieved through the combined results of 4 well-known tools for miRNA target prediction (miRanda (Enright et al. 2003), Target scan (Lewis et al. 2003), RNA22 (Miranda et al 2006) and miRWalk (Dweep et al. 2011)). Among the 42 potential targets of miR-190a related to the MAPK signalling pathway,

KRAS has an intrinsic GTPase activity which act upstream ERK ½ (Cox and Der 2010). For this reason, we have evaluated the protein levels of KRAS, and the data obtained show that alterations in the miR-190a levels were able to modulate this target in MAECs. This result is supported by the study carried out by Hao et al. demonstrating, that KRAS is directly regulated by miR-190a in HCT166 cells via a highly conserved binding site (Yang et al 2014). We further prove here the role of KRAS in the MGO-induced endothelial insulin-resistance by showing that its silencing in MAECs prevents the MGO effect on both the basal ERK 1/2 hyper-phosphorylation and the reduced insulin-stimulated IRS-1/Akt/eNOS signalling pathway. Besides miR-190a, we have also evaluated a possible role on the insulin-signalling of the other miRNAs found to be down-regulated by MGO. While very little is known about miR-450a to support its selection as a candidate for further investigation on its potential role in MGO-treated MAECs, previous studies highlight miR-214 and miR-126 attractive candidates, since they have a role in the control of endothelial cell function. Indeed, it has been demonstrated that miR-125 downregulates IRS1, suppressing AKT activation (Duan et al 2015, Ryu. While, miR-214 has been reported to activate the PI3K/Akt signalling by targeting PTEN expression in several cell types, (besides targeting IRS and Akt in C2C12 myoblasts Wang et al. 2016, Yang et al. 2008, Zhang and Zhang 2017, Liu et al. 2017, Yang et al. 2013, Xin et al. 2016). As we have found no difference in the levels of the key components of the IRS1/Akt/eNOS signalling in MAECs exposed to MGO, we have shifted our focus towards negative regulators of the insulin signalling. Indeed, their upregulation as a consequence of the reduced levels of miRNAs induced by MGO, would provide a reasonable explanation for the decrease of insulin responsiveness observed in MGO-treated MAECs. Through several bioinformatics tools, we have identified different phosphatases as a potential target of both miR-214 and miR-126. We have evaluated the effect of MGO on the levels of the following proteins: PTP1B, which binds and subsequently dephosphorylates the insulin receptor (Wang et al. 2001); the lipid phosphatase PTEN, which dephosphorylates PIP3 and antagonizes the PI3K signalling (Conche and Sauer 2014); and the serine phosphatases PHLPP1 and PHLPP2, which specifically dephosphorylates Akt at the serine 473 residue and inactivates it. We have not observed any alterations in the protein levels of PTP1B and PHLPP1 in MAECs treated with MGO. Surprisingly, despite PTEN is a widely validated target of miR-214, in our experimental model, its protein levels are not modified by MGO. One possible explanation for the lack of

PTEN regulation by miR-214 in our cellular model is that the binding site for miR-214 in the 3'UTR of mouse PTEN overlaps with the binding site for several other miRNAs in accordance with the microRNA.org prediction. This suggests that other miRNAs highly expressed in MAECs may regulate PTEN in a mutually exclusive fashion and independently from any changes in miR-214 levels upon MGO treatment. Based on our search on 10 different miRNA target prediction programs to retrieve information on any interaction between PHLPP2 and specific miRNAs, PHLPP2 results to be a predicted target of both miR-214 and miR-126. Interestingly, the inhibition of the endogenous miR-214 in MAECs is sufficient to cause a significant increase in PHLPP2 protein levels. This increase is comparable to that induced by MGO, while miR-214 overexpression results in decrease of PHLPP2 levels in MAECs the phosphatase levels are significantly decreased. Differently, we have not observed alterations in PHLPP2 protein levels, after modulation miR-126 in MAECs. Taken together, these results suggest an inverse correlation between PHLPP2 and miR-214, but not with miR-126, supporting the bioinformatic target prediction only for miR-214. Moreover, for the first time, we prove a direct regulation of miR-214, as demonstrated by the experiments performed with both PHLPP2 by a target site protector specific for the binding site of miR-214 in the 3'UTR of mouse PHLPP2 and a reporter gene assay with the 3'UTR of mouse PHLPP2 cloned downstream of the Firefly luciferase gene. In order to test the role of miR-214 in the MGO effect on PHLPP2 levels in MAECs, miR-214 was inhibited or overexpressed in presence of MGO. No further increase is observed in the former case, thus excluding that two different mechanisms are due to miR-214 and MGO. Differently, a reversion in the PHLPP2 expression is obtained when the MGO-dependent downregulation of miR-214 is specifically bypassed in when MAECs were treated with both MGO and miR-214 inhibitor.

It is well known that PHLPP2 can directly dephosphorylate Akt to inhibit its signalling activity in endothelial cells (Sun et al. 2016). Once validated PHLPP2 as direct target of miR-214, we then verified whether the negative effect of MGO on the insulin signalling pathway in MAECs may be mediated by miR-214 downregulation, by testing the Akt phosphorylation levels on serine 473 following the specific inhibition of miR-214 in MAECs. As expected, the following increase of PHLPP2 leads to a decreased phosphorylation levels of Akt, thus mimicking the MGO-dependent effect on the insulin sensitivity in endothelial cells. Moreover, when MAECs were transfected with miR-214 mimic, a rescue effect on Akt activation and

PHLPP2 levels occurred, strengthening our hypothesis that the downregulation of miR-214 may contribute to the MGO-dependent effect through its new target, PHLPP2.
Therefore, in this study, also provided evidence of a negative effect played by miR-214 on the responsiveness to insulin in MAECs, by regulating PHLPP2.

2.8 Conclusion

Our study demonstrates for the first time that MGO modulates miR-190a, miR-450a, miR-126 and miR-214. Among these, miR-190a and miR-214 mediate the endothelial insulin-resistance induced by MGO in MAECs, by targeting KRAS and PHLPP2, respectly. Thus, we indicate here both miR-190a and miR-214 as a new players in the MGO negative effect on endothelial cell function. Further investigations will be useful for the identification of novel therapy for preserving endothelial sensitivity and preventing the progression of vascular complications.

2.9 Material and Methods

Reagents

Media, sera and antibiotics for cell culture were from Lonza (Walkersville, MD, USA). MGO (40% in water) were from Sigma-Aldrich (St Louis, MO, USA). U0126 was from ENZO Lifescience (Florence, Italy). Insulin was from Eli Lilly (Florence, Italy). The antibodies used were anti-p-thr308-Akt, anti-p-tyr-IRS1 (Millipore, Billerica, MA, USA), anti-p-ser616-IRS1 (Life Technologies, Carlsbad, CA, USA), anti-p-tyr-IR, anti-Akt, anti-p-ser473-Akt, anti-PTEN, anti-eNOS, anti-p-ser1177-eNOS, anti-p-thr497-eNOS (Cell Signalling Technology, Beverly, MA, USA), anti-ERK1/2, anti-p-ERK1/2, anti-14-3-3, anti-β-actin, anti-PTP1B and anti-Akt (Santa Cruz, CA, USA), anti-KRAS (Abcam, Cambridge, UK) and anti-α-tubulin (Sigma-Aldrich, St Louis, MO, USA), anti-PHLPP1 and anti-PHLPP2 (Bethly Laboratories, Montgomery, TE, USA). All other chemicals were from Sigma-Aldrich (St Louis, MO, USA). Protein electrophoresis and western blot reagents were from Bio-Rad (Richmond, VA, USA) and chemiluminescence reagents from Pierce (Rockford, IL, USA).

Cell Culture

Mouse aortic endothelial cells (MAECs) were kindly provided by T.H Fleming (University of Heidelberg, Heidelberg, Germany). MAECs were plated in T75 flasks and grown in Dulbecco's Modified Medium (DMEM) containing 1 g/l glucose supplemented with 10% (v/v) FBS, 2 mmol/l L-glutamine and 0.1 mmol/l non-essential amino acids. Cell cultures were maintained at 37 °C in a humidified atmosphere containing 5% (v/v) CO_2. Cells were starved in serum-free medium containing 0.25% (w/v) albumin bovine serum (BSA) for 16 h, treated with MGO 500 μmol/l and then exposed or not to 100 nmol/l insulin for 10 min. Where indicated, cells were pre-treated for 30 min with U0126 15 μmol/l and then treated with MGO 500 μmol/l for 16h.

MiRNA Target Prediction

miRWalk2.0, a comprehensive atlas of microRNA–target interactions, was used (Dweep and Gretz 2015) for target prediction of specific miRNAs.

Cell transfection

miR-190a levels were modulated by transfecting MAECs with miR-190a-mimic (mmu-miR-190a-5p miRIDIAN Mimic) 0.5 nM or with miR-190a-inhibitor (mmu-miR-190a-5p miRIDIAN Harpin Inhibitor), miR-214 levels were modulated by transfecting MAECs with 0.5, 5, or 50 nmol/L miR-214-mimic (mmu-miR-214 miRIDIAN Mimic) or miR-214-inhibitor (mmu-miR-214 miRIDIAN Harpin Inhibitor). miR-126 levels were modulated by transfecting MAECs with 0.5, 5 and 50 nmol/L miR-126-mimic (mmu-miR-126 miRIDIAN Mimic) or miR-126-inhibitor (mmu-miR-126 miRIDIAN Harpin Inhibitor). DharmaFECT 4 was used as transfecting agent, according to the manufacturer's instructions (Dharmacon, part of GE Healthcare, Lafayette, CO). miRIDIAN microRNA Mimic negative control #1 and miRIDIAN microRNA Harpin Inhibitor Negative control #1 (Dharmacon, Lafayette, CO, USA) were used as negative controls of miRNA-mimic and miRNA-inhibitor transfection, respectively. After 48 h, the cells were directly harvested in the case of miR-inhibitor or harvested after MGO treatment and analyzed as described below. For study of miR-190a, KRAS protein levels were reduced in MAECs transfected with a specific siRNA 50 nM or a siRNA with a scrambled sequence used as a negative control, both of which purchased from Integrated DNA Technologies (IDT, Coralville, IA, USA). TransIT-TKO from Mirus Bio LLC (Madison, WI, USA) was used as transfecting reagent, according to the manufacturer's instructions.

Mice

Mice Glo1-knockdown (Glo1-KD) mice were generated and characterized as previously described (Queisser et al. 2010, Bierhaus et al. 2012, Giacco et al. 2014). Mice were housed in a temperature-controlled (22 °C) room with a 12 h light/dark cycle, in accordance with the Guide for the Care and Use of Laboratory Animals published by the National Institutes of Health (Marsch and Studer 1999), and experiments were approved by the ethics committee of the MIUR. Reduced Glo1 mRNA levels were confirmed by quantitative PCR. For vascular insulin signalling, a bolus of insulin (0.15 U/g bodyweight) was i.p. administrated to mice 10 min before they were killed by cervical dislocation. Aortic tissues were then collected and processed as follow.

Western blot Analysis

MAECs were solubilized in lysis buffer (50 mmol/L HEPES pH 7.5, 150 mmol/L NaCl, 10 mmol/L EDTA, 10 mmol/L Na2P2O7, 2 mmol/L Na3VO4, 100mmol/L NaF, 10% glycerol, 1% Triton X-100) for 2 h at 4 °C. Protein lysates were clarified by centrifugation at 16,000× g for 20 min. Cell lysates were then separated by SDS-PAGE and transferred into 0.45 µm Protran Nitrocellulose Membrane (Sigma-Aldrich). Upon incubation with primary and secondary antibodies (for a full list of the antibodies, see above), immunoreactivity bands were detected by chemiluminescence and densitometric analysis was performed using ImageJ software.

Measurement of NO

NO was measured in cell culture medium. After treatments, culture medium was collected, centrifuged at 1000g for 15 min and the supernatant fraction was used as a sample solution for the detection, using Nitrate/Nitrite Assay Colorimetric Kit (Sigma-Aldrich). This assay uses the Griess reaction, resulting in the formation of a chromophoric azo-derivative, which absorbs light at 540–570 nm.

miRNA reverse transcription, miScript PCR Array and Real Time-PCR.

Total RNA was isolated from MAECs and mouse aorta samples after homogenization in Qiazol using miRNeasy mini kit (QIAGEN, Hilden, Germany), according to manufacturer's instructions. After quantification with Nanodrop 2000 spectrophotometer (Thermo Scientific, Mirra et 2017), total RNA was reverse transcribed using the miScript II RT Kit (QIAGEN) and analyzed by the Diabetes miRNA PCR Array (QIAGEN; http://sabiosciences.com/mirna_pcr_product/HTML/MIMM-115Z), according to the manufacturer's instructions. The PCR array was provided in ready-to-use 96 well-plate, which contains 84 miRNA-specific primers and different snoRNA/snRNA specific primers, used as normalization controls. One plate was used for each experimental condition. Resulting data were analyzed by the free data analysis software, available at http://pcrdataanalysis.sabiosciences.com/mirna. The differential expression of miRNAs was then validated by Real Time-PCR using the miScript SYBR Green PCR Kit (QIAGEN) and specific miScript Primer Assays. The levels

of all differential expressed miRNAs were quantified as expression units relative to U6 snRNA, used as housekeeping smallRNA. Specific primers used for amplification were purchased from QIAGEN:

Mm_miR-190_3 miScript Primer Assay, MS00032438
Mm_miR-214_2 miScript Primer Assay, MS00032571
Mm_miR-34a_1 miScript Primer Assay, MS00001428
Mm_miR-126-5p_1 miScript Primer Assay, MS00006006
Mm_miR-129-3p_1 miScript Primer Assay, MS00006013
Mm_miR-199a-5p_1 miScript Primer Assay, MS00032529
Mm_miR-214_2 miScript Primer Assay, MS00032571
Mm_miR-320_3 miScript Primer Assay, MS00011767
Mm_miR-335_1 miScript Primer Assay, MS00002142
Mm_miR-375_2 miScript Primer Assay, MS00032774
Mm_miR-381_2 miScript Primer Assay, MS00032802
Mm_miR-450a_1 miScript Primer Assay, MS00025886
Mm_miR-451_1 miScript Primer Assay, MS00002408
RNU6B_13 miScript Primer Assay, MS00014000

Target Site Inhibition Assays.

The miScript miR-214 Target Protector (miR-214 TP) was designed based on the sequence of the target site for the miR-214 in the 3'UTR of the mouse PHLPP2 mRNA and obtained from Qiagen (Qiagen, Germantown, MD, USA). The miScript Target Protector is a single-stranded modified RNA that is complementary to the binding site of the miRNA of interest and covers the flanking region of the binding site, thus interfering specifically with the interaction of the miRNA with a single target and leaving the regulation of other targets of the same miRNA unaffected. After transfection, a miScript Target Protector binds to its specific miRNA-binding site, blocking miRNA access the site and preventing gene downregulation by a specific miRNA. MAECs were co-transfected with both 0.1 nmol/L miR-214 TP and 50 nmol/L miR-214 mimic using DharmaFECT 4 (Dharmacon), according to manufacturer's instructions. Forty-eight hours after transfection, cells were harvested and PHLPP2 protein levels were analyzed as described below.

Luciferase Reporter Assays.

The mouse PHLPP2-3'UTR sequence was inserted into pEZX-MT06, a Firefly/Renilla Duo-Luciferase reporter vector (GeneCopoeia, Rockville, MD, USA) (Carroll et al. 2014). Here, Firefly luciferase is the reporter gene controlled by the 3'UTR of interest and Renilla luciferase is the internal control.
MAECs were plated in 6-well plates and co-transfected with 100 ng of the pEZX-MT06 control reporter vector or the pEZX-MT06/PHLPP2-3'UTR reporter vector and 50 nmol/L miR-214 mimic or a non-targeting control oligonucleotide (mimic control) using DharmaFECT 4 (Dharmacon), according to manufacturer's instructions. Twenty-four hours post transfection, Firefly and Renilla luciferase activities were determined in cell lysates using the Dual-Luciferase Reporter Assay System (Promega, Madison, WI, USA) and a luminometer (Orion I, Berthold Detection Systems, Pforzheim, Germany) according to the manufacturer. Results were expressed as the ratio of Firefly to Renilla activity. The experiments were performed in triplicate.

Statistic Procedures.

Data are expressed as means ± SD and ± SEM, as indicated in figure legends. Comparison between groups were performed using Student's t-test or the one-way analysis of variance followed by Tukey multiple comparison tests, as appropriate, using GraphPad Prism 6.01 software (GraphPad, San Diego, CA, USA). A p-value of less than 0.05 was considered statistically significant.

2.10 Bibliography

Ahmed N., Thornalley P. J. (2006) Advanced glycation endproducts: what is their relevance to diabetic complications? Endocrinology & Metabolism 18/143 https://doi.org/10.1111/j.1463-1326.2006.00595.x

Alessi D.R., Deak M., Casamayor A., Caudwell F.B., et al. (1997) 3-Phosphoinositide-dependent protein kinase-1 (PDK1): structural and functional homology with the Drosophila DSTPK61 kinase. Curr Biol. 7(10):776-89

Beisswenger P.J. (2014) Methylglyoxal in diabetes: link to treatment, glycaemic control and biomarkers of complications. Biochemical Society Transactions42(2)450-456; DOI: 10.1042/BST20130275

Beisswenger P. J., Howell S. K., O'Dell R. M., Wood M.E., Touchette A. D, Szwergold B. S. (2001) α-Dicarbonyls Increase in the Postprandial Period and Reflect the Degree of Hyperglycemia Diabetes Care 24(4): 726-732. https://doi.org/10.2337/diacare.24.4.726

Bierhaus A., Fleming T., Stoyanov S., Leffler A., Babes A., Neacsu C., Sauer S.K., Eberhardt M., Schnölzer M., Lasitschka F., Neuhuber W.L., Kichko T.I., Konrade I., Elvert R., Mier W., Pirags V., Lukic I.K., Morcos M., Dehmer T., Rabbani N., Thornalley P.J., Edelstein D., Nau C., Forbes J., Humpert P.M., Schwaninger M., Ziegler D., Stern D.M., Cooper M.E., Haberkorn U., Brownlee M., Reeh P.W., Nawroth P.P. (2012) Methylglyoxal modification of Nav1.8 facilitates nociceptive neuron firing and causes hyperalgesia in diabetic neuropathy. Nat Med. 18(6):926-33. doi: 10.1038/nm.2750

Carroll A.P., Goodall G.J., Liu B. (2014) Understanding principles of miRNA target recognition and function through integrated biological and bioinformatics approaches. Wiley Interdiscip. Rev. RNA, 5, 361–379.

Chang L., Chiang S.H. , R Saltiel A. (2004) Insulin Signaling and the Regulation of Glucose Transport . Mol Med (7-12): 65–71 doi: 10.2119/2005-00029.Saltiel

Conche C., Sauer K. (2014) Uncovering the PI3Ksome: phosphoinositide 3-kinases and counteracting PTEN form a signaling complex with intrinsic

regulatory properties. Mol Cell Biol. 15;34(18):3356-8. doi: 10.1128/MCB.00920-14.

Cox A.D., Der C.J. (2010) Ras history: the saga continues Small GTPases, 1 (1) pp. 2-27, 10.4161/sgtp.1.1.12178

Dávalos A., Goedeke L., Smibert P., Ramírez C. M., Warrier N. P., Andreo U., Cirera-Salinas D., Rayner K., Suresh U., Pastor-Pareja J. C., Esplugues E., Fisher E.A., Penalva L. O. F., Moore K.J., Suárez Y., Lai e. C, and Carlos Fernández-Hernando. (2011) miR-33a/b contribute to the regulation of fatty acid metabolism and insulin signaling. PNAS 108 (22) 9232-9237; https://doi.org/10.1073/pnas.1102281108

De Caterina R. (2000) Endothelial dysfunctions: common denominators in vascular disease. Curr Opin Lipidol. 11(1):9-23.

Devaux Y., Stammet P., Friberg H., Hassager C., Kuiper M. A., Wise M. P., Nielsen N. and for the Biomarker subcommittee of the TTM trial (Target Temperature Management After Cardiac Arrest, NCT01020916). (2015) MicroRNAs: new biomarkers and therapeutic targets after cardiac arrest? Devaux et al. Critical Care 19:54 DOI 10.1186/s13054-015-0767-2

Duan Q, Yang L, Gong W, Chaugai S, Wang F, Chen C, Wang P, Zou MH, Wang DW. (2015) MicroRNA-214 Is Upregulated in Heart Failure Patients and Suppresses XBP1-Mediated Endothelial Cells Angiogenesis. J Cell Physiol. Aug;230(8):1964-73. doi: 10.1002/jcp.24942.

Dweep H., Gretz N. (2015) miRWalk2.0: a comprehensive atlas of microRNA-target interactions. Nat Methods. 12(8):697. doi: 10.1038/nmeth.3485.

Dweep H., Sticht C., Pandey P., Gretz N. (2011) miRWalk–database: prediction of possible miRNA binding sites by “walking” the genes of three genomes J. Biomed. Inform., 44 (5) pp. 839 847, 10.1016/j.jbi.2011.05.002

El-Osta A., Brasacchio D., Yao D., Pocai A., Jones P.L., Roeder R.G., Cooper M.E., Brownlee M. (2008) Transient high glucose causes persistent epigenetic changes and altered gene expression during subsequent normoglycemia J. Exp. Med., 205 pp. 2409-2417, 10.1084/jem.20081188

Enright A.J., John B., Gaul U. , Tuschl T. , Sander C. , Marks D.S. (2003) MicroRNA targets in drosophila Genome Biol 5 (1) p. R1, 10.1186/gb-2003-5-1-r1

Eringa E.C., Stehouwer C.D., Nieuw Amerongen G.P., et al. (2004) Vasoconstrictor effects of insulin in skeletal muscle arterioles are mediated by ERK1/2 activation in endothelium. Am J Physiol Heart Circ Physiol 287:H2043–H2048 https://doi.org/10.1152/ajpheart.00067.2004

Fiory F., Lombardi A., Miele C.. Giudicelli J., Beguinot F. Van Obberghen E. (2011) Methylglyoxal impairs insulin signalling and insulin action on glucose-induced insulin secretion in the pancreatic beta cell line INS-1E. Diabetologia 54:2941–2952 DOI 10.1007/s00125-011-2280-8

Giacco F., Du X., D'Agati V.D., Milne R., Sui G., Geoffrion M. and Brownlee M. (2014) Knockdown of Glyoxalase 1 Mimics Diabetic Nephropathy in Nondiabetic Mice. Diabetes Jan; 63(1): 291-299 https://doi.org/10.2337/db13-0316

Guo Q., Mori T., Jiang Y., Hu C., Osaki Y., Yoneki Y.; Sun Y.; Hosoya T.; Kawamata A., Ogawa S., Nakayama M, Miyata T., Ito S. (2009) Methylglyoxal contributes to the development of insulin resistance and salt sensitivity in Sprague–Dawley rats. Journal of Hypertension. 27(8):1664–1671, DOI: 10.1097/HJH.0b013e32832c419a

Jia X., Wu L. (2007) Accumulation of endogenous methylglyoxal impaired insulin signaling in adipose tissue of fructose-fed rats. Mol. Cell. Biochem., 306, pp. 133-139, 10.1007/s11010-007-9563-x

Laga M., Cottyn A., Van Herreweghe F., Vanden Berghe W., Haegeman G., Van Oostveldt P., Vandekerckhove J., Vancompernolle K. (2007) Methylglyoxal suppresses TNF-alpha-induced NF-kappaB activation by inhibiting NF-kappaB DNA-binding Biochem. Pharmacol., 4 (4), pp. 579-589, 10.1016/j.bcp.2007.05.026

Lewis B.P., Shih I.H., Jones-Rhoades M.W., Bartel D.P., Burge C.B. (2003) Prediction of mammalian microRNA targets Cell, 115 (7) pp. 787-798, 10.1016/S0092-8674(03)01018-3

Lind M., Odén A., Fahlén M., Eliasson B. (2010) The shape of the metabolic memory of HbA1c: re-analysing the DCCT with respect to time-dependent effects. Diabetologia. Jun;53(6):1093-8. doi: 10.1007/s00125-010-1706-z

Liu H., Zhang N., Tian D. (2014), MiR-30b is involved in methylglyoxal-induced epithelial-mesenchymal transition of peritoneal mesothelial cells in rats Cell. Mol. Biol. Lett., 19 (2) pp. 315-329, 10.2478/s11658-014-0199-z

Liu J., Chen W., Zhang H., Liu T., Zhao L. (2017) miR-214 targets the PTEN-mediated PI3K/Akt signaling pathway and regulates cell proliferation and apoptosis in ovarian cancer. Oncol. Lett. 14, 5711–5718 https://doi.org/10.3892/ol.2017.6953

Magenta A., Greco S., Gaetano C., Martelli F. (2013) Oxidative Stress and MicroRNAs in Vascular Diseases Int. J. Mol. Sci., 14(9), 17319-17346; https://doi.org/10.3390/ijms140917319

Marchand A., Atassi F., Mougeno t., Clergue M., Codoni V., Berthuin J., Proust C., Trégouët D.A., Hulot J.-S., Lompré A.M. (2016) miR-322 regulates insulin signaling pathway and protects against metabolic syndrome-induced cardiac dysfunction in mice Biochimica et Biophysica Acta 1862 611–621 DOI:0.1016/j.bbadis.2016.01.010

Marsch S.C.U., Studer W. (1999) Editorial Guidelines to the use of laboratory animals: what about neuromuscular blocking agents? Cardiovascular Research. 42565–566 www.elsevier.com/locate/cardiores www.elsevier.nl/locate/cardiores

Mir A.R., Uddin M., Alam K., Ali A. (2014) Methylglyoxal mediated conformational changes in histone H2A-generation of carboxyethylated advanced glycation end products Int. J. Biol. Macromol., 69 pp. 260-266, 10.1016/j.ijbiomac.2014.05.057

Miranda K.C., Huynh T., Tay Y., Ang Y.S, Tam W.L., Thomson A.M., Lim B., Rigoutsos I. (2006) A pattern-based method for the identification of microRNA binding sites and their corresponding heteroduplexes Cell, 126 (6) pp. 1203-1217, 10.1016/j.cell.2006.07.031

Mirra P., Nigro C., Prevenzano I., Leone A., Raciti G.A Formisano P., Beguinot F., and Miele C. The Destiny of Glucose from a MicroRNA Perspective (2018) Front Endocrinol (Lausanne) 9: 46. doi: 10.3389/fendo.2018.00046

Mirra P., Nigro C., Prevenzano I., Procopio T., Leone A., Raciti G.A., Andreozzi F., Longo M., Fiory F., Beguinot F., Miele C. (2017) The role of miR-190a in methylglyoxal-induced insulin resistance in endothelial

cells. Biochim Biophys Acta Mol Basis Dis. Feb;1863(2):440-449. doi: 10.1016/j.bbadis.2016.11.018.

Muniyappa R., Iantorno M., Quon M.J. (2007) Insulin action and insulin resistance in vascular endothelium. Current Opinion in Clinical Nutrition and Metabolic Care: Volume 10 - Issue 4 - p 523–530 doi: 10.1097/MCO.0b013e32819f8ecd

Nigro C., Raciti G.A., Leone A., Fleming T.H., Longo M. Prevenzano I., Fiory F., Mirra P., D'Esposito V., Ulianich L., Nawroth P.P., Formisano P., Beguinot F, Miele C. (2014) Methylglyoxal impairs endothelial insulin sensitivity both in vitro and in vivo. Diabetologia. 57(7):1485-94. doi: 10.1007/s00125-014-3243-7

Nigro C., Leone A., Raciti G.A., Longo M., Mirra P., Formisano P., Beguinot F., Miele C. (2017) Methylglyoxal-Glyoxalase 1 Balance: The Root of Vascular Damage. Review. Int J Mol Sci doi: 10.3390/ijms18010188.

Palsamy P., Bidasee K.R., Ayaki M., Augusteyn R.C., Chan J.Y., Shinohara T. (2014) Methylglyoxal induces endoplasmic reticulum stress and DNA demethylation in the Keap1 promoter of human lens epithelial cells and age-related cataracts Free Radic. Biol. Med., 72 , pp. 134-148, 10.1016/j.freeradbiomed.2014.04.010

Poy M.N., Spranger M., Stoffel M. (2007) microRNAs and the regulation of glucose and lipid metabolism. Diabetes Obes Metab. Suppl 2:67-73 DOI:10.1111/j.1463-1326.2007.00775.x

Pujol-López M., Ortega-Paz L., Garabito M., Brugaletta S., Sabaté M., Dantas A. P. (2017) miRNA Update: A Review Focus on Clinical Implications of miRNA in Vascular Remodeling. AIMS Medical Science, 4(1): 99-112. doi: 10.3934/medsci.2017.1.99.

Qaid M. M., Abdelrahman M.M. (2016) Role of insulin and other related hormones in energy metabolism. Qaid & Abdelrahman, Cogent Food & Agriculture, 2: 1267691 http://dx.doi.org/10.1080/23311932.2016.1267691

Queisser M. A, Yao D., Geisler S., Hammes H.P., Lochnit G., Schleicher E. D., Brownlee M. and. Preissner K. T. (2010) Hyperglycemia Impairs Proteasome Function by Methylglyoxal. Diabetes Mar; 59(3): 670-678 https://doi.org/10.2337/db08-1565

Rabbani N. and Thornalley P. J. (2014) The Critical Role of Methylglyoxal and Glyoxalase 1 in Diabetic Nephropathy. Diabetes 63(1): 50-52 https://doi.org/10.2337/db13-1606

Rask-Madsen C., King G.L. (2013) Vascular complications of diabetes: mechanisms of injury and protective factors. Cell Metab. Jan 8;17(1):20-33. doi: 10.1016/j.cmet.2012.11.012

Riboulet-Chavey A., Pierron A., Durand I., Murdaca J., Giudicelli J. and Van Obberghen E. (2006) Methylglyoxal Impairs the Insulin Signaling Pathways Independently of the Formation of Intracellular Reactive Oxygen Species. Diabetes 55(5): 1289-1299.https://doi.org/10.2337/db05-0857

Ryu H. S., Park S.Y., Ma D., Zhang J., Lee W. (2011) The Induction of MicroRNA Targeting IRS-1 Is Involved in the Development of Insulin Resistance under Conditions of Mitochondrial Dysfunction in Hepatocytes. https://doi.org/10.1371/annotation/2faafaa7-e359-4711-af5b-3597c705388d

Sandoo A., van Zanten J. J.C.S V., S Metsios G., Carroll D., and D Kitas G. (2010) The Endothelium and Its Role in Regulating Vascular Tone. Open Cardiovasc Med J. 4: 302–312 doi: 10.2174/1874192401004010302

Schalkwijk C.G., Stehouwer C.D. (2005) Vascular complications in diabetes mellitus: the role of endothelial dysfunction. Clin Sci (Lond).109(2):143-59 DOI: 10.1042/CS20050025

Scherrer U., Randin D., Vollenweider P., Vollenweider L., Nicod P. (1994) Nitric oxide release accounts for insulin's vascular effects in humans. J Clin Invest. 94(6):2511-5 DOI: 10.1172/JCI117621

Shan-Shan L., Yang W., Xin J. and Chun J. (2015) The SUR2B subunit of rat vascular KATP channel is targeted by miR-9a-3p induced by prolonged exposure to methylglyoxal. Am. J. Phys. Cell Physiol., 308 (2) pp. C139-C145, 10.1152/ajpcell.00311.2014

Stehouwer C.D., Lambert J., Donker A.J., van Hinsbergh V.W. (1997) Endothelial dysfunction and pathogenesis of diabetic angiopathy. Cardiovasc Res. 34(1):55-68

Sun X., Lin J., Zhang Y., Kang S., Belkin N., Akm K. Wara, Basak Icli , Naomi M. Hamburg , Dazhu Li , and Mark W. Feinberg. (2016) MicroRNA-181b Improves Glucose Homeostasis and Insulin Sensitivity by Regulating Endothelial Function in White Adipose Tissue Circulation Research. 118:810–821

Thangarajah H., Yao D., Chang E.I., Shi Y., Jazayeri L., Vial I.N., Galiano R.D., Du X.L., Grogan R., Galvez M.G., Januszyk M., Brownlee M., Gurtner G.C. The molecular basis for impaired hypoxia-induced VEGF expression in diabetic tissues. Proc. Natl. Acad. Sci. U. S. A., 106 (32) (2009), pp. 13505-13510, 10.1073/pnas.0906670106

Valenti G., Quinn H.M., Heynen G.J.J.E.[1], Lan L., Holland J.D., Vogel R., Wulf-Goldenberg A., Birchmeier W. (2017) Cancer Stem Cells Regulate Cancer-Associated Fibroblasts via Activation of Hedgehog Signaling in Mammary Gland Tumors. Cancer Res. Apr 15;77(8):2134-2147. doi: 10.1158/0008-5472.CAN-15-3490

Virkamäki A., Ueki K., and Ronald C. Kahn (1999) Protein–protein interaction in insulin signaling and the molecular mechanisms of insulin resistance. J Clin Invest. 103(7):931-943. https://doi.org/10.1172/JCI6609

Wang X., Shen E., Wang Y., Li J., Cheng D., Chen Y., Gui D., Wang N. (2016) Cross talk between miR-214 and PTEN attenuates glomerular hypertrophy under diabetic conditions. Sci. Rep., 6 31506 DOI:10.1038/srep31506

Wang X.Y., Bergdahl K., Heijbel A., Liljebris C., Bleasdale J.E. (2001) Analysis of in vitro interactions of protein tyrosine phosphatase 1B with insulin receptors. Molecular and Cellular Endocrinology [173(1-2):109-120] DOI: 10.1016/S0303-7207(00)00402-0

Woulfe D. Jiang H., Morgans A., Monks R., Birnbaum M., and Brass L. F. (2004). Defects in secretion, aggregation, and thrombus formation in platelets from mice lacking Akt2 J Clin Invest. 113(3): 441–450. doi: 10.1172/JCI200420267

Xin R., Bai F., Feng Y., Jiu M., Liu X., Bai F., Nie Y., Fan D. (2016) MicroRNA-214 promotes peritoneal metastasis through regulating PTEN negatively in gastric cancer. Clin. Res. Hepatol. Gastroenterol., 40, 748–754 https://doi.org/10.1016/j.clinre.2016.05.006

Yang H., Junyu Y., Shenyi Y., Hanshuo Z., Yu F., Changhong S., Jin G. and Jianzhong Jeff X. (2014) The synergistic regulation of VEGF-mediated angiogenesis through miR-190 and target genes RNA, 20 (8), pp. 1328-1336, 10.1261/rna.044651.114

Yang H., Kong, W., He L., Zhao J.J., O'Donnell J.D., Wang J. Wenham, R.M.; Coppola, D.; Kruk, P.A.; Nicosia, S.V. (2008) MicroRNA expression profiling in human ovarian cancer: mir-214 induces cell survival and cisplatin resistance by targeting PTEN. Cancer Res. 68, 425–433 DOI: 10.1158/0008-5472.CAN-07-2488

Yang T.S., Yang X.H., Wang X.D., Wang Y.L., Zhou B., Song Z.S. (2013) MiR-214 regulate gastric cancer cell proliferation, migration and invasion by targeting PTEN. Cancer Cell Int., 13, 68 10.1186/1475-2867-13-68

Yao D., Taguchi T., Matsumura T., Pestell R., Edelstein D., Giardino I., Suske G., Rabbani N., Thornalley P.J., Sarthy V.P., Hammes H.P., Brownlee M. (2007) High glucose increases angiopoietin-2 transcription in microvascular endothelial cells through methylglyoxal modification of mSin3A J. Biol. Chem., 282 (42), pp. 31038-31045, 10.1074/jbc.M704703200

Zhang Q., Zhang S. (2017)_miR-214 promotes radioresistance in human ovarian cancer cells by targeting PTEN. Biosci. Rep. DOI: 10.1042/BSR20170327

Zhang Y., Sun X., Icli B. and Feinberg M. W. (2017) Emerging Roles for MicroRNAs in Diabetic Microvascular Disease: Novel Targets for Therapy Endocrine Reviews 38: 145–168 doi: 10.1210/er.2016-1122

Zheng H., Zeng Y., Zhang X., Chu J., Loh H.H., Law P.Y. (2010) mu-Opioid receptor agonists differentially regulate the expression of miR-190 and NeuroD Mol. Pharmacol., 77 (1) pp. 102-109, 10.1124/mol.109.060848